STUDY ON ZEOLITE-SEBS COMPOSITE/PERFORATED POLYOLEFINS (LDPE AND BOPP) DOUBLE-LAYERED FILMS FOR IMPROVING ETHYLENE PERMEATION

SARAWUT LAOWAKUL

A THESIS SUBMITTED IN PARTIAL FULFILLMENT
OF THE REQUIREMENT FOR THE DEGREE OF
MASTER OF SCIENCE IN POLYMER TECHNOLOGY
FACULTY OF SCIENCE
KING MONGKUT'S INSTITUTE OF TECHNOLOGY LADKRABANG
2011

KMITL - 2011 - SC - M - 014 - 004

หัวข้อวิทยานิพนธ์	การศึกษาฟิล์มสองชั้นของซีโอไลต์-เอสอีบีเอส คอมโพสิต/พอลิโอลิฟินส์ (แอลดีพีอีและบีโอพีพี) ที่เจาะรูเพื่อช่วยการแพร่ผ่านของก๊าซเอทิลีน
นักศึกษา	นายศราวุธ เลาวกุล
รหัสประจำตัว	51067903
ปริญญา	วิทยาศาสตรมหาบัณฑิต
สาขาวิชา	เทคโนโลยีพอลิเมอร์
พ.ศ.	2553
อาจารย์ผู้ควบคุมวิทยานิพนธ์	รศ.ดร.ตะวัน สุขน้อย
อาจารย์ผู้ควบคุมวิทยานิพนธ์ร่วม	ผศ.ดร.ชลลดา ฤตวิรุฬห์ ผศ.ดร.สุภารัตน์ รักชลธี ดร.อศิรา เฟื่องฟูชาติ

บทคัดย่อ

ในงานวิจัยนี้ ได้ทำการเตรียมฟิล์มสองชั้นของซีโอไลต์-เอสอีบีเอสคอมโพสิต/พอลิโอลิฟินส์ (แอลดีพีอีและบีโอพีพี) ที่เจาะรูเพื่อช่วยเพิ่มความสามารถในการแพร่ผ่านของก๊าซเอทิลีนโดยมีการผสมซีโอไลต์ปริมาณ 5% โดยน้ำหนักในสไตรีน-เอทิลีนบิวทิลีน-สไตรีน จากนั้นทำการเตรียมฟิล์มโดยกระบวนการหล่อแบบสารละลาย (50 ไมครอน) และกระบวนการเคลือบหมุนเหวี่ยง (30 40 และ 50 ไมครอน) ส่วนฟิล์ม LDPE และ BOPP (30 ไมครอน) ทำหน้าที่เป็นชั้นเสริมแรง ทำการปรับเปลี่ยนเปอร์เซ็นต์การเจาะรู (0-100) และขนาดของรู (2 3 และ 5 มิลลิเมตร) ฟิล์มคอมโพสิตสองชั้นที่สามารถเตรียมโดยกระบวนการลามิเนต และกระบวนการกดอัด ได้นำมาตรวจพิสูจน์เอกลักษณ์ด้วยกล้องจุลทรรศน์อิเล็กตรอนแบบส่องกราด กล้องจุลทรรศน์แบบแสงดิฟ-เฟอร์เรนเชียลสแกนนิ่งแคลอรีมิเตอร์ และเทอร์โมกราวิเมตริกแอนนาไลเซอร์ หลังจากนั้นทำการทดสอบการแพร่ผ่านของไอน้ำ ก๊าซออกซิเจน ก๊าซคาร์บอนไดออกไซด์ ก๊าซเอทิลีน และทำการทดสอบสมบัติการดึงยืด จากการศึกษาพบว่าฟิล์มคอมโพสิตที่มีการเจาะรู 40 เปอร์เซ็นต์ ขนาดรู 2 มิลลิเมตรและความหนาของ SEBS 30 ไมครอนมีความสามารถในการแพร่ผ่านก๊าซเอทิลีนที่สูงเมื่อทำการผสมซีโอไลต์ 5% โดยน้ำหนัก พบว่าความสามารถในการแพร่ผ่านก๊าซเอทิลีนยิ่งเพิ่มสูงขึ้น นอกจากนี้การผสมซีโอไลต์ยังช่วยเพิ่มความสามารถในการยึดติดของฟิล์มสไตรีน-เอทิลีนบิวทิลีน-สไตรีนและชั้นเสริมแรง เมื่อมีการทดสอบก๊าซเอทิลีนในระบบก๊าซผสม ปรากฏว่าความสามารถในการแพร่ผ่านของก๊าซเอทิลีนผสมในก๊าซคาร์บอนไดออกไซด์มีค่าต่ำเมื่อเทียบกับก๊าซเอทิลีนที่ผสมก๊าซไนโตรเจน หรือก๊าซออกซิเจน

Title thesis	Study on zeolite-SEBS composite/perforated polyolefins (LDPE and BOPP) double-layered films for improving ethylene permeation
Student	Mr. Sarawut Laowakul
Student ID.	51067903
Degree	Master of Science
Program	Polymer Technology
Year	2011
Thesis Advisor	Assoc.Prof.Dr. Tawan Sooknoi
Thesis Co-Advisors	Asst.Prof.Dr. Chonlada Ritvirulh
	Asst.Prof.Dr. Suparat Rukchonlatee
	Dr. Asira Fuongfuchat

ABSTRACT

In this research the zeolite-styrene ethylene-butylene styrene/perforated polyolefins (LDPE and BOPP) double-layered films were fabricated for packaging film with improved ethylene permeability. SEBS film was modified with 5% w/w zeolite and prepared via solution casting (50 μm thickness) and spin coating (30, 40 and 50 μm thickness). As received LDPE film (30 μm thickness) and BOPP film (30 μm thickness) were used as supporting layers with various percentages of perforated areas (0-100%) and sizes (2, 3 and 5 mm). The composite double-layered films were prepared by lamination, hot-compression and characterized by scanning electron microscope (SEM), optical microscope (OM), differential scanning calorimeter (DSC) and thermogravimetric analyzer (TGA). The water vapor, oxygen, carbon dioxide and ethylene permeabilities of the composite double-layered films were evaluated together with the tensile properties. It was found that the 40% perforated area, 2 mm perforated size and SEBS (30 μm thickness), double-layered films possessed high ethylene transmission rate (ETR). Adding 5% w/w zeolite into SEBS of double-layered films can somewhat increase ETR of the double-layered films using LDPE as a supporting layer. Moreover, zeolite can also increase adhesion at the interface between SEBS and supporting layers. When the permeation of ethylene was determined in the presence of other gases, the ethylene permeability of the double-layered films in CO_2 was relatively low as compared to that in the presence of N_2 and air zero due to competitive adsorption.

ACKNOWLEDGEMENT

The author would like to express his profound gratitude to his advisors, Assoc.Prof.Dr. Tawan Sooknoi, Asst.Prof.Dr. Chonlada Ritvirulh, Asst.Prof.Dr. Suparat Rukchonlatee, and Dr. Asira Fuongfuchat for their supervisions, helpful suggestion and encouragement throughout this thesis. It is also grateful to Assoc.Prof.Dr. Ittipol Jangchud and Assoc.Prof.Dr. Suwabun Chirachanchai for serving as the chairperson and the committees, and giving valuable comments.

The author would like to extend this sincere appreciation to all of his teachers, friends and research team for their constant guidance advice, support and encouragement.

Sincere thanks to Dr. Doungporn Sirikittikul, Miss Methawadee Thirasat and Miss Phatchareeya Raksa for their advice, helpful suggestion and kindness.

Sincere thanks to the Department of Chemistry, Faculty of Science, King Mongkut's Institute of Technology Ladkrabang for equipment, chemicals and facilities.

Sincere thanks to the National Metal and Materials Technology Center114 Thailand Science Park Paholyothin Rd., Klong 1, Klong Luang, Pathumthani 12120 Thailand for equipment and scholarship.

Finally, the author dedicates his thesis to parents and family for the constant love and encouragement.

Sarawut Laowakul

CONTENTS

CONTENTS (Continued)

CONTENTS (Continued)

CONTENTS (Continued)

LIST OF TABLES

LIST OF TABLES (Continued)

LIST OF FIGURES

LIST OF FIGURES (Continued)

CHARTER 1

INTRODUCTION

1.1 Motivation

The fresh fruits and vegetable can be rotten, leading to short shelf life. This is because, after harvesting, biochemical reactions and physical changes in the fresh fruits and vegetables continue, and thus the produces still consume oxygen and produce water, carbon dioxide and ethylene gases. In particular, ethylene gas a plant hormone can accelerate the ripening process of fruits and vegetable. Such biochemical reactions can be delayed by controlling the oxygen and ethylene content in the packaging, thus the shelf life of fresh fruits and vegetable could be extended. If the ethylene gas in the packaging can be particularly controlled or reduced, a ripening of fruit and vegetable could be delayed. In some applications, the ethylene gas can be removed by placing a packet of potassium permanganate in the fresh fruit and vegetable package. However, the contamination of manful potassium permanganate to the fresh produces has been concerned to the human health. Alternatively, the ethylene gas can be reduced by keeping the fresh produces in cold storage. However, temperature fluctuation in only 3 – 5 °C can trigger ethylene production and activity. Thus, a proper packaging should generate a modified atmosphere inside that can lower the rate of respiration, i.e., reduce oxygen consumption, less production of carbon dioxide and ethylene gases in the packaging **[1-3]**.

Today, packaging films are produced mainly from polyolefins as they possess high flexibility, good optical clarity, good seal ability, long shelf life, dimensional stability during sterilization and bioinert. In addition, it is generally cost effective. However, polyolefin packaging exhibits moderate permeability for water vapor, oxygen, carbon dioxide and ethylene **[4]**. Therefore, it is not suitable as packaging for extending shelf life of fresh fruits and vegetables. In order to solve this problem the commercial perforated packaging was widely used. However, perforated films cannot readily control the packaging atmosphere and may be easy contaminated. In the previous work **[5]**, it was found that zeolite-SEBS/LDPE double-layered films showed high ethylene permeability as compared to oxygen and carbon dioxide. However, LDPE supporting layer limited gas permeability of zeolite composite double-layered films. Hence, it is interesting to develop double-layered films which can improve gas permeation by using perforated

supporting film. In addition, gas transports can be enhanced with a lower SEBS film thickness by spin coating. However, perforation may cause inferior tensile properties of film. Hence, effect of perforation size was included in the study.

In this study the zeolite-styrene-ethylenebutylene-styrene (SEBS) composite/perforated polyolefins (LDPE and BOPP) double-layered films were fabricated for controlling atmosphere in the packaging. The zeolite-SEBS/perforated polyolefins (LDPE and BOPP) films were characterized by scanning electron microscopy (SEM), optical microscopy (OM), thermogravimetric analyzer (TGA) and Differential scanning calorimeter (DSC). The water vapor, oxygen, carbon dioxide and ethylene permeability of the composite double-layered films was evaluated together with the tensile properties. The effect of percentage of perforated area, perforation size, type of supporting layer (LDPE and BOPP films), SEBS thickness and zeolite contents in SEBS on ethylene permeation were investigated.

1.2 Objectives

This study aims to achieve zeolite-SEBS composite/perforated polyolefins (LDPE and BOPP) double-layered films with high ethylene permeability.

1.2.1 To obtain the zeolite-SEBS composite/perforated polyolefins (LDPE and BOPP) double-layered films.

1.2.2 To understand the effect of percentage of perforated area and perforated size in supporting layers (LDPE and BOPP) on ethylene permeation.

1.2.3 To understand the effect of thickness and zeolite contents in SEBS layer on ethylene permeation.

1.3 Scope of study

The scope of study on zeolite-SEBS composite/perforated polyolefins (LDPE and BOPP) double-layered films as follow :

1.3.1 Preparation of SEBS and zeolite-SEBS film by solution casting (50 μm thickness) and spin coating (30, 40 and 50 μm thicknesses).

1.3.2 Preparation of perforated polyolefins (LDPE and BOPP) films with various percentages of perforated areas (0-100%) and perforated sizes (2, 3 and 5 mm).

1.3.3 Fabrication of the zeolite-SEBS composite/perforated polyolefins (LDPE and BOPP) double-layered films using lamination and compression technique.

1.3.4 Characterization of composite double-layered films on thermal and morphological properties.

1.3.5 Study on permeation of oxygen, carbon dioxide, water vapor and ethylene in composite double-layered films with suitable perforated area of LDPE and BOPP layers.

1.3.6 Study on tensile properties of composite double-layered films.

1.4 Expected results

To obtain zeolite-SEBS composite/perforated polyolefins (LDPE and BOPP) double-layered films packaging that can enhance ethylene permeation leading to extend life time of fresh vegetables or fruits and possess acceptable tensile properties.

CHAPTER 2

THEORY AND LITERATURE REVIEW

2.1 Respiration in fresh produces and ethylene gas as plant hormone [2,6-7]

Respiration of fresh fruits and vegetable is metabolism that consumes oxygen and then, produces carbon dioxide gas and water vapor. Furthermore, ethylene gas can be generated by some of the produces (such as tomato). Classification of some produces according to ethylene production rate is shown in Table 2.1. Ethylene gas is natural plant hormone that can affect on the fresh produces in so many different ways. The most detrimental effects are senescence (aging) and ripening acceleration of the fresh produces. When the fresh produces are stored in enclosed areas, the ethylene level is raised. So, they have an unusually fast deterioration in the present of with just a small amount of this gas. The post-harvest "life" of the produce is short and it must be discarded as waste. Hence, to keep produce from ripening too quickly, as much ethylene as possible should be removed from the surrounding air. In practical term, a removal as much ethylene out of the packaging as possible is the best way to cut down on premature aging and ripening and prolong the post-harvest life of fruits and vegetable.

Table 2.1 Classification of the fresh produces that is classified by ethylene production rate **[8]**.

Class	Range at 20 °C (68 °F) ($\mu l\ C_2H_4$ /Kg-hr)	Commodities
Very low	Less than 0.1	Asparagus, cauliflower, cherry, citrus, grape, jujube, strawberry, pomegranate, leafy vegetables, root vegetables, potato, most cut flowers.
Low	0.1-1.0	Blueberry, cranberry, cucumber, eggplant, okra, olive, pepper, persimmon, pineapple,
Moderate	1.0-10.0	Banana, fig, guava, honeydew, melon, mango, plantain, tomato
High	10.0-100.0	Apple, apricot, avocado, cantaloupe, kiwifruit (ripe), nectarine, papaya, peach, pear, plum
Very high	More than 100.0	Cherimoya, mammee apple, passion fruit

2.2 Membrane technology

2.2.1 Membrane description [9-10]

The diversity of membrane based separation systems makes it difficult to categorize them clearly. The systems are typically labeled either on the basis of type of membrane employed, or on the driving force applied to assist penetrant transport through the membrane. The type of membranes used for separation are classified as porous, non-porous (tight) and liquid membranes. With each type of membrane used, further classification is based on the type of applied driving force for the penetrant. Membranes are available in different configurations : plate and frame, tubular, hollow fiber and spiral wound. They are made of various materials such as polymer, metal and ceramic.

The basic concept of membrane separation is shown in Figure 2.1. A feed stream enters the system of membrane and a suitable driving force (such as concentration or pressure differences) is applied across the membrane. This leads to preferential transport of one or more components. Certain components (solutes, solvents, or gases) pass through the membrane. Other components do not pass through the membrane or pass through very slowly. The selective transport (called permeation) forms the basis of membrane separations, which generally involves the separation of solutes or fluid. The stream contains the components that permeated through membrane is called the permeate (or filtrate) and the stream containing retained components is called the retentate (or concentrate).

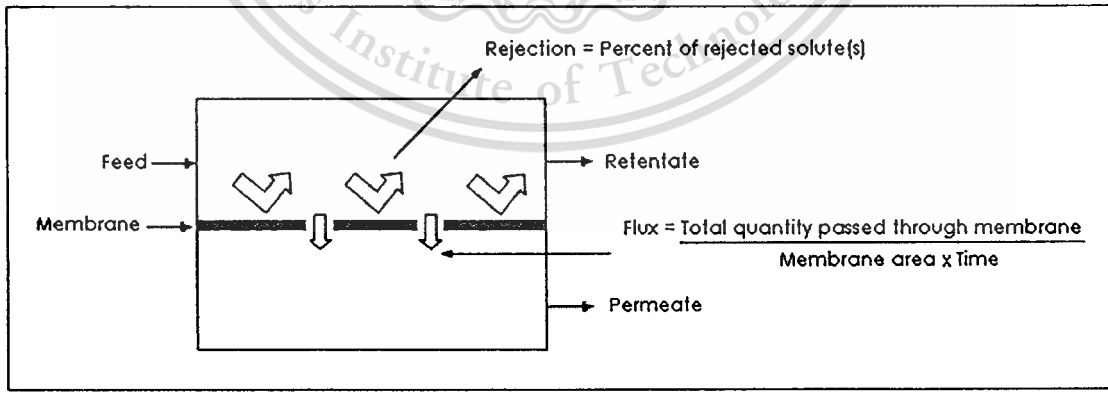

Figure 2.1 Transport of membrane [11].

2.2.2 Application of membrane [12]

Membrane technology has become a dignified separation technology over the past decennia and is being used increasingly in a broad range of applications. The main force of membrane technology is the fact that it works without the addition of chemicals, with a relatively low energy use, easily and well-arranged process conductions. The important property of membrane, which is exploited in every application, is the ability of a membrane to control the permeation of chemical species in contact with it. Applications of membrane is shown in Table 2.2

Table 2.2 Industrial applications of membrane separation processes **[12]**.

1. Reverse osmosis:

Desalinization of brackish water

Treatment of wastewater to remove a wide variety of impurity

Treatment of surface and ground water

Concentration of foodstuffs

Removal of alcohol from beer and wine

2. Dialysis:

Separation of nickel sulfate from sulfuric acid

Hemodialysis (removal of waste metalbolites, excess body water, and restoration of electrolyte balance in blood

3. Eletrodialysis:

Production table salt from seawater

Treatment of wastewater from electroplating

Demineralization of cheese whey

Production of ultra pure water for the semiconductor industry

4. Microfiltration:

Sterilization of drug

Purification of antibiotic

Separation of mammalian cell from liquid

5. Ultrafiltration:

Preconcentration of milk before making cheese

Recovery of vaccine and antibiotic from fermentation broth

Color removal from Kraft black in paper making

Table 2.2 Industrial applications of membrane separation processes (continued).

6. Pervaporation:
Dehydration of ethanol-water azeotrope
Removal of water from organic solvent
Removal of organic from water
7. Gas permeation:
Separation of CO_2 and H_2 from methane and other hydrocarbons
Adjustment of the H_2/CO ratio in synthesis gas
Recovery of helium
Recovery methane from biogas
8. Liquid membrane:
Recovery of zinc from wastewater in the viscose fiber industry

2.2.3 Gas permeation of polymer membrane [11,13-14]

Gas permeation is based on gas dissolution in a membrane, followed by diffusion of the gas through the thickness of the membrane, under the influence of the applied driving force. The relative sorption and diffusion rates of gases then lead to separation of the gas mixture. In this membrane process, membrane devices for gas or vapor separation usually operate under continuous steady-state conditions with three streams (feed, permeate and retentate streams). Gas is made to pass through the membrane by applying a pressure difference on either side of the membrane. This pressure difference causes a difference in dissolved gas concentration between the two faces of the membrane and hence a diffusional gas flows through the membrane. Membrane selectivity is based on the relative permeation rates of the components through the membrane.

Membranes utilized in separations process need to possess both high selectivity and high permeation (high permselectivity). The selectivity of the membrane to specific gas molecules is the ability of the molecules to transport through the membrane. Transportation of molecules through the polymer is dependent upon a number of polymer properties : crosslinking density (if present), chain stiffness, glass transition temperature (T_g), crystallinity (if present), crystallite size and distribution, and solubility of the molecules in the polymer membrane.

Chain stiffness and crystallinity affect the free volume of the polymer. Crystallites restrict the free volume, making diffusion more difficult. Increasing the chain stiffness in the amorphous regions essentially restricts the free volume. Having small, uniformly distributed crystallites in the polymer creates more tortuous pathways for the diffusing molecules. Polarity due to functional groups inside the membrane and van der waals forces due to hydrocarbon fragments can also have a significant influence on separation processes, depending on the nature of the gas molecules.

Permselective polymeric membranes can be divided into two basic categories : glassy and rubbery. Glassy polymers have low chain intrasegmental mobility and long relaxation times, while rubbery polymers exhibit the opposite characteristics, namely high intrasegmental mobility and short relaxation times. Permeation behavior in each type of polymer is shown in Table 2.3.

Table 2.3 Permeation behavior of polymeric materials **[14]**.

Glassy polymer	Rubbery polymer
Diffusion controlled permeation	Solubility controlled permeation
Permeation dependent upon size of permeating molecules	Permeation dependent upon ability to dissolve intermolecular interaction and increase moving polymer segment

Membrane separation processes offer numerous industrial advantages over distillation or disposal. Energy requirements are lower, providing for lower overhead costs. The equipment necessary for liquid and gas separations is significantly more compact, simple to build, and reasonably easy to operate. Handling various volumes of separated product is accomplished without having to utilize different equipments because the equipment can be scaled up or operated at partial capacity without problems occurring. Furthermore, permselective membranes have utility in not only industrial processes involving basic chemicals but also in commercial products. Polymer films, such as polyethylene, used in packaging meats, fruits, and vegetables need to have a certain amount of oxygen permeability and diffusion through the packaging while holding back water. This minimum diffusion, especially in meat packaging, allows the meat to retain a more desirable coloring for the consumer.

2.3 Polymer

2.3.1 Low density polyethylene (LDPE)

Low density polyethylene (LDPE) is a thermoplastic made from oil. It was the first grade of polyethylene, produced in 1933 using a high pressure process via free radical polymerization. It's manufacture employs the same method today.

2.3.1.1 Structure of LDPE [16-18]

LDPE is a synthetic polymer that is formed by addition polymerization of ethylene monomer as shown in Figure 2.2. When ethylene molecules are polymerized to form polyethylene, they form long chains of carbon atoms in which each carbon also is bonded to two hydrogen atoms except the end carbon atom (bonded to three hydrogen atoms). LDPE structure and a repeating unit can be represented in Figure 2.3

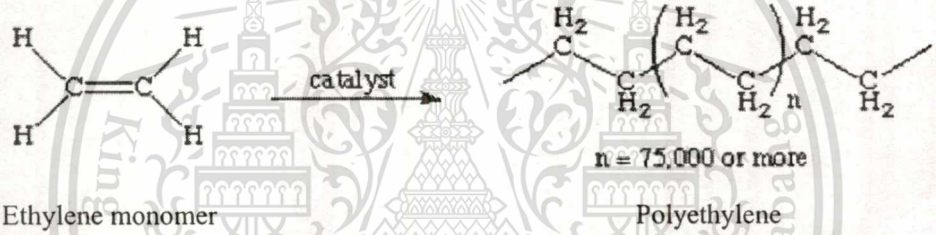

Figure 2.2 Addition polymerization of ethylene monomer **[17]**.

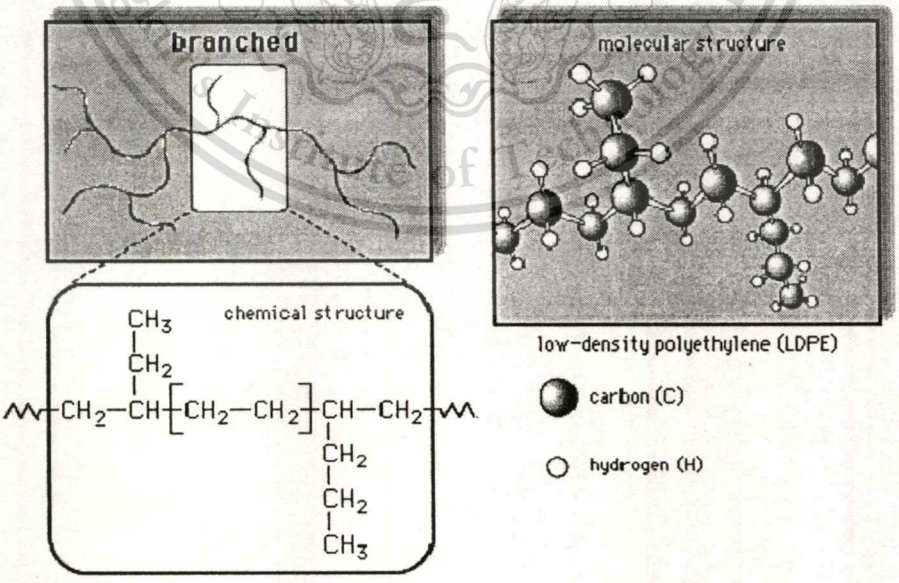

Figure 2.3 LDPE structure **[18]**.

Branching can influence a number of physical properties including tensile strength and crystallinity of polyethylene (PE). LDPE has a high degree of short and long chain branching, which means that the chains do not pack into the crystal structure so well. It has, therefore, less strong intermolecular forces as the instantaneous-dipole induced-dipole attraction is less. This results in a lower tensile strength and increased ductility. The high degree of branching with long chains gives molten LDPE unique and desirable flow properties. In addition, comparing with HDPE, the major difference between LDPE and HDPE is the degree of branching of the polymer chain. HDPE is composed of linear, non-branched chains, while LDPE chains are branched. These different structures are compared in Figure 2.4. This cause leads to some different properties of LDPE and HDPE. Hence, they are suitable for different applications.

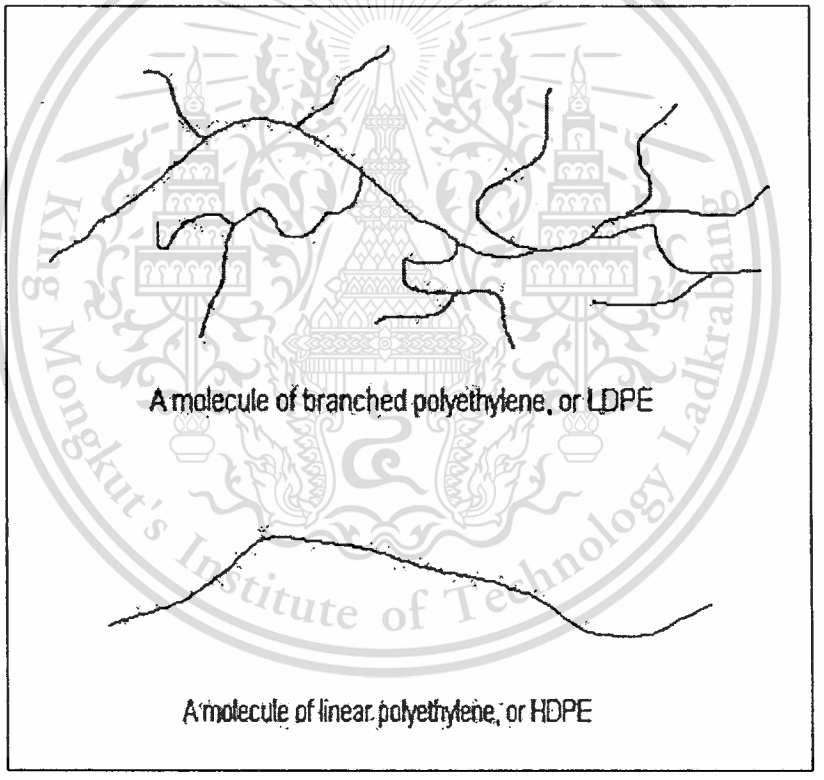

Figure 2.4 Structure of LDPE and HDPE **[16]**.

2.3.1.2 Properties of LDPE [15]

LDPE is defined by a density range of 0.910 - 0.940 g/cm³. This is due to more side chain branching. Melting temperature of LDPE is typically 105 – 115 °C and glass transition temperature is about -120 °C. It is translucent materials with low working temperature. It is unreactive at room temperatures, except by strong oxidizing agents, and some solvents cause

swelling. Chemicals resistance is shown in Table 2.4. It is soft, flexible, tough and low tensile strength while high impact strength. It possesses poor temperature resistance which it can withstand temperatures of 80 °C continuously to 95 °C for a short time. LDPE exhibits low moisture permeability. Some of the benefits of the LDPE include its excellent electrical insulation properties, design versatility and low cost.

Table 2.4 Chemical resistance of LDPE **[15]**.

Level	Solvent or chemical reagent
Excellent resistance (no attack)	Diluted and concentrated acids, alcohols, bases and esters
Good resistance (minor attack)	Aldehydes, ketones and vegetable oils
Limited resistance (moderate attack suitable for short-term use only)	Aliphatic and aromatic hydrocarbons, mineral oils, and oxidizing agents
Poor resistance (not recommended for use)	Halogenated hydrocarbons.

2.3.1.3 Applications of LDPE [15].

LDPE is widely used for manufacturing various containers, dispensing bottles, wash bottles, tubing, plastic bags for computer components, and various molded laboratory equipment. Its most common use is in plastic bags. Other products made from it include :

- Trays & general purpose containers
- Food storages and laboratory containers
- Corrosion-resistant work surfaces
- Weldable and machinable parts
- Parts that require flexibility
- Very soft and pliable parts
- Six-pack soda can rings
- Extrusion coating layers on paperboard and aluminum laminated for beverage cartons.
- Computer components, such as hard drives, screen cards and disk-drives.
- Playground slides

2.3.2 Polypropylene (PP) [19].

PP is a thermoplastic polymer, made by the chemical industry. It was first polymerized to a crystalline isotactic polymer by Giulio Natta and his coworkers in March of 1954. This pioneering discovery led to large-scale commercial production of isotactic polypropylene from 1957 onwards. Syndiotactic polypropylene was also first synthesized by Giulio Natta and his coworkers.

2.3.2.1 Structure of PP [19].

PP is a synthetic polymer that is formed by addition polymerization of propylene monomer as shown in Figure 2.6 When propylene molecules are polymerized to form polypropylene, they form long chains of carbon atoms in which one carbon also is bonded to one hydrogen atom and one methyl group except the end carbon atom (bonded to three hydrogen atoms). Stereoisomer of PP can be represented in Figure 2.5

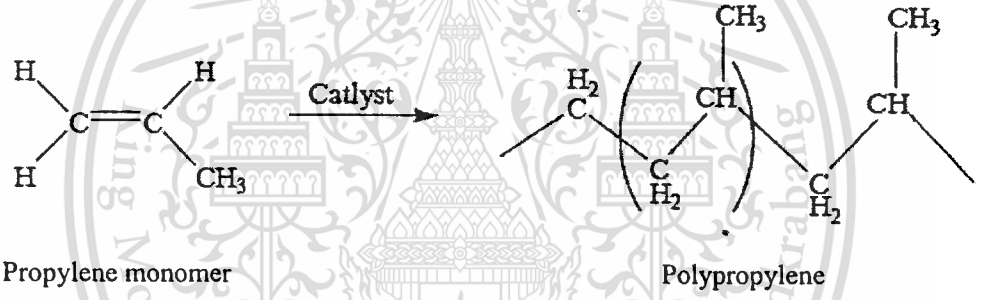

Figure 2.5 Addition polymerization of propylene monomer [19].

Tacticity (isotactic, syndiotactic and atactic) can influence a number of physical properties including tensile strength and crystallinity of polypropylene (PP). Isotactic polymers are usually semicrystalline and often form a helix conformation. Syndiotactic polypropylene made by metallocene catalysis polymerization, is crystalline with a melting point of 130 – 171 °C.

Isotactic polymers

Isotactic polymers are composed of isotactic macromolecules (IUPAC definition). In isotactic macromolecules all the substituents are located on the same side of the macromolecular backbone. An isotactic macromolecule consists of 100% meso diads. Polypropylene formed by Ziegler-Natta catalysis is an isotactic polymer.

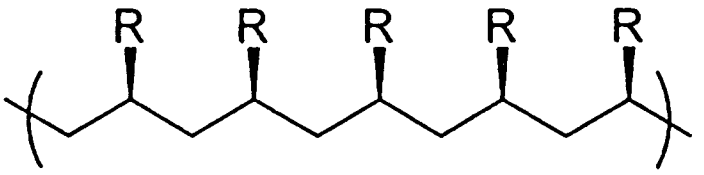

Figure 2.6 Structure of isotactic PP [19].

Syndiotactic polymers

In syndiotactic or syntactic macromolecules the substituents have alternate positions along the chain. The macromolecule consists 100% of racemo diads.

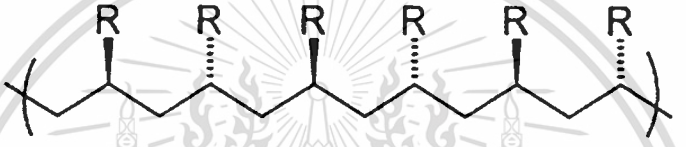

Figure 2.7 Structure of syndiotactic PP [19].

Atactic polymers

In atactic macromolecules the substituents are placed randomly along the chain. The percentage of meso diads is between 1 and 99%. With the aid of spectroscopic techniques such as NMR it is possible to pinpoint the composition of a polymer in terms of the percentages for each triad.

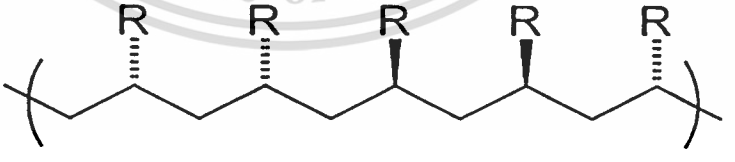

Figure 2.8 Structure of atactic PP [19].

2.3.2.2 Properties of PP [19]

PP is defined by a density range of 0.855 - 0.946 g/cm³. Melting temperature of PP is typically 130 – 171 °C and glass transition temperature is about -20 °C. It is translucent materials with low working temperature. It is unreactive at room temperature, except by strong oxidizing agents, and some solvents cause swelling. Chemical resistance is shown in Table 2.5. It is rigid and low tensile strength and impact strength. It possesses poor temperature resistance which it can withstand temperatures of 90 °C continuously to 105 °C for a short time. PP exhibits low moisture permeability, design versatility and low cost.

Table 2.5 Chemical resistance of PP [20].

Level	Solvent or chemical reagent
Excellent resistance (no attack)	Dilute and concentrated acids, alcohols, bases and mineral Oils
Good resistance (minor attack)	Aldehydes, esters, aliphatic hydrocarbons, ketones and vegetable oils
Limited resistance (moderate attack suitable for short-term use only)	Aromatic and halogenated hydrocarbons and oxidizing agents
Poor resistance (not recommended for use)	Sulphide, chloride and ether

2.3.2.3 Applications of PP [21]

PP is resistant to fatigue. It was used in a wide variety of applications, including packaging, textiles, stationary, plastic parts and reusable containers of various types, laboratory equipment, loudspeakers, automotive components, and polymer banknotes. An addition polymer made from the monomer propylene, it is rugged and unusually resistant to many chemical solvents, bases and acids. A common form of polypropylene in packaging application is biaxially oriented polypropylene (BOPP). These BOPP sheets are used to make a wide variety of products including clear bags. When polypropylene is biaxially oriented, it becomes clear and serves as an excellent packaging material for artistic and retail products. Other products made from it include :

- Autoclaveable packaging and containers for usage in biohazardous environments
- Fittings and connectors, storage containers, sinks, and hoods

2.3.3 Styrene ethylene-butylene styrene block copolymer (SEBS) [22-25]

SEBS is one type of thermoplastic elastomers consist styrenic block copolymer (SBC). Figure 2.9 shows the typical structure of a linear SBC. The styrene end-blocks are rigid polymers. The mid-block is composed of rubbery polymer, i.e., ethylene-butylene block for SEBS.

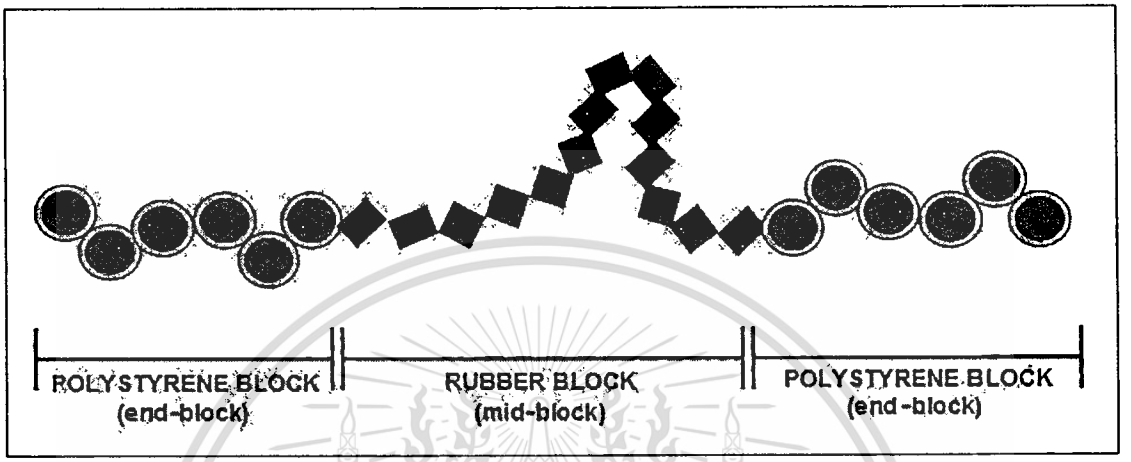

Figure 2.9 Schematic drawing of a linear styrenic triblock copolymer [23].

SEBS has two glass transition temperatures (T_g), an upper one about 95°C associated with the polystyrene domains and a lower one about -55°C associated with ethylene-butylene blocks. These two phases structures give SEBS high strength at end-use temperatures and also provides low viscosity and easy thermoplastic processing at elevated temperatures.

SEBS is high performance thermoplastic elastomer (TPEs) designed for use without valcanization. It has fully saturated mid-blocks for the ultimate in stability, which is high resistance to degradation by oxygen, ozone and UV light, and low color. However, it is the most difficult SBC to tackify. SEBS combines high elasticity and low temperature flexibility with resistance to water, acids, and alkalis. It also has a wide range of Shore hardness values depending on styrene content. In addition, SEBS is also the highest in tensile strength comparing to other TPEs.

Because of their better thermal stability, SEBS compounds are used for more demanding applications in all market segments. One key application is grips where the soft touch, anti slip properties, good resistance to oil and grease are needed. In addition, SEBS shows major properties including transparency and easy to color, soft touch, room temperature compression set, high tear strength and elasticity, excellent surface appearance, non slip, and low hardness (down to 5 Shore A).

2.3.4 Polymer as packaging films [26-29]

There are numerous packaging materials in food packaging applications including paper, fibre board, glass, tinplate, aluminium and various types of plastics. In this thesis, plastic films are focused.

Plastic films are high performance materials, which play an essential part in modern life. They are mostly used in packaging applications along with some applications in agricultural, medical and engineering fields. Plastic films are perfectly stable, easy to work with and can be lighter than tissue. However, they do not have voids in the surface that allow an ink or coating to penetrate into it. Many packages required transparency because people wanted to see what they were buying. Since then, many plastic films were added to the list of packaging films. Plastic films for packaging are available in the form of pouch, bags, film rolls, sheets, foils etc. Food packaging includes bags for bread and rolls, in-store bags for produce and bulk foods, candy wrap and bags, bag-in-a-box, carton liners for cereal and cake mixes, milk bags, grocery bags and wrappers for fresh food, prepared red meat, poultry and fish.

The main purpose of food packaging is to protect the food from microbial and chemical contamination, oxygen, water vapor and light. The type of packaging used therefore has an important role in determining the shelf life of food.

Packaging is described as "active" when it performs some roles in the preservation of the food other than providing an inert barrier to outside influences. It can control, and even react to, events taking place inside the package. Active packaging employs a packaging material that interacts with the internal gas environment to extend the shelf-life of food. The packaging material can either removing gases from or adds gases to the headspace of a package. Table 2.6 sets out some areas of atmosphere control in which active packaging is being successfully used.

Table 2.6 Use of active packaging **[30]**.

Active Packaging System	Application
Oxygen scavenging	Most food classes
Carbon dioxide production	Most food affected
Water vapor removal	Dried and mould-sensitive foods
Ethylene removal	Horticultural produce
Ethanol release	Baked foods (where permitted)

2.3.5 Required characteristics of plastic films for modified atmosphere packaging of fresh fruit products [31]

Modified atmosphere packaging (MAP) is a special class of active packaging. Gas composition in headspace of this type of package can be modified by active agent or displacement of mixed gas (active action) and balance produce's respiration and packaging film permeation (passive action)

The desirable characteristics of polymeric film for MAP depend on the respiration rate of the produce at the transit and storage temperature and on the MA condition, i.e., O_2 and CO_2 concentrations, for the packaged produce. For most produce, a suitable film must be much more permeable to CO_2 than O_2. The principles for selected of packaging material were illustrated.

1. Type of packaging
2. Gas/water vapor permeability
3. The physical properties, i.e., machinability, strength, clary, and durability
4. Sealing reliability
5. Printability
6. Resistant to chemical degradation
7. Nontoxic and chemically inert
8. Commercial suitability with economic feasibility

2.4 Zeolite

2.4.1 ZSM-5 [32-35]

ZSM-5 (also known as MFI) is an aluminosilicate zeolite with a high silicon and low alumininum content (high Si/Al ratio). It is composed of several pentasil units linked together by oxygen bridges to form pentasil chains as shown in Figure 2.10. A pentasil unit consists of eight five-membered rings. In these rings, the vertices are Al or Si and O is assumed to be bonded between the vertices. The structure of ZSM-5 is a channel framework that provided by 10 membered rings, as represented in Figure 2.11 (a). The pore structure is depicted schematically in Figured 2.11 (b); there are straight and elliptical pores in the cross section intersected by the horizontal pores in a zigzag pattern.

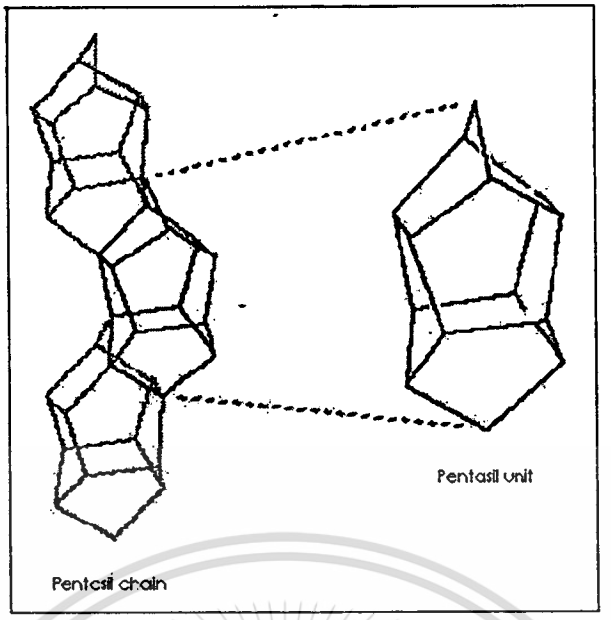

Figure 2.10 Pentasil unit and pentasil chain **[33]**.

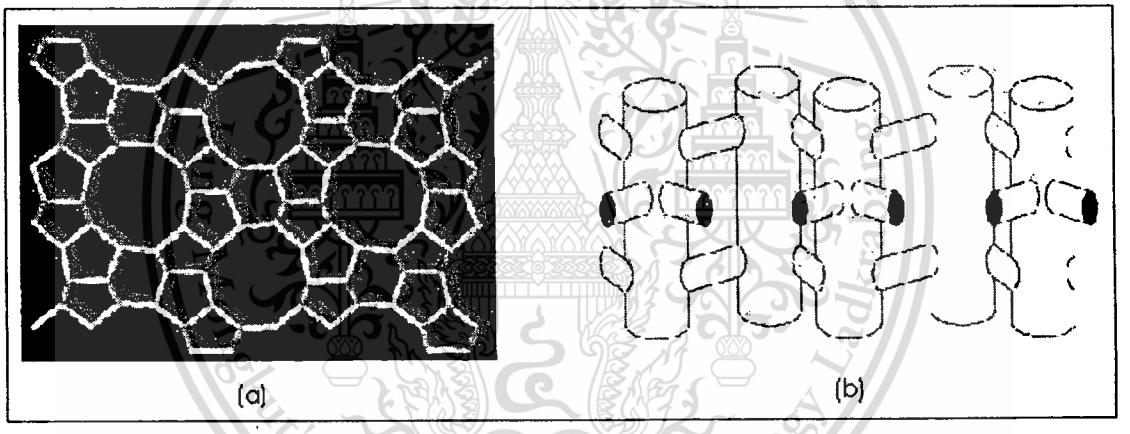

Figure 2.11 (a) Framework structure of ZSM-5 and (b) schematic diagram of the pore structure of ZSM-5 **[8-9]**.

ZSM-5 has an estimated pore size of the channel running parallel of 5.4 – 5.6 Å. This size is approximately in the dimensional range of aromatic molecules, so that ZSM-5 has a high shape-selectivity in catalytic reaction. In addition, its broad range SiO_2/Al_2O_3 (30-100) makes ZSM-5 useful for various applications.

2.4.2 Zeolite as adsorbent [32,36-37]

Zeolites are inorganic crystalline materials with uniform sized pores of molecular dimensions. Zeolite is well adsorbent. This is because it has high surface area. The pores of zeolite are precisely uniform in size and molecular dimensions. Therefore, porous structures can

be used to sieve molecules having certain kinetic diameter and smaller than those of the pore sizes. Depending on the size of these pores, molecules may be readily adsorbed, slowly adsorbed or completely excluded. The selectivity in sieving is also based on polarity of the zeolite and the sieved molecule; for instance, hydrocarbon is hydrophobic molecule that prefers hydrophobic zeolite (high Si/Al). Due to their unique characteristics, zeolites are commercially used for drying and purifying liquids and gases, and for various industrial separation processes, i.e., zeolite A (LTA) is very effective adsorbent and it can remove water from a moist gas with a very low partial pressure. Its adsorption capacity provides more than 35% of their weight in water. Other applications of zeolite adsorptions are shown in Table 2.7.

Table 2.7 Application of zeolite adsorption **[32]**.

Application	Zeolite
Removal of water from natural gas	NaA
Adsorption of water from organic solvent	KA
Adsorption of VOC from water	Silicalite
Separation of SO_x, NO_x from air	Silicalite
Separation of H_2S from nature gas	CaA
Separation of n-butane/i-butane	MFI

2.5 Literature reviews

Modifield atmosphere packaging (MAP) refers to the technique of sealing active respiring produces in polymeric films packaging, in which the O_2 and CO_2 levels within the package can be modified for extending shelf life of the fresh produces.

Ethylene can be removed by adsorption and decomposition. It was reported that potassium permanganate ($KMnO_4$) is commonly used to remove the ethylene in fresh fruit packaging. Ethylene decomposition capability of potassium permanganate is 950 μL of ethylene/7g $KMnO_4$.hr. However, $KMnO_4$ is toxic and has intense purple color **[38-39]**. It can contaminate fresh produces and hence affect to human health. In addition, 1-methylcyclopropene (1-MCP) was reported to treat sweet basil leave, 0.4 g/m^3 of 1-MCP can significantly decrease ethylene activity **[40]**.

In addition to adsorption and decomposition, gas permeability of films was also studied for removing ethylene. Ethylene and oxygen permeability of polyethylene films **[41]** (LDPE, LLDPE and HDPE) were investigated. It was reported that LDPE showed relatively higher ethylene (30.8 cm^3/m^2.day.atm) and oxygen (16.6 cm^3/m^2.day.atm) permeations as compared to LLDPE and HDPE. For the film with various thicknesses (50, 80 and 100 μm), thickness does not significantly affect both gas permeabilities. It was also reported that for LDPE, ethylene permeability is higher than oxygen permeability at high temperatures.

In addition to PE film, the ethylene permeability of wheat gluten film was studied as a function of relative humidity (RH) (from 0 to 100%) and temperature (from 3 to 45°C) **[42]**. The film exhibited ethylene permeability approximately 608 cm^3.mm/m^2.day.atm. At high temperature and relative humidity (25 °C and 75%RH), the wheat gluten film exhibited higher ethylene permeation. However, its ethylene permeability was not different from the reference LDPE in the same study.

To improve gas permeability perforated PE film was investigated. For example, effect of various perforated sizes of PE bags for packaging broccolis, spinaches, tomatoes and cucumbers were studied with different perforated sizes (1, 5 and 9 mm). It was reported that perforated size 1 mm served best for keeping fresh produces **[43]**.

Ethylene, oxygen and carbon dioxide permeabilities of SEBS 1652 were investigated **[12]**. It was reported that SEBS 1652 showed ethylene, oxygen and carbon dioxide permeabilities about 4200 cm^3.mm./m^2.day, 1000 cm^3.mm./m^2.day and 2500 cm^3.mm./m^2.day, respectively.

Alternatively, an inclusion of finely dispersed minerals such as zeolites or clays into packaging films can be used for the modified atmosphere packaging. For example, ethylene permeability of zeolite/LDPE and zeolite/SEBS composite film were studied **[12]**. It was reported that zeolite incorporated into LDPE and SEBS can increase ethylene permeation. ZSM-5 (280) with high Si/Al ratio incorporated into LDPE showed the higher ethylene permeability as compared to that with low Si/Al ZSM-5(50), Ferrierite, Beta and silicalite. Nevertheless, SEBS containing silicalite showed the highest ethylene permeability. However, adhesion between SEBS and silicalite particle is poor, resulting in interfacial void between SEBS and silicalite.

In the previous work **[5]**, ethylene permeability of ZSM-5 (280)/SEBS was higher than that of the ZSM-5 (280)/LDPE. However, SEBS is sticky. Thus, polyolefins were used as supporting for SEBS. Therefore, ethylene permeability of zeolite-SEBS/LDPE double-layered films was studied. It was reported that in the double-layered films with SEBS containing ZSM5 (280) (5 and 10%w/w), ethylene permeability of zeolite-SEBS/LDPE double-layered composite film cannot be clearly improved owing to the limited gas permeability of LDPE supporting layer. It was also reported that the ethylene permeability of film with well dispersed (WD) zeolite is higher than that of film with surface rich (SR). In addition, the incorporation of zeolite also decreased the carbon dioxide permeation. This is because carbon dioxide is relatively high polar and can be soluble in the polystyrene segment. The interaction between zeolite and polystyrene segment causes an increase in the chain rigidity. However, oxygen permeability was not readily affected by the incorporation of zeolite.

In addition to gas permeation study, tensile properties of SEBS/LDPE double-layered zeolite composite films were reported. It was found that the incorporated zeolite particles with various contents also acted as reinforcing filler leading to improve tensile properties of the film when loading was less than 10%w/w. In addition, when the zeolite content was higher than 10 %w/w the ultimate tensile strength was significantly dropped. It was also reported that in a view of zeolite dispersion, there was no significant difference of tensile properties between the double-layered films with surface rich and double-layered films with well dispersed films.

In this study the zeolite-SEBS composite/perforated polyolefins (LDPE and BOPP) double-layered films were fabricated for applications of modified atmosphere packaging. SEBS films were modified with zeolite 5% w/w and prepared via solution casting (50 μm thickness) and spin coating (30, 40 and 50 μm thicknesses). As received LDPE film (30 μm thickness) and BOPP

film (30 μm thickness) were used as supporting layers with various percentages of perforated areas (0-100%) and sizes (2, 3 and 5 mm).

CHARTER 3

Experimental details

3.1 Chemical and materials

1. Air Zero (Purity 99.9%, TIG Co., LTD.)
2. Distilled water
3. Ethylene (C_2H_4), (Purity 99.9%, TIG Co., LTD.)
4. Standard ethylene (C_2H_4), (Ethylene balance in Nitrogen 589 ppm, TIG Co., LTD.)
5. Ethanol (Commercial Grade)
6. Nitrogen gas (Purity 99.9%, TIG Co., LTD.)
7. Styrene ethylene-butylene styrene (SEBS 1652, KRATON)
8. Toluene (99.9%, Fisher Scientific)
9. Zeolite NH_4ZSM5 (280)(CBV28014, Zeolyst)
10. Low density polyethylene (LDPE, JJ4324,TPI Polene Public Co., LTD)
11. Biaxial oriented polypropylene (BOPP, A.J. Plast Public Co., LTD)

3.2 Apparatus

1. Laboratory glassware
2. Balance
3. Sand bath
4. Magnetic stirrer/hot plate with temperature controller system (RCT basic : IKA)
5. Sonicator
6. Glass mold
7. Glass plate
8. Casting blade
9. Vacuum oven
10. Micrometer
11. Laminator (LPD2313 : Fuji Lamipacker)
12. Compression machine (Labtech : LP 20)
13. Viscometer (CT-1000 : Cannon)
14. Scanning electron microscope (JEOL)
15. Thermogravimetric analyzer (Pyris 1 TG : Perkin Elmer)

16. Differential scanning calorimeter (DSC-50 : Shimadzu)
17. Perforation device
18. Universal testing machine (LR 5K : LLOYD Instrument)
19. Permeation cell
20. Permeation rig
21. Gas chromatograph with Flame Ionization Detector (FID) (CP-3800 : Varian)
22. Carbon dioxide permeability analyzer (CO_2-TRAN : Mocon)
23. Oxygen permeability analyzer (O_2-TRAN : Mocon)
24. Water vapor permeability analyzer (7000 : ILLINOIS Instrument)
25. Optical microscope (DINO)

3.3 Characterization of composite films

3.3.1 Determination of morphology using scanning electron microscope (SEM)

The morphology of zeolite-SEBS composite/perforated polyolefins (LDPE and BOPP) double-layered films were determined by scanning electron microscope (JEOL). The sample was cryogenic cracked and then placed onto the sample holder. Then it was coated with gold thin film by ion sputtering. The coated sample was placed in the sample chamber. Scanning electron micrographs were taken at the magnifications of 750x and 3500x.

3.3.2 Determination of perforated size using optical microscope (OM)

The perforation size of film was determined by optical microscope (DINO). The sample was prepared by carefully placing films onto the glass slide. Then it was covered by a cover glass. The sample was placed in the sample stage of optical microscope and was taken at the magnifications of 55x, 60x and 70x

3.3.3 Determination of zeolite content in SEBS by thermogravimetric analyzer (TGA)

The zeolite content was investigated by a Pyris 1 TG : Perkin Elmer thermogravimetric Analyzer. Approximately 10-20 mg of zeolite-SEBS film was placed in a platinum pan hanging from a microbalance and nitrogen was introduced as a carrier gas. The sample was heated under air zero (50 ml /min) from 50°C to 750°C at a heating rate of 10°C/min.

3.3.4 Determination of melting temperature (T_m), crystallization temperature (T_c) and % crystallinity using differential scanning calorimeter (DSC)

The T_m, T_c and %crytallinity of LDPE and BOPP films were determined by a DSC-50 : Shimadzu differential scanning calorimeter. Approximately 5-10 mg of sample was placed in aluminum pan. The sample was heated from 50°C to 200°C with a heating rate of 10°C/min in N_2 atmosphere.

3.4 Film preparation

3.4.1 SEBS film

The specification of SEBS is shown in Table 3.1. The neat SEBS film was prepared by a solution casting and spin coating techniques.

Table 3.1 Specification of SEBS1652 resin used in the experiment [44].

Property	Value
Styrene content, %w/w	29.0 to 30.8
MFI (230 °C, 5kg) g/10min	5
Specific gravity	0.91
Viscosity (Solution in toluene 20%w and at 25 °C) cP	400 to 525
Elongation at break %	500
Tensile strength, psi	4500
300% Modulus, psi	700
Hardness (Shore A, 10 s)	69

3.4.1.1 SEBS film by solution casting

Table 3.2 SEBS film by solution casting.

Formula	Concentration (%w/w)	SEBS (g)/ toluene (g)
SEBS (~ 50 μm thickness)	25	16.2 / 48.6

The neat SEBS films were prepared by dissolving 16.2 g of the SEBS in 48.6 g of toluene for 24 hr to obtain the polymer solution. The mixture was heated to approximately 80°C under stirring for 19 hr and then transferred into a sonicator for another 30 min. After that, the solution with temperature around 55°C was casted onto a glass plate using a casting blade and allowed to dry for a day. The film was then removed from the glass plate by immersing in ethanol. Finally, the film was dried in vacuum oven at 60°C until a constant weight was obtained. The films thickness was approximately 50 μm.

3.4.1.2 SEBS film by spin coating

Table 3.3 SEBS film by spin coating.

Formula	Speed (rpm)	Concentration (%w/w)	SEBS (g)/toluene (g)
SEBS (~ 30 μm thickness)	600	23	20 / 66.9
SEBS (~ 40 μm thickness)	600	25	20 / 60
SEBS (~ 50 μm thickness)	400	25	20 / 60

The SEBS films (30, 40 and 50 μm) were prepared by spin coating with controlled speeds as shown in the Table 3.3. The neat SEBS films were prepared by dissolving 20 g of the SEBS in 66.9 and 60 g of toluene for 24 hr to obtain the polymer solutions with different concentrations, i.e., 23 %w/w and 25 %w/w, respectively. The mixtures was heated to approximately 80°C under stirring for 19 hr and then transferred into a sonicator for another 30 min. After that, the solution with temperature around 55°C was spin coated on a spinning glass plate as suffuse control speeds. They were allowed to dry for a day. The film was then removed from the spinning glass plate by immersing in ethanol. Finally, the film was dried in vacuum oven at 60°C until a constant weight was obtained.

3.4.2 Zeolite-SEBS film

In this work, commercial ZSM-5 with a specification shown in Table 3.4 was used without further modification.

Table 3.4 Specification of zeolite ZSM-5 [45].

Property	Data
SiO_2/Al_2O_3 mole ratio	280
Nominal cation form	Ammonium
Na_2O weight %	0.05
Surface area m^2/g	400
Specific gravity	> 1
Pore size Å	5.5

3.4.2.1 Zeolite-SEBS composite film by solution casting

The zeolite/SEBS film was prepared as composition shown in Table 3.5

Table 3.5 Zeolite-SEBS film by solution casting.

Formula	SEBS (g)	ZSM-5 (280) (g)	Total toluene (mL)
5%ZSM-5	15.39	0.81	48.6

The zeolite-SEBS film was prepared by dissolving 15.39 g of the SEBS1652 in 38.6 g of toluene in a 250 flask for 24 hr. The mixture was heated to approximately 80°C under stirring for 16 hr. In another flask, 0.81 g of ZSM-5 in 10 g of toluene was sonicated for 30 min. The polymer solution was added into the stirring mixture of zeolite and toluene at 80°C. The mixture was continuously stirred for 3 hr. After that, the mixture was sonicated for 30 min at 50 °C. The mixture was casted on a glass plate using a casting blade and allowed to dry for 24 hr. The film was removed from the glass plate while the glass plate was soaking in ethanol. The film was allowed to dry for a day. Finally, the zeolite-SEBS composite film was dried in a vacuum oven at 60°C for another 24 hr.

3.4.2.2 Zeolite-SEBS composite film by spin coating

Table 3.6 Zeolite-SEBS film by spin coating.

Formula	Speed (rpm)	ZSM-5 (280) (g)/ toluene (g)	SEBS (g)/ toluene (g)	Solution (%w/w)
SEBS (~ 30 μm thickness)	600	1/5	19/64.9	23
SEBS (~ 40 μm thickness)	600	1/5	19/55	25
SEBS (~ 50 μm thickness)	400	1/5	19/55	25

The SEBS films (30, 40 and 50 μm) were prepared by spin coating with controlled speeds as shown in the Table 3.6. The zeolite-SEBS films were prepared by dissolving 19 g of the SEBS1652 in 64.9 and 55 g of toluene in 250 flasks for 24 hr to obtain the polymer solutions. The mixtures were heated to approximately 60°C under stirring for 16 hr. In a separated flask, 1 g of ZSM-5 in 5 g of toluene was sonicated for 30 min. While, zeolite was vigorously stirred in toluene at 60°C, the polymer solution was added into the stirring mixture and continued stirring for 30 min. After that, the mixture was transferred into a sonicator for another 30 min. The mixture was poured into a spinning glass plate as suffuse control speeds. It was allowed to dry for 24 hr. The film was removed from the glass plate while the mold was immersed in ethanol. Finally, the zeolite-SEBS film was dried in a vacuum oven at 60°C for another 24 hr.

3.4.3 LDPE and BOPP films

LDPE (JJ4324,TPI Polene Public Co., LTD) and BOPP (BOPP, A.J. Plast Public Co., LTD) films with approximately 30 μm thickness as received from MTEC. The LDPE and BOPP specifications are described in Table 3.7

Table 3.7 Specification of supporting layers (LDPE and BOPP films) **[15,46].**

Properties	LDPE	BOPP
Density (g/cm^3)	0.922	0.910
Tensile Strength (N/mm^2)	>11.0	>130
Tensile Strength (Yield point) (N/mm^2)	>11.0	>22
Tensile Elongation (at Break) (%)	>600	>60
Impact Resistance (J/m^2)	>160	-

3.4.4 Perforated supporting films

The supporting layer, i.e., LDPE or BOPP, was immersed in liquid nitrogen for 5 min and then perforated by puncher. The percentage of perforated areas was varied as shown in the Table 3.8 and various perforated sizes were shown in Table 3.9

Table 3.8 Percentage of perforated areas.

sample	Percentage of perforated areas
1	0.00
2	2.25
3	6.25
4	12.25
5	20.25
6	30.25
7	42.25
8	64.00
9	90.25

*The percentage of perforated areas was calculated by comparing perforated size with diameter of membrane cell (20 mm).

Table 3.9 Perforated size of perforation.

Film	Perforated size (mm)
LDPE or BOPP	2
	3
	5

3.4.5 Double-layered films

The double-layered films containing supporting layer (LDPE or BOPP with thickness of 30 μm) and SEBS film (or zeolite-SEBS composite film with thickness of 30, 40 and 50 μm) were fabricated. A gloss coated paper was used for supporting SEBS film (or zeolite-SEBS composite film) and a photo paper (back side) used for supporting layer side. Then they were adjoined by running through the laminator as shown in Figure 3.1 Finally, the adjoined film was compressed by hot compression with the condition as shown in Table 3.10

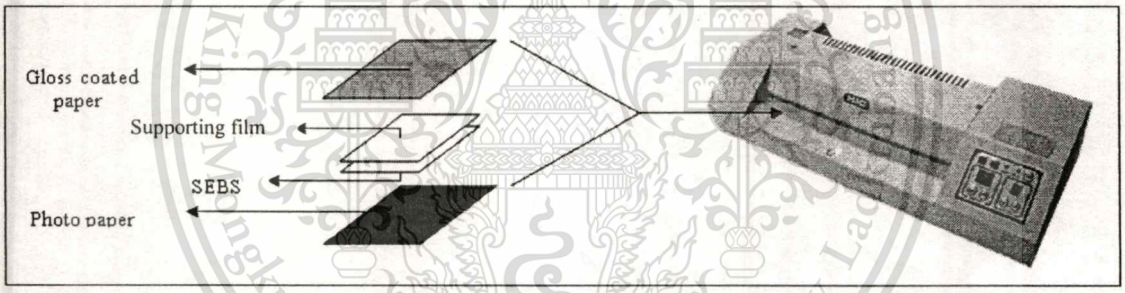

Figure 3.1 Schematic of film layers in an adjoining step.

Table 3.10 Hot press conditions.

Factor	Type of films	
	LDPE	BOPP
Temperature of hot pressing (°C)	100	145
Pressure of hot pressing (psi)	1800	1800
Time of hot pressing (min)	12	12
Temperature of cold pressing (°C)	6	6
Pressure of cold pressing (psi)	1800	1800
Time of cold pressing (min)	6	6

3.5 Permeation test

3.5.1 Ethylene permeability of film using homemade permeation cell equipped with FID gas chromatograph

The film was fixed between two metal o-rings with an inside diameter of 20 mm using epoxy adhesive. The component is called a membrane cell, as shown in Figure 3.2.

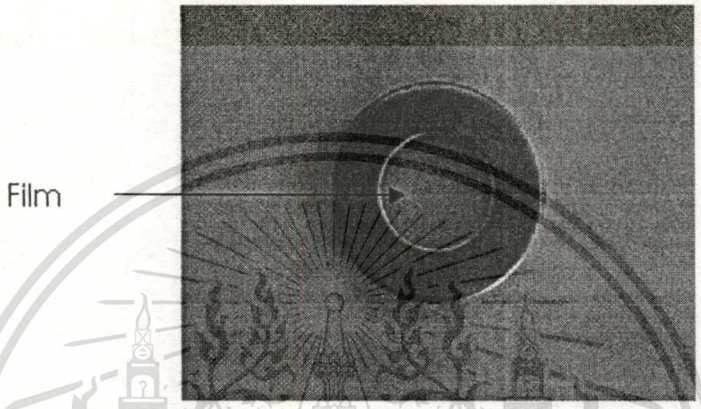

Figure 3.2 Membrane cell : the film was fixed with the metal ring center.

The membrane cell was assembled with 4-ways Pyrex glass tube using Viton o-ring. The component is called the permeation cell, as shown in Figure 3.3. The schematic diagram of permeation test is shown in Figure 3.4.

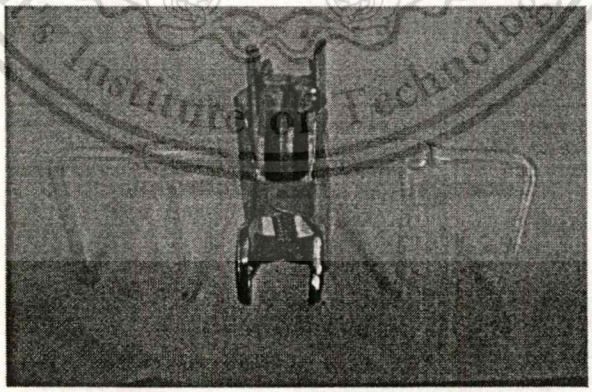

Figure 3.3 Permeation cell.

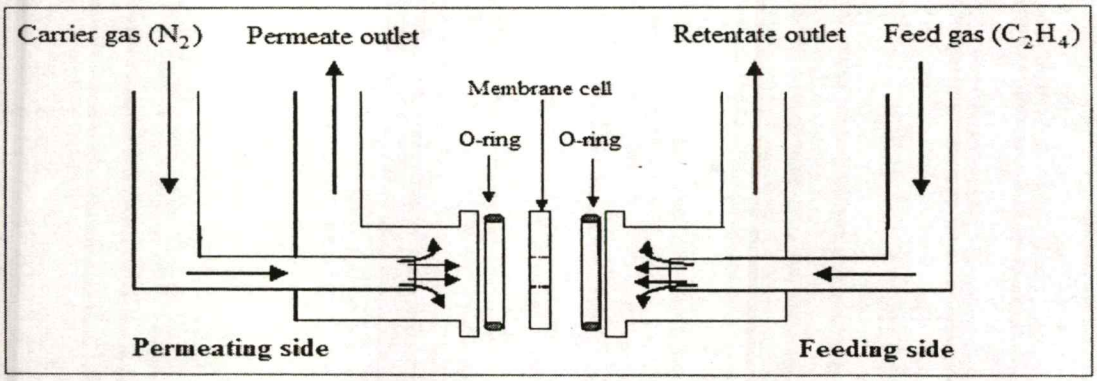

Figure 3.4 Diagram of the permeation test.

The feed gas (ethylene or diluted ethylene) as compositions shown in Table 3.11 and carrier gas (nitrogen) at a flow rate of 30 ml/min were connected to the feeding and the permeating sides, respectively.

Table 3.11 Composition of the feed gas.

Ethylene concentration (%v/v)	**Feed gas**	
	C_2H_4 flow rate (ml/min)	**N_2, CO_2, or Air zero** flow rate (ml/min)
20	6	24
40	12	18
60	18	12
80	24	6
100	30	-

The flow rate of the feed gas and the carrier gas were controlled by mass flow controllers. As the feed gas flows across the film surface, some of the gas can diffuse through the film to the permeating side. The permeated gas was swept by a carrier gas into the permeate outlet. On the other hand, some of the gas that cannot diffuse through the film was flowed to retentate outlet. The permeate outlet was connected to the sampling valve of gas chromatograph while the retentate outlet was connected to a needle valve and finally, to the vent. The gas flow system for ethylene permeation unit is illustrated in Figure 3.5.

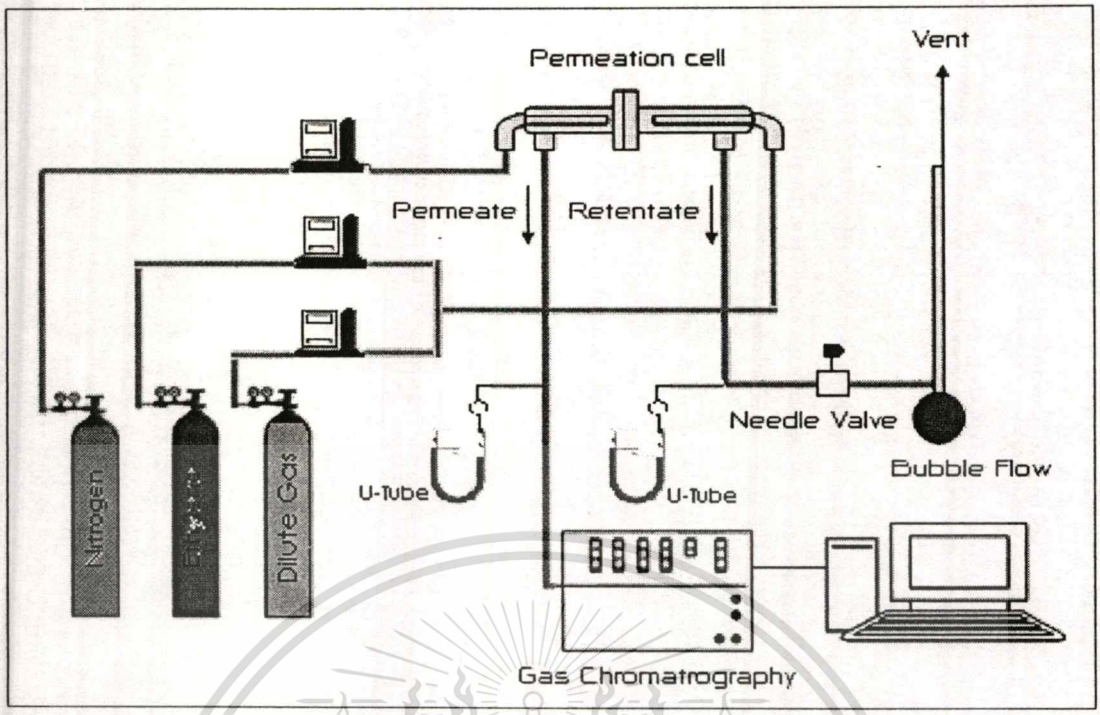

Figure 3.5 Diagram of the ethylene permeation unit.

The U-tube glass contained distillation water was connected to both retentate and permeate outlets for measuring the pressure drop. The pressure drop in retentate outlet was adjusted by a needle valve to balance with that of the permeate outlet. During pressure drop adjustment, a dense membrane (aluminum foils) was preliminary used instead of the film in the permeation cell.

For ethylene permeation testing, the dense membrane was replaced by the tested film. The permeate compositions were analyzed by gas chromatograph (Varian model 3800) with Porapak Q column. The injection port, the column oven, and FID detector were set to 200, 150, 200 ^{o}C, respectively. The permeate gas was periodic analyzed by FID detector every 10 min in order to determine permeability at the steady state.

3.5.2 Oxygen permeation of film using oxygen permeability analyzer

The oxygen permeation of film was investigated by oxygen permeability analyzer (Mocon Oxtran Model 2/21). Approximate 5×5 cm of sample was cut by cutting template. Then the sample was placed into cell. The oxygen permeation of every double-layered films was measured using atmosphere pressure at 23ºC. The oxygen was diluted by nitrogen gas as a carrier gas.

3.5.3 Carbon dioxide permeation of film using carbon dioxide permeability analyzer

The carbon dioxide permeation of film was investigated by carbon dioxide permeability analyzer (Mocon Permeation Model 4/41). Approximate 5×5 cm of sample was cut by cutting template. Then the sample was placed into cell. The carbon dioxide permeation of every double-layered films was measured using atmosphere pressure at 23°C. The carbon dioxide was diluted by nitrogen gas as a carrier gas.

3.5.4 Water vapor permeation of film using water permeability analyzer

The water vapor permeation of film was investigated by water vapor permeability analyzer (Water Vapor Transmission 7000 series, ILLINOIS Instrument). Approximate 25 cm^2 of sample was placed into cell. The water vapor permeation of every double-layered films was measured using atmosphere pressure at 28°C and relative humidity of 90%.

3.6 Peeling property testing

Peeling properties of the films were determined by a universal testing machine. The T-shape specimen of peeling test is illustrated in Figure 3.6. The film specimens were cut into a size of 10x80 mm and the peeling testing conditions are shown in Table 3.12

Table 3.12 Peeling test conditions.

Lists	Films	
	DB_BOPP	5Z_DB_BOPP
Load cell	100 N	100N
Test speed	100 mm/min	100 mm/min

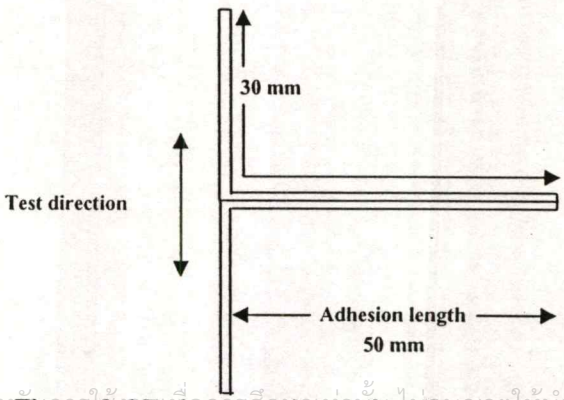

Figure 3.6 T-shape specimen of peeling test.

3.7 Tensile property testing

Tensile properties of the films were determined by a universal testing machine. The tensile properties including stress at yield and Young's modulus were measured according to ASTM D882 **[47].** The film specimens were cut into a size of 10x80 mm (Figure 3.7) and the tensile testing conditions are shown in Table 3.13

Table 3.13 Tensile test conditions.

Lists	Films (or supporting layer)	
	LDPE	BOPP
Load cell	100 N	5 KN
Test speed	100 mm/min	100 mm/min
Gauge length	25 mm	25 mm

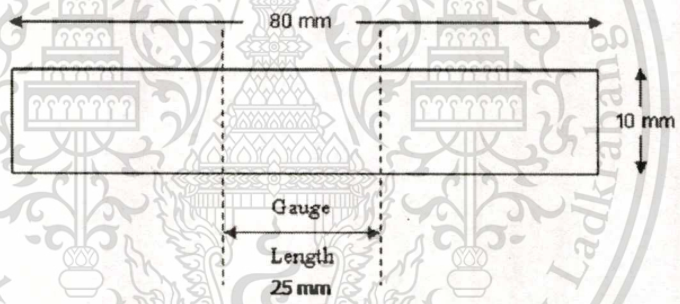

Figure 3.7 Size and shape of tensile test specimen.

Stress at yield and Young's modulus can be calculated from the following equations.

Stress at yield = F_y / A (3.1)

Young's modulus = Stress / Strain (3.2)

Where F_y = Force at yield point (N)

A = Initial cross-section area (mm^2)

Note Young's modulus can be calculated from the slope of stress-strain curve at 2% and 4% elongations.

CHAPTER 4

RESULTS AND DISCUSSION

4.1 Characterization of the films

4.1.1 Thickness of single-layered and double-layered films

Thickness of the single-layered LDPE, BOPP, SEBS, zeolite-SEBS composite films and the double-layered films between SEBS (or zeolite-SEBS composite) and LDPE or BOPP films are shown in Table 4.1

Table 4.1 Thickness of the single-layered and double-layered films.

Sample	Composition	Thickness (μm)
LDPE (30)[a]	95%w/w LDPE + 5%w/w Anti-blocking agent	33±3
BOPP (30)[b]	100%w/w BOPP	33±2
SEBS (50)[c]	100%w/w SEBS	53±3
SEBS (30)[d]	100%w/w SEBS	32 ± 1
SEBS (40)[d]	100%w/w SEBS	42 ± 1
SEBS (50)[d]	100%w/w SEBS	52 ±1
5Z_SE (30)[d]	95 %w/w SEBS + 5%w/w ZSM-5	32±2
5Z_SE (40)[d]	95 %w/w SEBS + 5%w/w ZSM-5	40±1
5Z_SE (50)[d]	95 %w/w SEBS + 5%w/w ZSM-5	53±1
DB_LD[c]	SEBS 50 μm + LDPE 40% perforated area	83±4
DB_LD[d]	SEBS 30 μm + LDPE 40% perforated area	66±1
	SEBS 40 μm + LDPE 40% perforated area	75±1
	SEBS 50 μm + LDPE 40% perforated area	86±4
5Z_DB_LD[d]	5%w/w ZSM-5 + SEBS 30 μm + LDPE 40% perforated area	61±2
	5%w/w ZSM-5 + SEBS 40 μm + LDPE 40% perforated area	72±1
	5%w/w ZSM-5 + SEBS 50 μm + LDPE 40% perforated area	84±2

Table 4.1 Thickness of the single-layered and double-layered films (continued).

Sample	Composition	Thickness (μm)
DB_BOPP [d]	SEBS 30 μm + BOPP 40% perforated area	63±1
	SEBS 40 μm + BOPP 40% perforated area	72±1
	SEBS 50 μm + BOPP 40% perforated area	84±2
5Z_DB_BOPP [d]	5%w/w ZSM-5 + SEBS 30 μm + BOPP 40% perforated area	63±1
	5%w/w ZSM-5 + SEBS 40 μm + BOPP 40% perforated area	69±3
	5%w/w ZSM-5 + SEBS 50 μm + BOPP 40% perforated area	82±1

[a] From blown film process

[b] From stenter process

[c] SEBS from a blade solution casting technique

[d] SEBS from spin-coating process technique

The thickness of the supporting layer (either LDPE or BOPP) is ~ 30 μm. The film thickness of the double-layered films prepared from ~ 30, 40 and 50 μm SEBS layers are approximately ~ 60, 70 and 80 μm, respectively (Table 4.1). This suggests that the temperature and pressure used for compression process allow only adhesion between a supporting layer (LDPE or BOPP) and a SEBS layer without significant change in the thickness of the laminated layers.

4.1.2 Morphology

4.1.2.1 Dispersion of zeolite in the SEBS layer

Zeolite dispersion in SEBS can be observed from scanning electron microscope in three measurement zones, as schemed in Figure 4.1. It can be seen that the zeolite particles (5%w/w loading) were well dispersed in the SEBS layer, as shown in Figures 4.2 and 4.3. This is because the highly viscous media (23%w/w for spin coating or 25%w/w for solution casting) can suspend the zeolite particles during evaporation.

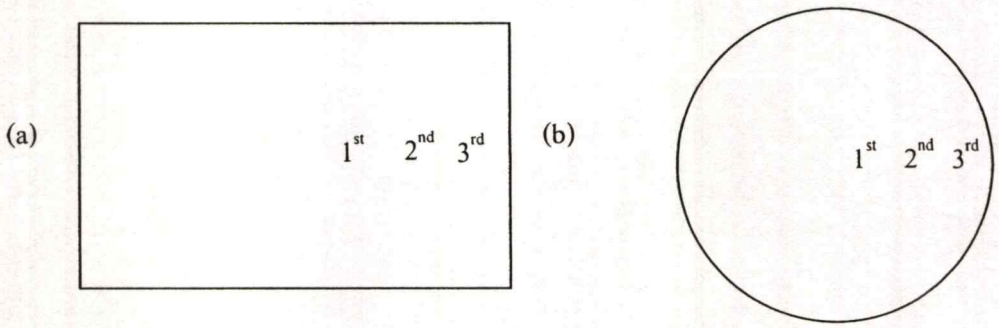

Figure 4.1 Schematic representation of surface measurement zone :
(a) solution casting technique and (b) spin coating technique.

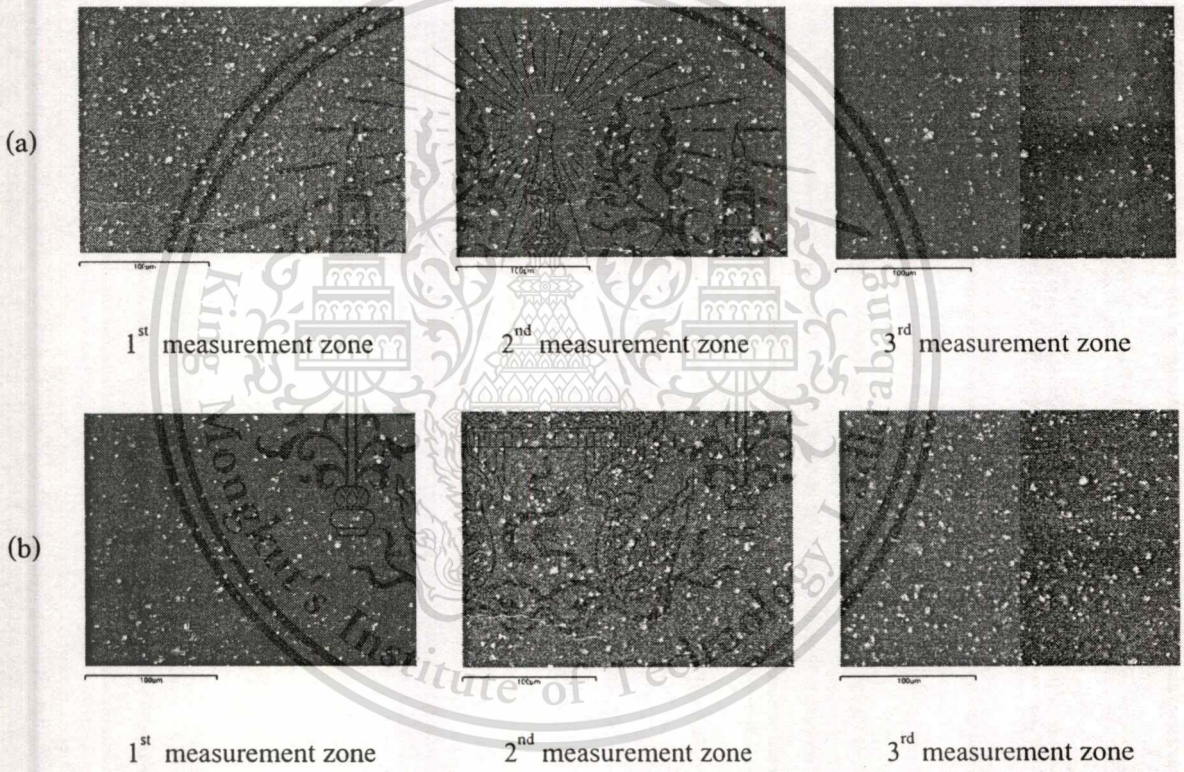

Figure 4.2 SEM micrograph (750x) of zeolite incorporated in SEBS film :
(a) SEBS by solution casting (25%w/w) and (b) SEBS by spin coating (23%w/w).

The cross-section of the double-layered films were also observed from scanning electron microscope, as shown in Figure 4.3. It can be seen that the adhesion between SEBS and zeolite particle is particularly good because no interfacial void between SEBS and zeolite can be observed.

(a) 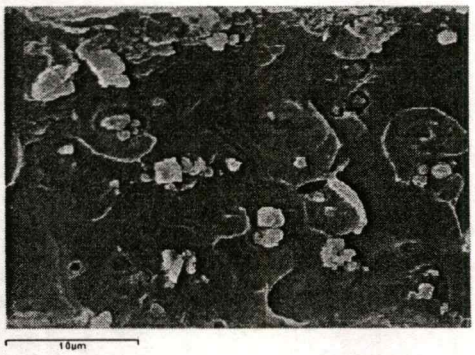 (b) 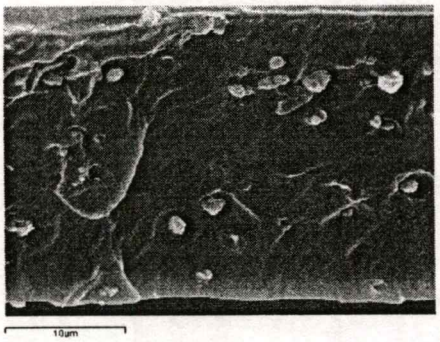

Figure 4.3 SEM micrograph (3500x) of zeolite incorporated SEBS (5Z_SEBS) :
(a) SEBS by solution casting (25%w/w) and (b) SEBS by spin-coating (23%w/w).

4.1.2.2 Perforated size

The perforated size of the supporting layers in the double-layered films was determined from optical micrograph as shown in Appendix F. It can be seen from Table 4.2 that the perforated size of the double-layered LDPE (DB_LD) and double-layered BOPP (DB_BOPP) are relatively similar to that of the parent LDPE and BOPP films, respectively. Thus, it is suggested that the fabrication process does not markedly modify perforated size of the supporting layers.

Table 4.2 Perforated size of single-layered and double-layered films.

Type / Size (mm)	LDPE		BOPP	
	Single-layered	**Double-layered**	**Single-layered**	**Double-layered**
2	2.0±0.1	2.0±0.1	2.0±0.1	2.0±0.1
3	3.5±0.1	3.4±0.1	3.5±0.1	3.5±0.1
5	5.5±0.1	5.5±0.1	5.5±0.1	5.5±0.1

* Average perforated sizes are calculated from 10 samples.

4.1.2.3 Adhesion of the double-layered films

The interphase between the two layers at the perforated areas was observed from scanning electron microscope, as shown in Figure 4.4.

It can be seen that the interphase at the perforated boundary of DB_LD is better than that of DB_BOPP. This is suggested that SEBS is highly amorphous with glass transition temperature approximately -55°C for ethylene-butylene block and 90°C for styrene block. In addition, LDPE

is semicrystalline with glass transition temperature approximately -120 ºC and melting temperature approximately 110ºC. BOPP is also semicrystalline with glass transition temperature approximately -20 ºC and melting temperature approximately 160ºC. When the double-layered films (SEBS and supporting layers) were fabricated at 100 ºC for LDPE and 145 ºC for BOPP using hot press process, These temperatures are higher than the glass transition temperatures of SEBS and supporting layers (LDPE and BOPP). Hence, the polymer chain can readily relax and the SEBS can fill up the perforated areas of the supporting layers, as schemed in Figure 4.5. In addition, the relaxation of the polymer chains can induce interdiffusion of amorphous phase between SEBS and supporting layers. Moreover, amorphous phase of LDPE is higher than that of BOPP. Therefore, the interdiffusion between SEBS and LDPE is higher than that of SEBS and BOPP. Adhesion between SEBS and LDPE is better than that SEBS and BOPP, see in Figure 4.4 (a) and (b).

In addition, zeolite (5%w/w) was incorporated in SEBS layer. It can be seen that the interphases at the perforated boundary of 5Z_DB_LD and 5Z_DB_BOPP are better than those of the DB_LD and DB_BOPP without zeolite. This suggests that with fabrication process under the pressure, zeolite in SEBS may lead to induce interlocking between SEBS and supporting layers, particularly in the case of 5Z_DB_BOPP.

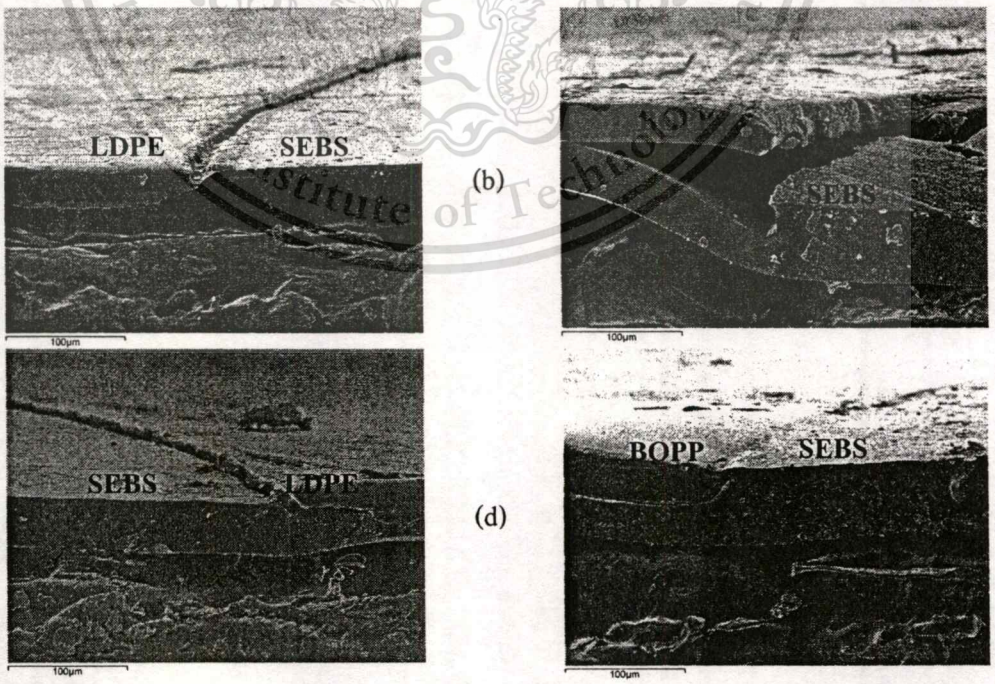

Figure 4.4 SEM micrograph (350X) at interphase btween SEBS and LDPE or BOPP films : (a) DB_LD, (b) DB_BOPP, (c) 5Z_DB_LD and (d) 5Z_DB_BOPP.

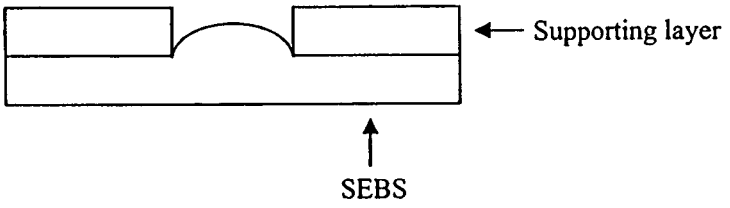

Figure 4.5 Schematic representation of SEBS filling up in perforated area supporting layer.

4.1.3 Zeolite content in SEBS layer

Zeolite content in SEBS layer (Table 4.3) was calculated from the weight of as remained after 700 °C in TGA (Appendix D).

Table 4.3 Zeolite content in SEBS layer.

SEBS preparation technique	Zeolite loading (%w/w)	Zeolite content at different positions (%w/w) (as Figure 4.1)		
		1st measurement zone	2nd measurement zone	3rd measurement zone
solution casting	5	4.8	4.8	4.8
spin coating	5	4.5	4.6	4.7

From Table 4.3, it can be seen that the zeolite content in three measurement zones are not significantly different. This confirms that zeolite is well dispersed in the SEBS film. The %weight of zeolite in SEBS was slightly lower than the target values (5%w/w). This is because zeolite might be lost during the preparation process. In addition, the weight percentage of zeolite in the films obtained from spin coating is lower than that from the solution casting. This is because zeolite in the films may be carried away by centrifugal force during the spin coating.

4.1.4 Thermal properties of the films

Since the film crystallinity can readily affect to gas permeability, supporting layer film (LDPE or BOPP ~30μm) and double-layered films were analyzed by differential scanning calorimetry (DSC). Melting (T_m) and crystallization (T_c) temperatures and %crystallinity of the films are shown in Table 4.4. Calculation of the % crystallinity and DSC thermograms are shown in Appendices C and E, respectively.

Table 4.4 T_m, T_c and % crystallinity of the parent films (LDPE and BOPP) and double-layered films.

Film	T_m (°C)		T_c (°C)	% Crystallinity
	Onset	Peak		
LDPE (30)	99	106	97	23
BOPP (30)	152	157	114	75
DB_LD	93	101	97	26
DB_BOPP	156	159	113	74
5Z_DB_LD	93	104	97	28
5Z_DB_BOPP	161	166	115	74

As, the SEBS is highly amorphous [22], it is suggested that the observed crystallinity of the double-layered films is contributed only from the supporting layer (LDPE or BOPP). It can be seen that the % crystallinity and melting temperature of the double-layered films are relatively similar to those of the parent film (LDPE or BOPP), as shown in Table 4.4.

4.1.5 Peeling property

Zeolite ZSM-5 (280) is hydrophobic and readily compatible with the SEBS matrix. Together with the small ZSM-5 particle size (approximate 1-2 μm), a strong interfacial interaction and hence good adhesion between the zeolite filler and the polymer matrix can be obtained. Zeolite loading in SEBS can induce high roughness of the SEBS. Generally, roughness can readily affect the adhesion between two layers. From Figure 4.4 the interphase at the perforated boundary of double-layered film with zeolite loading seems to be better than that of the double-layered film without zeolite loading, particularly for DB_BOPP. This is assumed that zeolite can induce interlocking between SEBS and BOPP, as mentioned in section 4.1.2.3. In order to prove this assumption, the peel testing of the DB_BOPP and 5Z_DB_BOPP films were performed and illustrated in Figure 4.6.

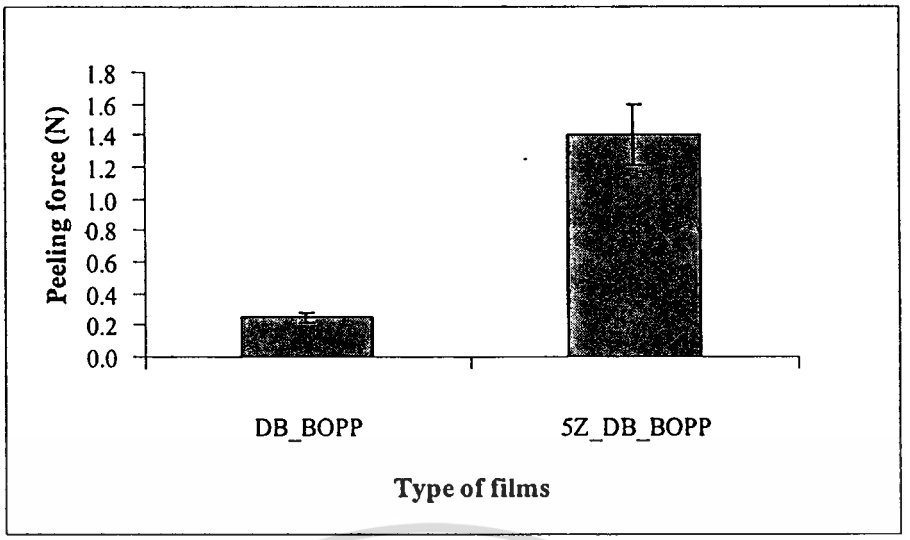

Figure 4.6 Peeling property of double-layered films with and without zeolite.

From Figure 4.6, it was found that 5Z_DB_BOPP film requires higher peeling force than DB_BOPP film. This suggests that the adhesion at the interphase at the perforated boundary of 5Z_DB_BOPP is better than that of the DB_BOPP film. This is due to the interlocking between BOPP and SEBS with the presence of zeolite ZSM-5.

4.1.6 Tensile properties

4.1.6.1 Tensile properties of the parent films

The tensile properties of the parent films; LDPE(30), BOPP(30) and SEBS(30) are shown in Figure 4.7. The LDPE and BOPP were tested on tensile properties for both transverse (TD) and machine (MD) directions. This is because the orientation of polymer chain can be induced depending on manufacturing processes. In the case of SEBS, isotropic properties of the films were obtained since the film was prepared from solution casting.

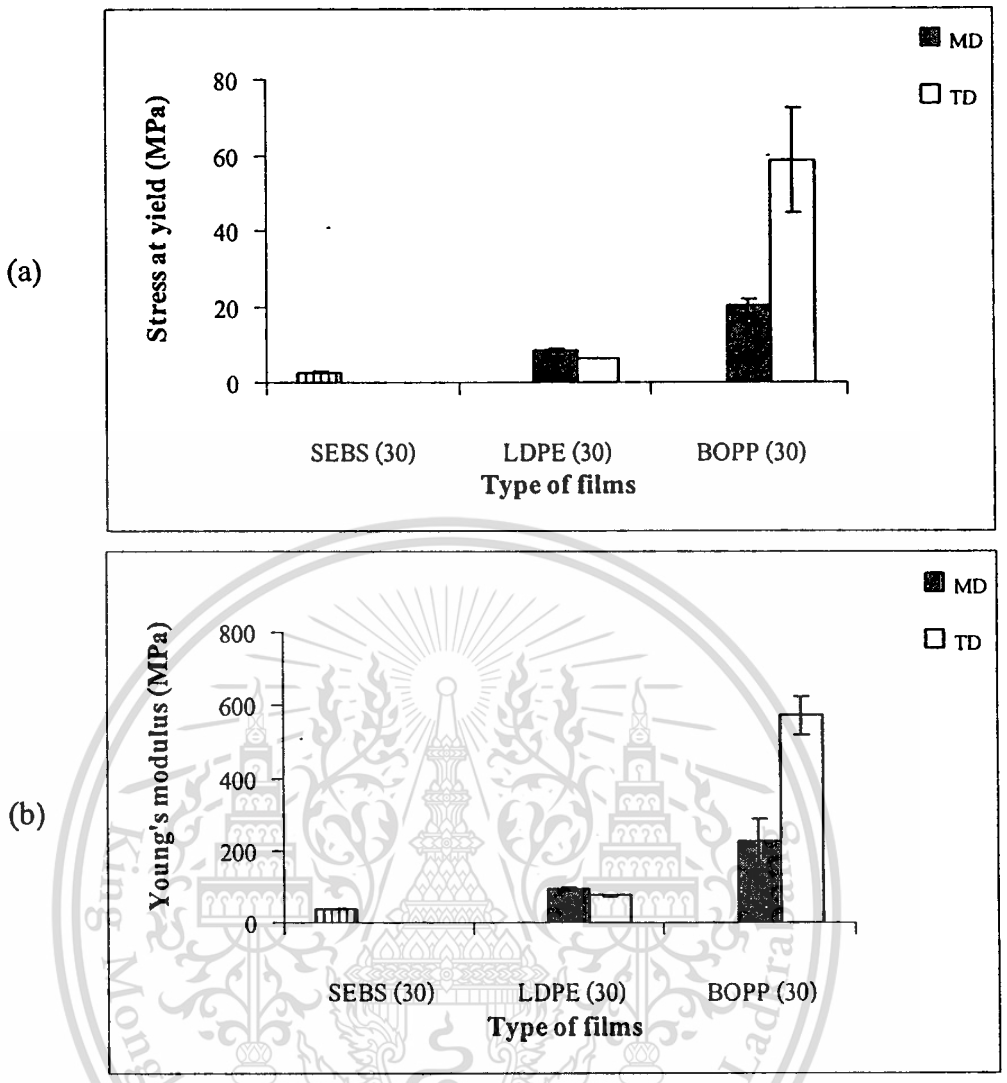

Figure 4.7 Tensile properties of the parent films : (a) stress at yield and (b) Young's modulus.

From Figure 4.7 (a), it is observed that SEBS can be easily deformed as shown by a low stress at yield when compared with LDPE and BOPP films. This is because the folded chains of the crystalline region in LDPE or BOPP require higher stress for deformation at the yield point. In opposite, there is only physical entanglement of polymer chains in SEBS which requires lower stress for the chain deformation. In addition, it can be seen that Young's modulus of SEBS is the lowest among the three polymers. This is because thermoplastic elastomer SEBS (Kraton® G1652) contains 70%w/w of ethylene-butylene units, providing softness and flexibility in its nature. Morover, SEBS film is highly sticky. It is difficult to fabricate and handle. SEBS film alone is not suitable for packaging application, although it can provide high ethylene transmission rate **[5,12]**.

More rigid structure of the BOPP provides higher tensile propereties as compared with LDPE. It was also found that the tensile properties of LDPE film in the MD are higher than those in the TD. This implies that a high draw ratio used in the blown film process of LDPE induced greater molecular orientation in the MD. In the case of BOPP film, the opposite results were observed; the tensile properties in the TD are higher than those in the MD. This suggests that the stenter process for BOPP film production induces greater orientation in the TD, as compared to the MD. Consequently, for further investigation on tensile properties of the double-layered films, only the DB_LD films in the MD and the DB_BOPP films in the TD were examined.

4.1.6.2 Effects of perforated area on tensile properties

In the previous work [5], LDPE as a supporting of DB_LD possessed a better tensile properties as compared to that of the SEBS single layer film. In addition, it can be easily handle and hence suitable for packaging application. Moreover, the ethylene permeability of the DB_LD film is higher than that of the LDPE film, but lower than that of the SEBS film this is because the crystalline phase of the LDPE acts as barrier for ethylene permeation. To overcome this problem, DB_LD can be improved ethylene permeation by perforating on LDPE supporting layer film. In order to study effect of perforated area on tensile properties of the DB_LD, tensile properties of double-layered films with various perforated areas (0-100%) were tested and illustrated in Figure 4.8.

(a)

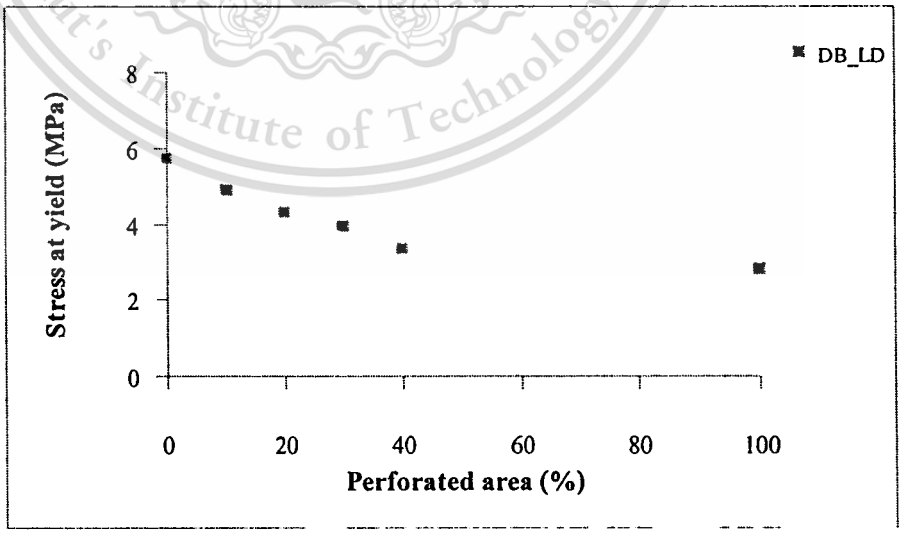

(b)

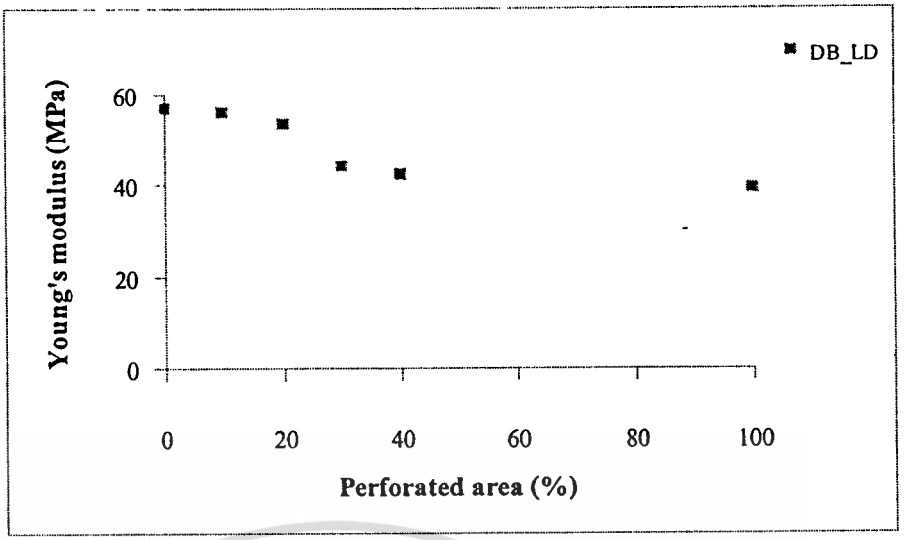

Figure 4.8 Tensile properties of the film with various perforated areas : (a) stress at yield and (b) Young's modulus.

From Figure 4.8, the tensile properties of DB_LD films (with perforated size of 2 mm) are decreased with increasing the perforated areas. This is because the continuous phase of LDPE providing the film strength is decreased. The tensile properties (stress at yield and Young's modulus) of the perforated films at higher than 40% perforated areas is immeasurable as the supporting layer was torn away at the initial load. Therefore, the film cannot be used for packaging. It is clearly seen that the tensile properties of the DB_LD film at 40% perforated areas are adequately higher than those of the SEBS film (as represented by 100% perforated area). Hence, the 40% perforated area of the supporting layer was selected for further study

4.1.6.3 Effects of perforated size on tensile properties

Tensile properties of DB_LD and DB_BOPP films with various perforated sizes (2, 3 and 5 mm) at the 40% perforated area were tested as shown in Figure 4.9.

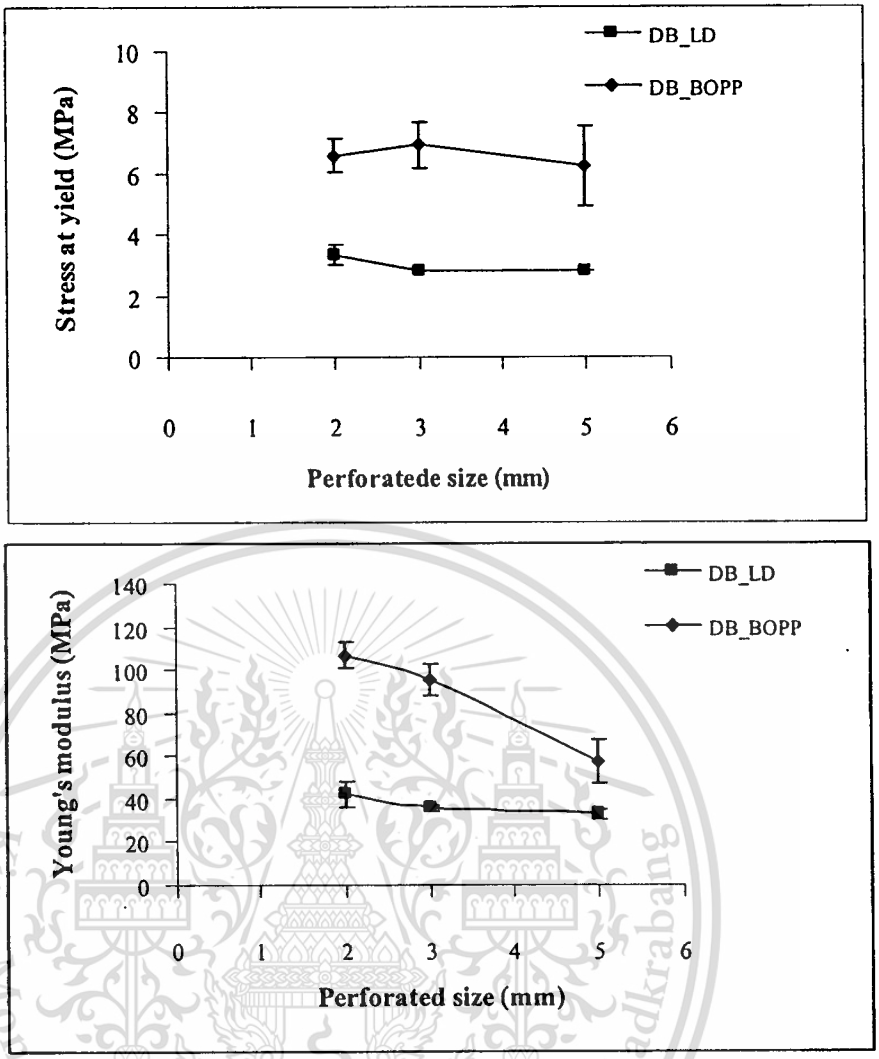

Figure 4.9 Tensile properties of the double-layered films with various perforated sizes : (a) stress at yield and (b) Young's modulus.

From Figure 4.9, it is observed that the tensile properties (stress at yield and Young's modulus) of the DB_BOPP film is higher than that of the DB_LD film. This is because the tensile properties of the parent BOPP are much higher than those of parent LDPE as mentioned earlier in section 4.1.6.1.

It was found that the DB_BOPP films with various perforated sizes have similar stress at yield. This is because the all DB_BOPP samples were perforated with the same perforated area (40%). However, Young's modulus of DB_BOPP is decreased with an increase in the perforated size. The observed tensile properties of DB_BOPP are contributed from BOPP layer rather than that from the SEBS layer. Accordingly, the plastic deformation is increased with increased

perforated size, particularly at perforated boundary of film, leading to the lower Young's modulus.

In the case of DB_LD, the perforated size does not alter the tensile properties of double-layered films. This is because the tensile properties of DB_LD are contributed from both layers due to similar flexible nature of both LDPE and SEBS. To maintain high tensile properties, perforated size of 2 mm was selected for further study on the effect of SEBS thickness.

4.1.6.4 Effects of SEBS thickness

Since the thickness of SEBS films and the incorporated zeolite can affect the tensile properties, tensile properties of DB_LD and DB_BOPP films (40% perforated area and 2 mm perforated size) with and without zeolite were examined as shown in Figure 4.10.

(a)

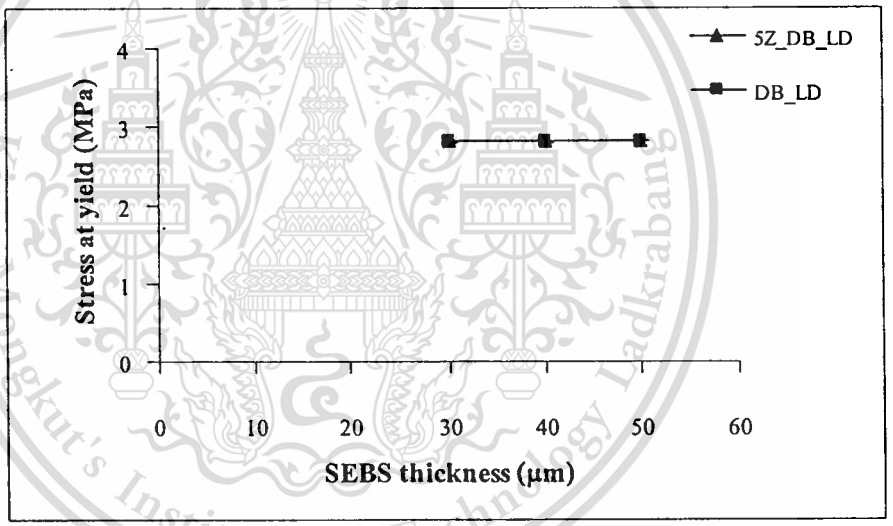

(b)

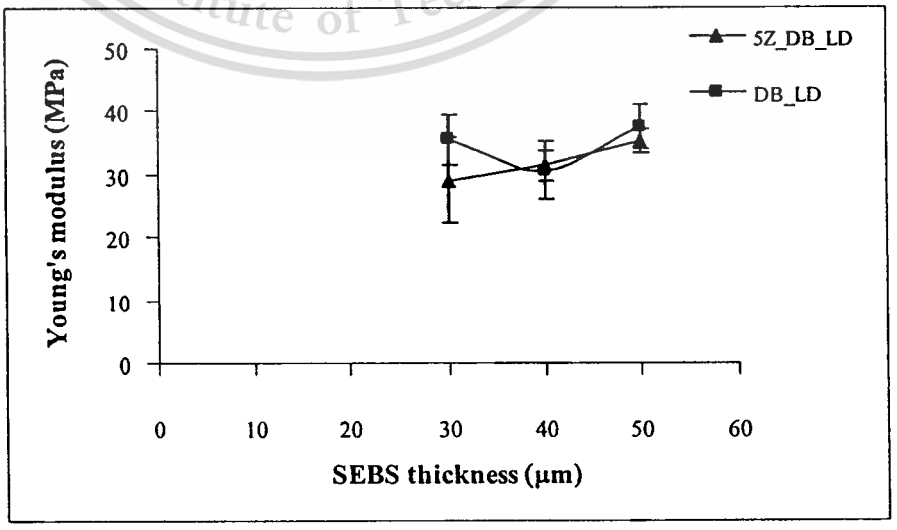

(c)

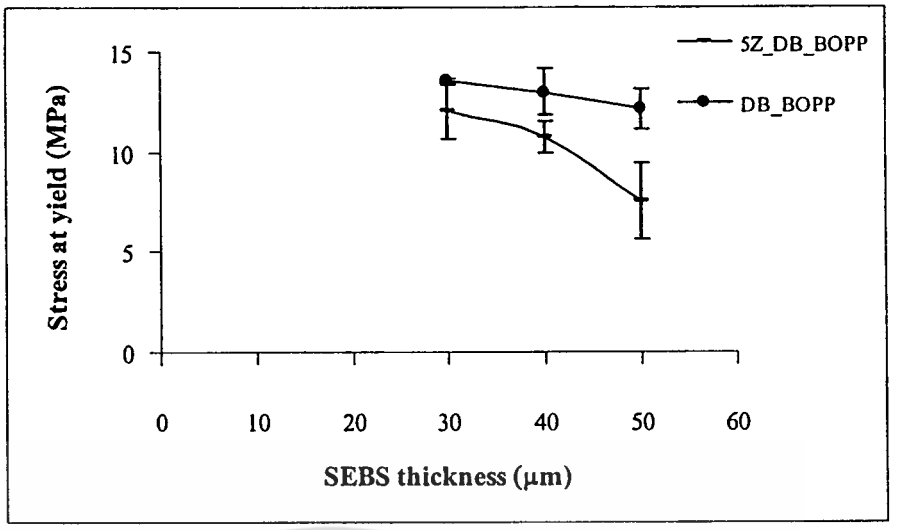

(d)

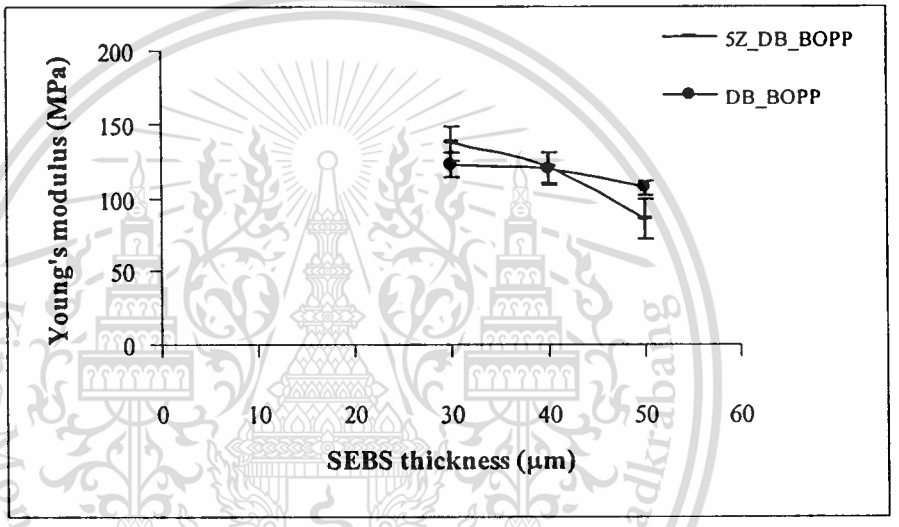

Figure 4.10 Tensile properties of the double-layered films with various SEBS thicknesses : (a, c) Stress at yield and (b, d) Young's modulus.

For DB_BOPP film, it was observed that the SEBS thickness does not significantly affect on tensile properties. This is due to adhesion at perforated boundary of film is poor and the tensile properties are mainly contributed from BOPP. However, zeolite was loaded in the double-layered films. It was found that the interphase at perforated boundary of 5Z_DB_BOPP is improved, as compared to that of DB_BOPP, as mentioned in section 4.1.5. Therefore, the tensile properties of the 5Z_DB_BOPP film is partly contributed from the SEBS layer. Hence, the tensile properties of 5Z_DB_BOPP are decreased with increasing SEBS thickness. This is because an increase thickness of the flexible SEBS phase requires lower force for deformation tensile, leading to the lower tensile properties of 5Z_DB_BOPP as observed.

For both DB_LD and 5Z_DB_LD films, the thickness of SEBS showed insignificant effect to the tensile properties of the double-layered films. This is because both SEBS and LDPE are flexible and possess similar tensile properties.

4.2 Permeation

4.2.1 Ethylene transmission rate (ETR) of the parent films

The ethylene transmission rates (ETR) of the SEBS (30), LDPE (30), BOPP (30) films were tested and the results are shown in Figure 4.11.

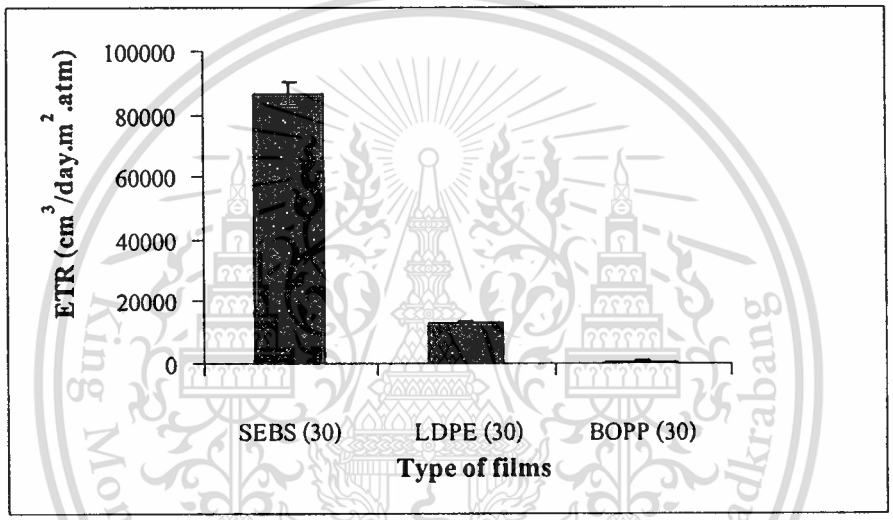

Figure 4.11 ETR of the parent films.

It was found that ETR of SEBS film is significantly higher than those of both LDPE and BOPP films (Figure 4.11). This is because the SEBS contains ethylene/butylene segments with relatively high free volume and flexibility. Thus the gas molecules can be soluble in the SEBS film and readily permeate through this film. Whilst, the crystalline phase in LDPE or BOPP is generally impermeable for gas molecules **[48].** Only the amorphous phase of LDPE or BOPP allows the gas permeation.

In the case of supporting films, it was found that ETR of LDPE film is higher than that of the BOPP film. This is again because the crystallinity of BOPP film is higher than that of the LDPE as shown in Table 4.4. The crystalline phase of BOPP generally acts as barrier for gas permeation.

The SEBS/LDPE double-layered films showed high ethylene permeability [5]. However, the supporting layer acts as barrier for gas permeation in double-layered films. Hence, gas permeation of double-layered films can be improved by perforated of the supporting layer film.

4.2.2 ETR of double-layered films with various perforated areas (0-100%)

ETR of DB_LD films (SEBS (50 μm)) with various perforated areas of the LDPE supporting layer was investigated as shown in Figure 4.12.

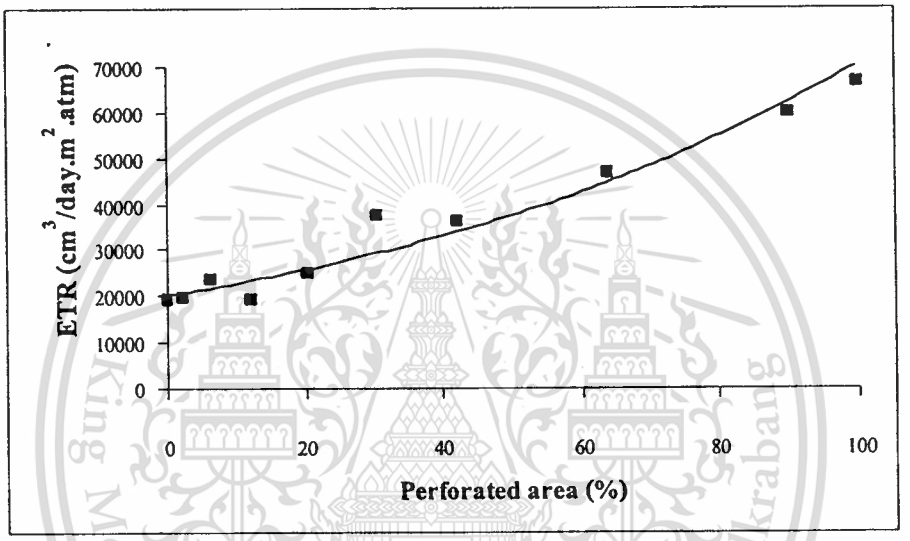

Figure 4.12 ETR of the DB_LD films with various perforated areas.

It can be seen that ETR of DB_LD films is increased with increasing perforated areas. This is because the LDPE supporting layer acts as gas barrier. Hence the higher perforated area provides a better gas permeation to the SEBS layer that possesses high gas permeability. However, the tensile properties (stress at yield and Young's modulus) of the film with perforated area at higher than 40% is immeasurable and the film cannot be use for packaging. Therefore, film with perforated area of 40% was selected for further study on the ethylene permeation.

4.2.3 ETR of double-layered films with various perforated sizes (2-5 mm)

For 40% perforated area, double-layered films (40% perforated area) with various perforated sizes were tested for ETR as shown in Figure 4.13.

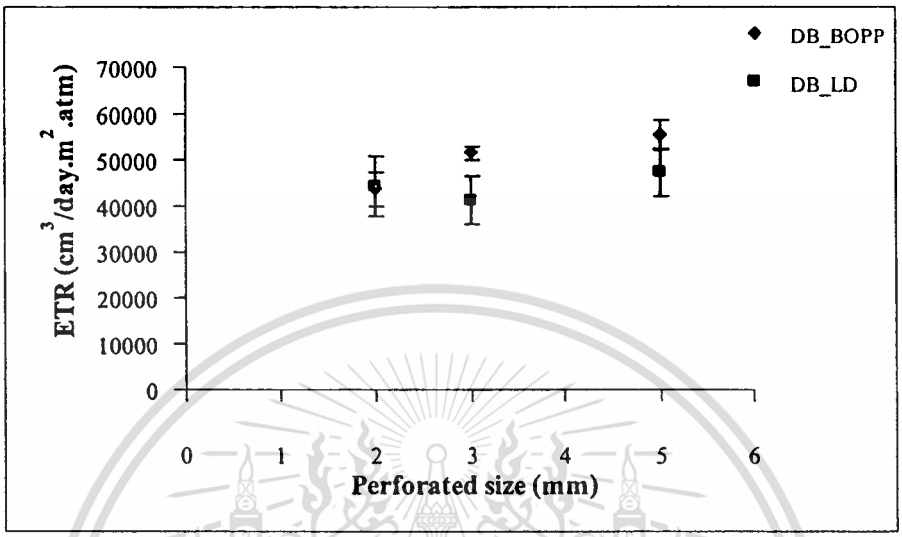

Figure 4.13 ETR of the double-layered films with various perforated sizes (2-5 mm).

It can be seen that no significant change in ETR of double-layered films is observed when perforated size is increased. As the double-layered films with various perforated sizes (2, 3 and 5 mm) consist of the same perforated area (40%), ethylene gas will permeate mostly at the perforated area. Therefore, to maintain high tensile properties of DB_LD or DB_BOPP film, perforated size of 2 mm was selected for further study on the effect of SEBS thickness.

Although, ETR of LDPE single-layered film is higher than that of BOPP single-layered film (Figure 4.11). The ETR of DB_BOPP is found to be higher than that of DB_LD. This is not expected and may result from a poor adhesion between interphase of SEBS and BOPP as compared to SEBS and LDPE as discussed earlier (section 4.1.2.3). Therefore, the ethylene gas can permeate not only through the perforated area, but also through the defects derived from the poor adhesion between interphase of SEBS and BOPP layers (Figure 4.14 (b)). While, ethylene gas will be permeate mostly at the perforated area in DB_LD (Figure 4.14 (a)). Accordingly, the observed ETR of the DB_BOPP cannot be trusted and the film cannot be referred to as a control sample.

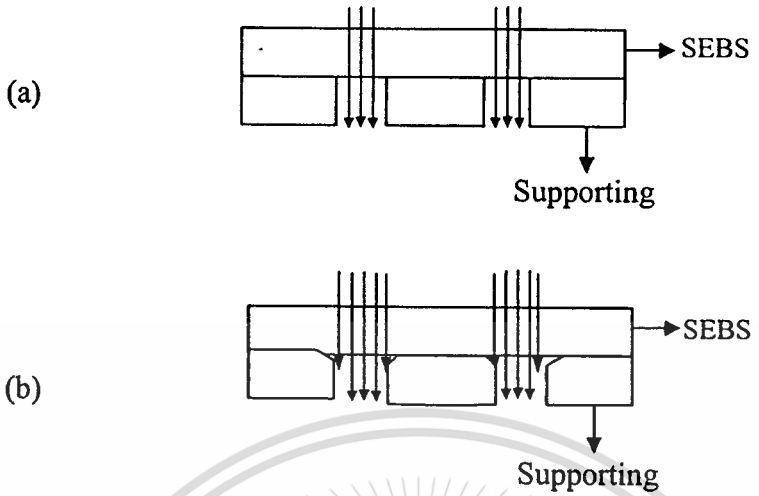

Figure 4.14 Schematic representation of adhesion : (a) good interphase and (b) poor interphase.

4.2.4 ETR of double-layered films with various SEBS thicknesses

Double-layered films (40% perforated area and 2 mm perforated size) with various SEBS thicknesses were tested for ETR as shown in Figure 4.15.

(a)

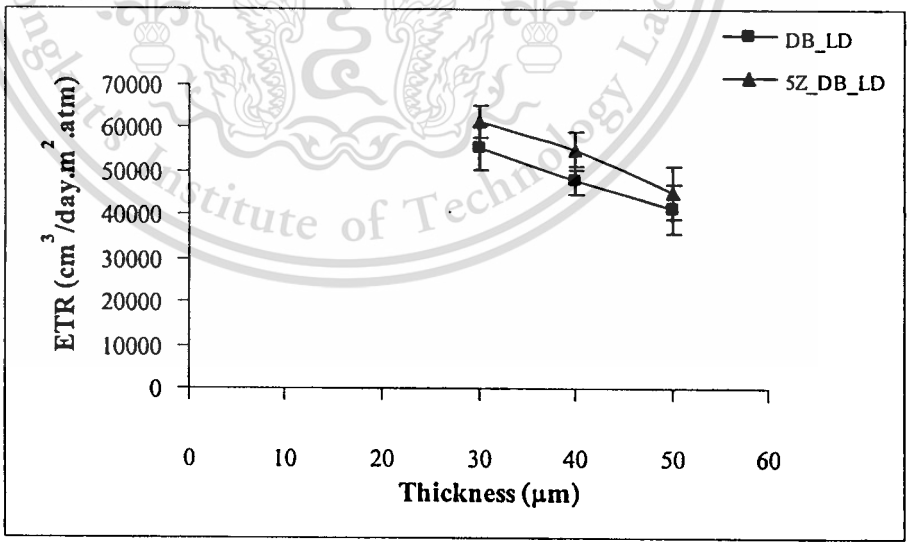

(b)

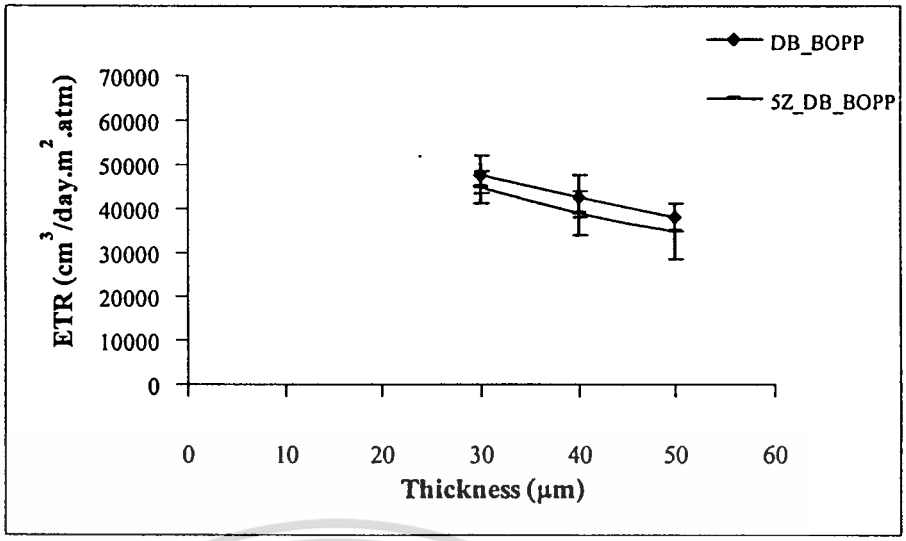

Figure 4.15 ETR of the double-layered films with various SEBS thicknesses : (a) DB_LD and (b) DB_BOPP.

It can be seen that ETR of double-layered films is increased with decreasing SEBS thicknesses. This is because diffusion path way is decreased when the SEBS thickness is decreased (Figure 4.16). The film becomes less transmission barrier as the thickness was reduced leading to a higher ETR as observed less transmission barrier. Therefore, SEBS with 30 μm was used for further study.

In the presence of zeolite, ETR of 5Z_DB_LD is higher than that of the DB_LD. This is because the ZSM-5 framework (Si/Al = 140) possessing 5.5 Å pore diameter, is highly hydrophobic. This provides a strong interaction with the ethylene gas, a hydrophobic molecule with 4.2 Å kinetic diameter [45]. Hence, the incorporated zeolite leads to a relatively higher ethylene adsorption. It is clearly seen that ETR of 5Z_DB_LD is higher than those of 5Z_DB_BOPP, particularly at the lower SEBS thickness. This is due to the lower crystallinity of LDPE as discussed previously. Moreover, when the zeolites was incorporated into DB_BOPP film, a better adhesion between SEBS and BOPP interphase can be obtained as shown in Figure 4.4. Hence, ETR of 5Z_ DB_BOPP is lower than that of DB_BOPP. However, the effect of zeolite incorporation cannot be determined for DB_BOPP since the ETR of DB_BOPP cannot be trusted due to the un-controlled defects as discussed earlier.

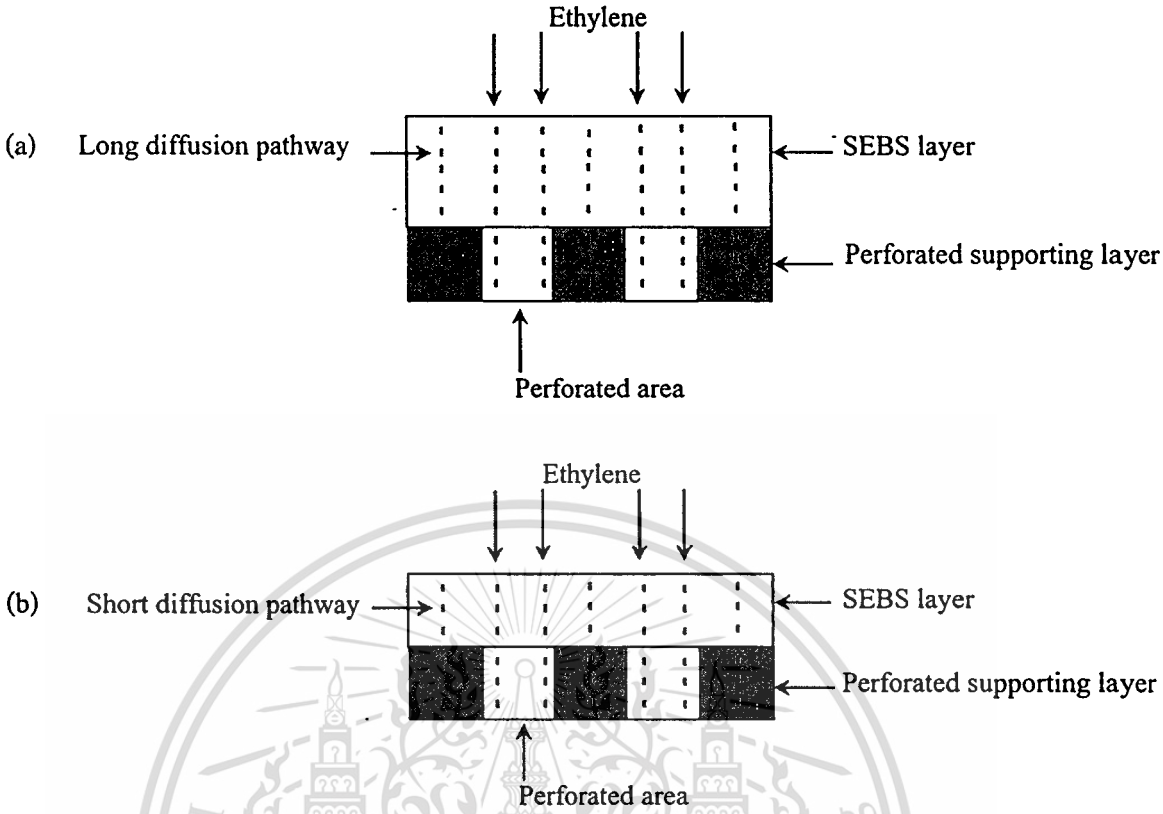

Figure 4.16 Diffusion pathway of ethylene gas :
(a) long diffusion pathway and (b) short diffusion pathway.

4.2.5 Gas transmission rate of the films for MAP

The ethylene, carbon dioxide and oxygen transmission rate of the SEBS (30), LDPE (30), BOPP (30) and double-layered films (40% perforated area and 2 mm perforated size) are shown in Figure 4.17.

(a)

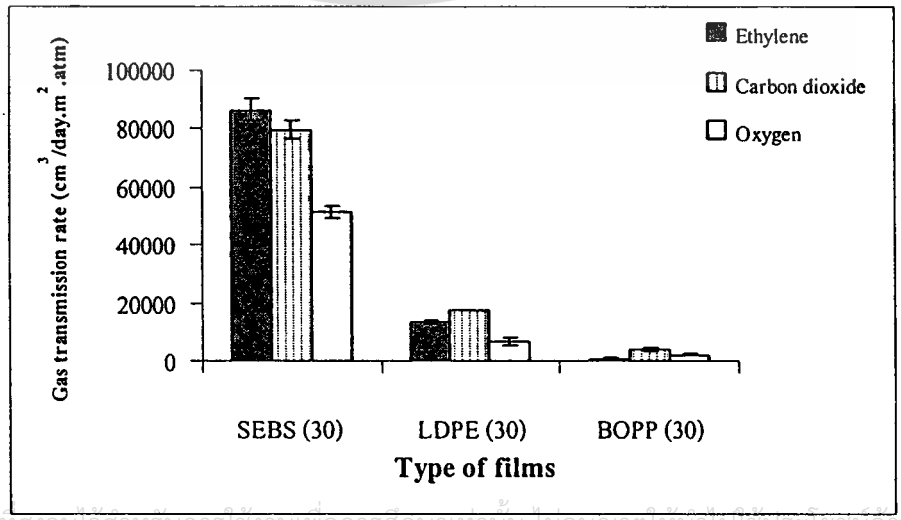

(b)

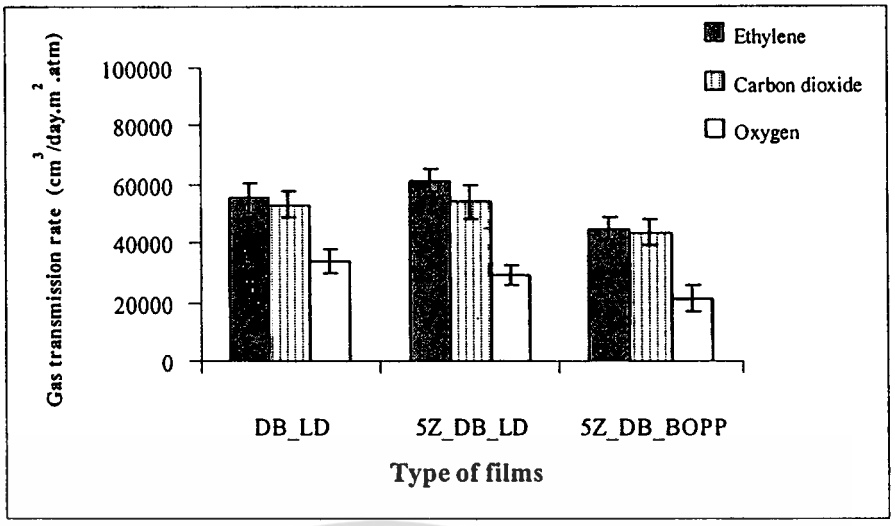

Figure 4.17 Ethylene, carbon dioxide and oxygen transmission selectivity :
(a) gas transmission rate of the parent films and
(b) gas transmission rate of the double-layered films.

From Figure 4.17, the gas transmission rate of SEBS is generally higher than those of LDPE and BOPP. This is due to nature of the film as discussed previously (section 4.2.1).

When LDPE and BOPP were used as supporting layer, the gas permeability of the double-layered films is higher than that of the LDPE and BOPP film, but certainly lower than that of SEBS film. (Figure 4.17 (a)) This is because gases permeate mostly through the perforated area of supporting layer, i.e., through the SEBS. However, the gases can also permeate through the supporting layer, as the both LDPE and BOPP possess some gases permeability (Figure 4.17 (b)). Hence, ethylene permeability of 5Z_DB_LD is higher than that of the 5Z_DB_BOPP, due to the lower crystallinity of LDPE as discussed previously.

For SEBS and double-layered films relatively higher permeation of ethylene can be observed as compared to oxygen and carbon dioxide. This is because the ethylene/butylene segment in SEBS is hydrophobic polymer which allows strong interaction with non-polar ethylene gas. While, in the both LDPE and BOPP, carbon dioxide permeation are higher than that of ethylene and oxygen. This is because carbon dioxide possesses strong interaction with the hydrophobic amorphous phase of both LDPE and BOPP as compared to oxygen and ethylene. Oxygen permeation of all films is relatively low. This is because oxygen possesses very weak molecular interaction and high vapor pressure (critical temperature -183 °C). Thus, it can only be slightly soluble and adsorbed in polymer matrix leading to low permeation as observed in Figure 4.17 (b).

The effect of incorporated zeolite can be clearly demonstrated for double-layered with LDPE supporting layer. It can be seen that when zeolite was loaded in the double-layered films the ethylene permeability is increased as compared to that without zeolite. This is because the ZSM 5 is selectitve for ethylene gas as discussed in section 4.2.4. This is also consistent with the adsorption isotherm of ZSM-5, as shown in Figure 4.18 (ethylene > carbon dioxide >> oxygen).

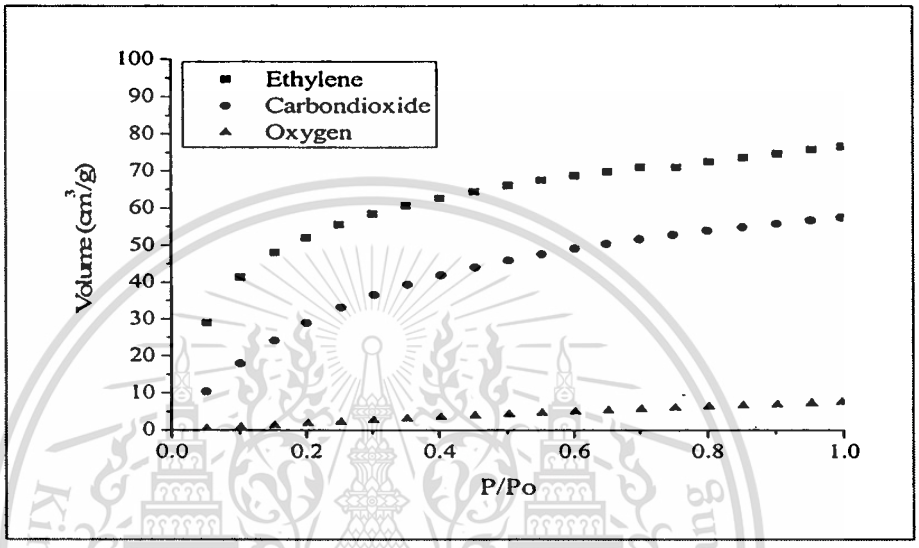

Figure 4.18 Adsorption isotherm by ZSM-5 zeolite [5,35].

Accordingly, a high concentration of ethylene is expected at the film surface leading to a higher concentration gradient across the film. This becomes a driving force for ethylene permeation and leads to a greater diffusion of ethylene gas through the film.

However, oxygen permeability of films slightly decreased was observed when zeolite was incoporated. This is because the presence of zeolite as filler would increase the films rigidity, decreasing the free volume of the polymer matrix.

In a similar manner carbon dioxide permeability insignificantly changes when zeolite is incorporated into the SEBS layer (Figure 4.17 (b)). This is not because carbon dioxide does not interact with zeolite but because carbon dioxide is relatively high polar and readily soluble in SEBS. Therefore, carbon dioxide can readily diffuse in the SEBS matrix and the presence of zeolite in the SEBS layer show insignificant effect.

From the gas transmission rate, gas permeatbility of the films can be calculated from the following equation 4.1

$$P = \frac{J \Delta x}{A \Delta p} \tag{4.1}$$

where P is the gas permeability ($cm^3.mm/m^2.day.atm$), J is the transmission rate of the permeated gas (cm^3/day), Δx is the film thickness (mm), A is the surface area of the film (m^2), Δp is the partial pressure difference of the analyte gas across the film (atm). The calculated permeability are listed in appendix H

The ratio of gas permeability for ethylene/oxygen $P(C_2H_4)/P(O_2)$ and carbon dioxide/oxygen $P(CO_2)/P(O_2)$ were calculated from pure gas permeation experiment to determine the ideal selectivity [49], as shown in Table 4.5.

Table 4.5 Permeability ratio of the parent and the double-layered films.

Film	$P(C_2H_4)/P(O_2)$	$P(CO_2)/P(O_2)$	ETR ($cm^3/m^2.day.atm$)
SEBS	1.7	1.6	86616±3936
LDPE	2.0	2.6	18365±830
BOPP	0.4	1.8	1531±101
DB_LD	1.6	1.6	55474±5144
5Z_DB_LD	2.1	1.9	61511±3800
5Z_DB_BOPP	2.1	2.1	44263±5969

It can be seen that ethylene permeability of SEBS is approximately 1.7 times higher than that of oxygen. The higher values at 2.0 times were found for LDPE. However, BOPP shows low ethylene permselectivity. With the C_2H_4/O_2 permeability ratio more than one, the film can regulate oxygen permeation but facilitate ethylene permeation. In other word, the film readily reduces the ethylene accumulation in the package. This is preferred because, in postharvest, the ethylene gas induces an unusually fast growth for example over-ripening, excessive softening and abscission of leaves and flowers. Thus, high ethylene permeation of film is a beneficial property for a smart packaging of fresh produces.

When LDPE and BOPP were used as supporting layer, it was also found that $P(C_2H_4)/P(O_2)$ of double-layered films exhibit high selectivity for ethylene gas. This is due to gases permeate mostly through the perforated area of supporting layer, as discussed earlier in section 4.2.2. Since SEBS alone possesses $P(C_2H_4)/P(O_2)$ approximately 1.7, it is reasonable for $P(C_2H_4)/P(O_2)$ of double-layered films to exhibit approximately 1.6.

Although the permeability ratio of SEBS parent film is lower than that of LDPE parent film. When consider the ETR of SEBS, it was found that the ETR of SEBS is higher than that of LDPE. It facilitates that the ethylene gas permeated through the SEBS film more than the LDPE film. Nevertheless, $P(C_2H_4)/P(O_2)$ of double-layered films is similar to that of LDPE parent film, the ETR of double-layered films is higher than that of LDPE. It can be used for MAP with ethylene removal ability.

It importantly points out that the increase in $P(C_2H_4)/P(O_2)$ ratio can be observed when zeolite was incorporated in the double-layered films due to selective adsorption of ethylene by zeolite as mentioned earlier. This indicates that the zeolite composite double-layered films can readily remove ethylene gas from the package and maintain capability for impeding the permeation of oxygen.

The appropriate atmosphere inside the package can also be achieved by increasing $P(CO_2)/P(O_2)$ ratio. Such gas dynamic results in a slow metabolism that allows the products to be kept for a longer period of time. A diagram of gas exchange is shown in Figure 4.19

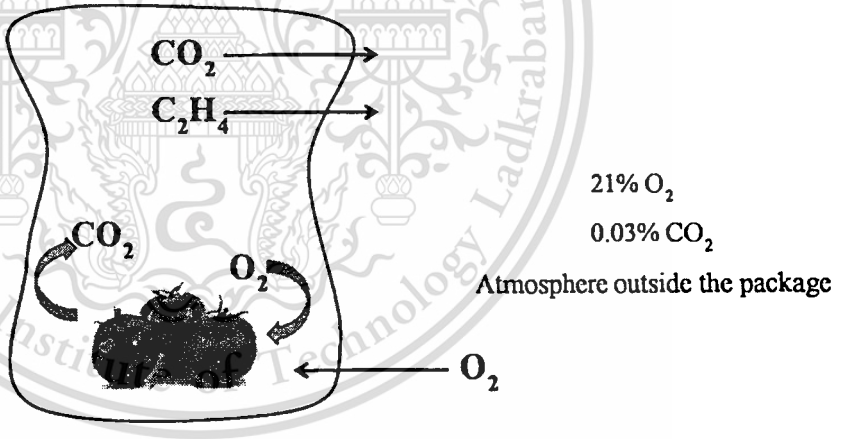

Figure 4.19 Diagram of a gas exchange through the film.

It can be seen from Table 4.5 that $P(CO_2)/P(O_2)$ are increased when zeolite was incorporated in the double-layered films. This is because zeolite can suppress oxygen permeability by increasing the films rigidity.

In addition to ethylene and permanent gases transmission rate, water also affects to shelf life of fresh fruit and vegetables. Hence, water vapor transmission rate (WVTR) of the SEBS (30), LDPE (30), BOPP (30) and double-layered films were also studied as shown in Figure 4.20.

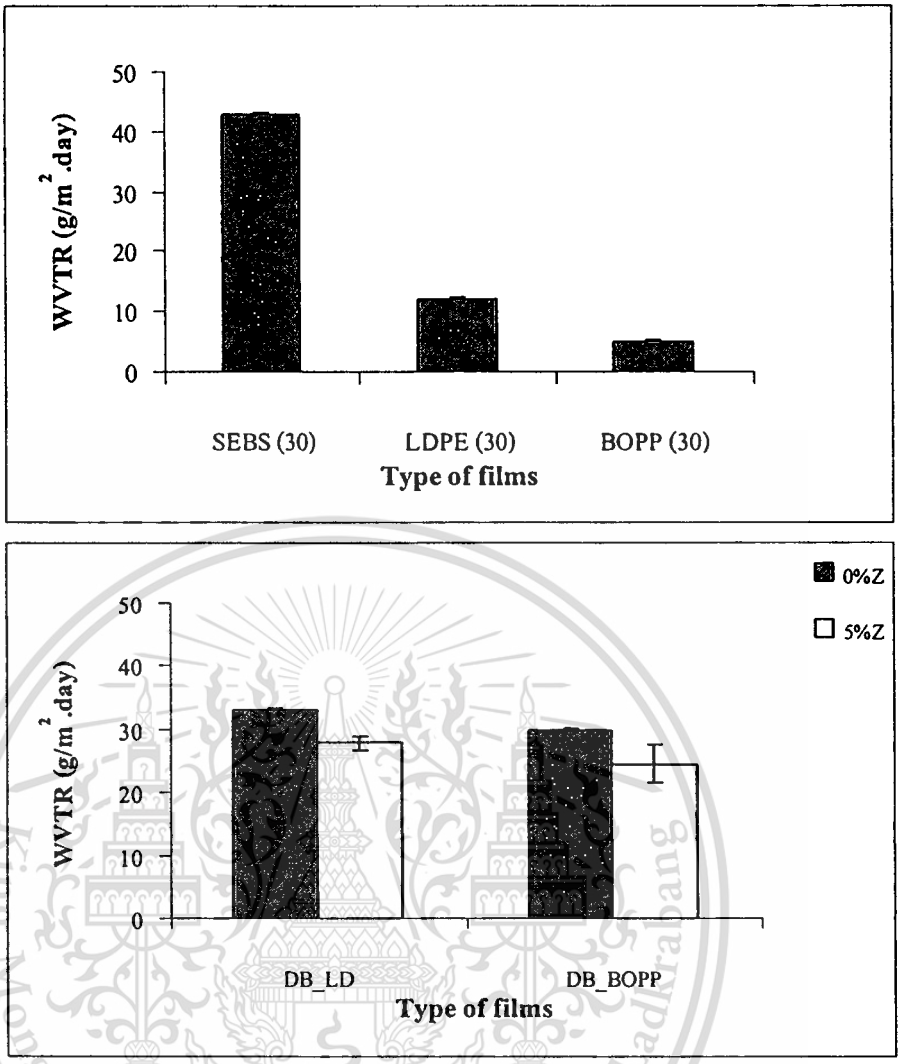

Figure 4.20 Water vapor transmission rate of the films.

It can also be seen that the water vapor transmission rate of SEBS is higher than that of both LDPE and BOPP. In a similar manner to other gases. However, the water vapor transmission rate (WVTR) of all films is much lower than ethylene, carbon-dioxide and oxygen transmission rate. This is because SEBS, LDPE and BOPP are non polar polymers, whereas water is high polar. Hence, water vapor possesses weak interaction with the polymer matrix. This leads to a low adsorption and consequently, low permeation of water in the polymer film **[50]**.

With the zeolite incorporation, there is no significant change in water vapor transmission rate of both DB_LD and DB_BOPP films (Figure 4.20 (b)). This is again because ZSM-5 is hydrophobic and does not interact well with water vapor, a high polar molecule. However, water vapor transmission rate of all zeolite composite double-layered films are in the range of 25-35 g/m^2.day, and can be applicable in the packaging **[50]**.

4.2.6 Relationship of ethylene transmission rate in the presence of other gases

Although, $P(C_2H_4)/P(O_2)$ and $P(CO_2)/P(O_2)$ are used widely to determine ideal selectivity for MAP, the values are obtained from pure gas permeation tests. Practically, there are several gases component in the packaging film. Hence permeation of ethylene in the presence of other gases is determined to evaluate the selectivity of gas permeation.

(a)

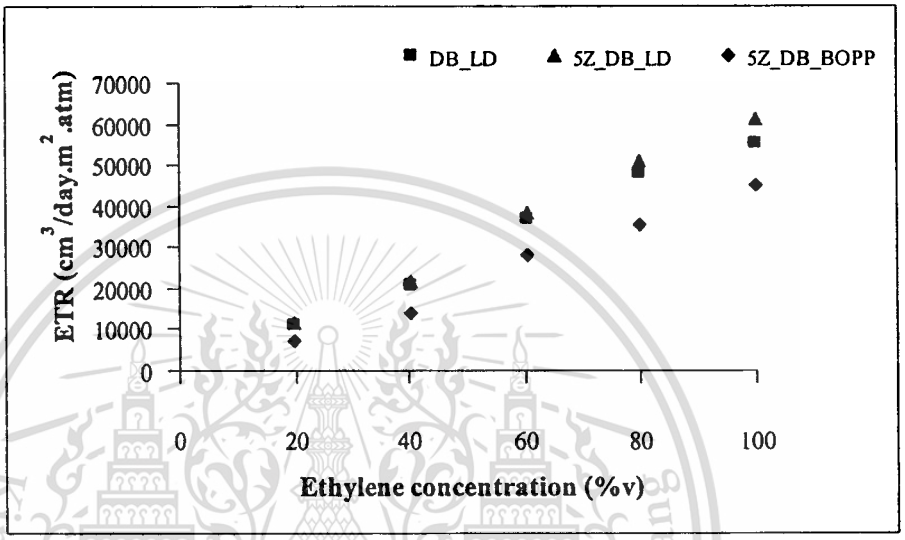

(b)

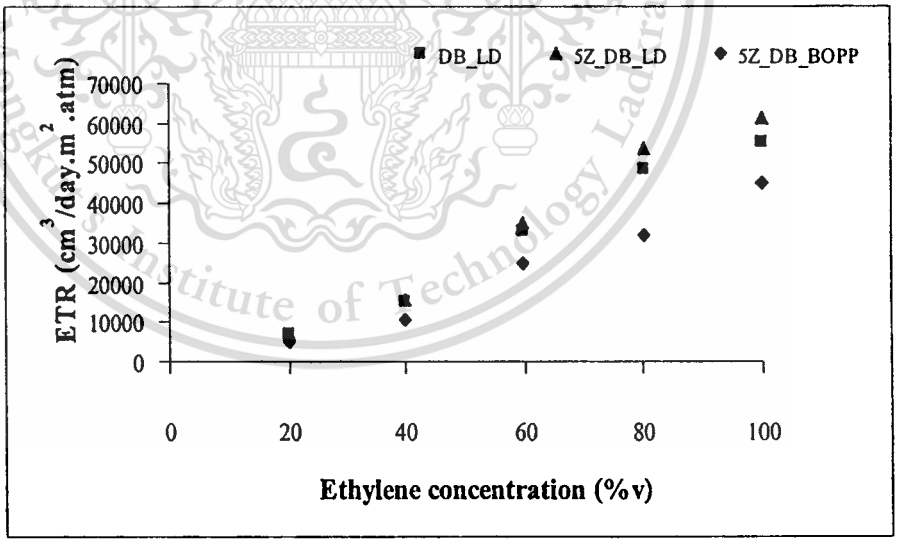

(c)

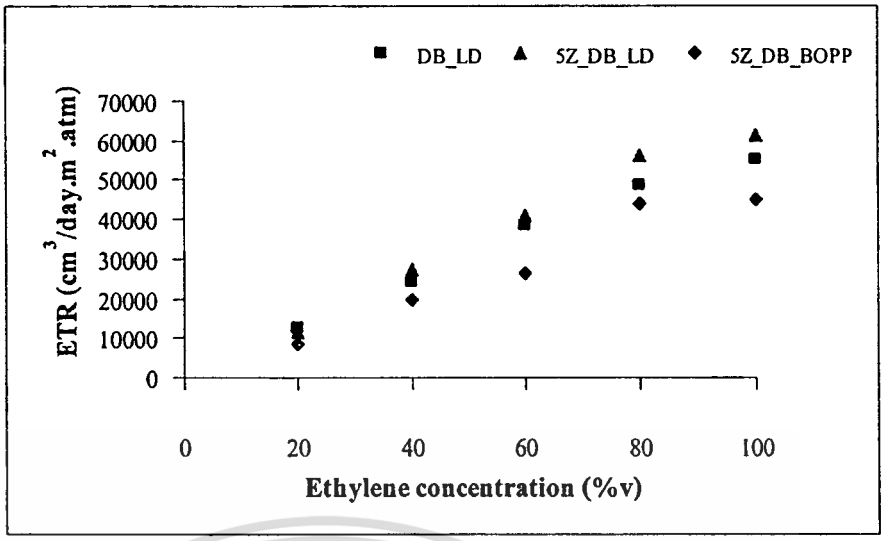

Figure 4.21 Relationship of ethylene transmission rate and feed concentration of DB_LD, 5Z_DB_LD and 5Z_DB_BOPP film (40% perforated area and 2 mm perforated size): (a) under nitrogen, (b) under air zero and (c) under carbon dioxide.

It can be seen from Figure 4.21 that ethylene flux is enhanced when the concentration of ethylene in the gas phase is increased for all gases mixtures. This is explained by Fick's law of diffusion as follow **[51]** :

$$J = -D\frac{\partial \phi}{\partial x} \tag{4.2}$$

where J is the diffusion rate of gas through the membrane per a unit area, D is diffusion coefficient or diffusivity, $\partial\phi$ is the concentration gradient of gas on the feed and permeate side of the membrane and ∂x is the distance or the film thickness, respectively. In this study, the constant ambient temperature (25 °C) was used for permeation test. This hence results in a constant diffusion coefficient (D) of the gas in the film. In addition, the film thickness was prepared within the same range and presumably no significant change in the thickness of the film tested. Therefore, the ethylene flux, which relates to permeability, depends only on the ethylene concentration of feed gas. As the ethylene concentration in the feeding side is increased, the higher concentration gradient can be obtained. Accordingly, the ethylene gas molecule can feasibly permeate increasingly throughout the film.

The ethylene transmission rate of double-layered films (i.e., DB_LD) with zeolite is higher than that without zeolite. This is because the ZSM-5 highly hydrophobic and provides a strong interaction with the ethylene gas, as discussed earlier. This leads to higher ethylene permeation

particularly at high ethylene concentration as shown by adsorption isotherm of ZSM-5 (Figure 4.18)

It can be seen for all ranges of ethylene concentration that ethylene transmission rate of DB_BOPP is lower than that of the DB_LD. This is again because the crystalline phase of BOPP shows better gas barrier properties than that of the LDPE.

From the ethylene transmission rate as a function of feed concentration, ethylene permeation (EP) of double-layered films under nitrogen, air zero and carbon dioxide can be calculated from the equation 4.1

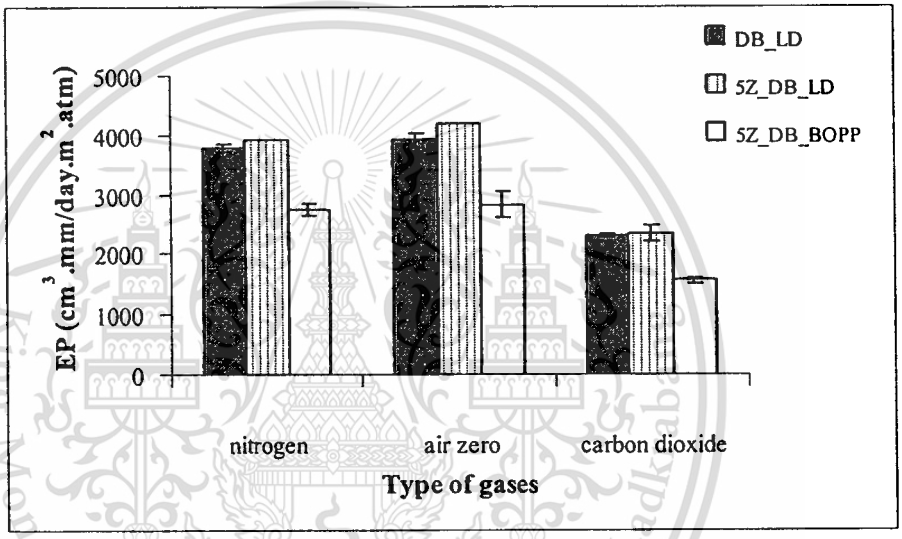

Figure 4.22 Relationship of ethylene permeability of the double-layered films with and without zeolite under nitrogen, air zero and carbon dioxide.

From Figure 4.22, it can be seen that ethylene permeability of the double-layered films in N_2 is somewhat similar to that in oxygen. This is because there is no competitive adsorption between C_2H_4 and N_2 or air zero. However, the ethylene permeability of the double-layered films in CO_2 is relatively low. This suggests that the mass transfer of ethylene from the gas phase onto such film surface would be inhibited by the competitive adsorption of CO_2. This leads to notably lower ethylene permeation, as compared to that in the C_2H_4-N_2 and C_2H_4-Air zero.

CHAPTER 5

CONCLUSION AND SUGGESTION

5.1 Conclusion

The double-layered films (DB_LD or DB_BOPP) were successfully improved ethylene permeability by perforating the supporting layer (40%). This is because ethylene gas will permeate mostly at the perforated area through SEBS layer. The ethylene/butylene segment in SEBS, which is hydrophobic and possesses high free volume and flexibility, allows stronger interaction and permeation for ethylene, as compared to carbon dioxide and air zero. In a similar manner, the permeation of carbon dioxide is higher than that of oxygen because carbon dioxide possesses strong interaction with the hydrophobic amorphous phase of SEBS as compared to O_2. It was also shown that the perforated size (2, 3 and 5 mm) insignificantly affected the gas permeation at the same perforated area (40%).

For the variation of SEBS thickness, the ethylene permeation is increased when a decrease in SEBS thickness was observed. This is simply because diffusion path way is shorter when the SEBS thickness is decreased. For both DB_LD and 5Z_DB_LD films, the thickness of SEBS insignificant affected the tensile properties of the double-layered films. This is because the tensile properties of the films are contributed from both SEBS and LDPE which are flexible and possess similar tensile properties. However, DB_BOPP film, it was observed that the SEBS thickness does not significantly affect on tensile properties. This is due to adhesion at perforated boundary of film is poor and the tensile properties are mainly contributed from BOPP. In addition the tensile properties of 5Z_DB_BOPP films are decreased with increasing SEBS thickness. This is because the tensile properties are partly contributed from the SEBS layer. Therefore, an increase in thickness of the flexible SEBS phase requires lower tensile deformation. SEBS thickness is increased, leading to lower tensile properties.

When zeolite (ZSM-5) was added into SEBS film, it can increase ethylene permeation of the double-layered films (DB_LD or DB_BOPP). This is because the hydrophobic frameworks of zeolite possess relative non-polar property. In addition, the microporosity of zeolite can strongly interact with small non-polar gas molecules, leading to high ethylene adsorption capacity and selectivity. However, an addition of zeolite insignificantly affected on carbon dioxide permeation. This is derived from the interaction between zeolite and polystyrene segment that causes an

increase in chain rigidity. Oxygen permeability also was not readily affected by the incorporation of zeolites. Moreover, no competitive adsorption between C_2H_4 and N_2 or Air zero was observed. However, the ethylene permeability of the double-layered films was inhibited by the competitive adsorption of CO_2.

The incorporated zeolite particles can also improve the adhesion between interphase of SEBS and supporting layers (LDPE and BOPP). In addition, there was no significant change in stress at yield and Young's modulus. However, 5%w/w zeolite was loaded in DB_BOPP film. Tensile properties of 5Z_DB_BOPP is lower than that of the DB_BOPP. This suggests that the zeolite induce defect in the 5Z_DB_BOPP film. With 40% perforated area, 2 mm perforated size and 30 μm SEBS thickness, the double-layered films possessed appropriate tensile properties and ethylene permeability/selectivity that can be used for MAP with ethylene removal ability.

5.2 Suggestions for future studies

5.2.1 It is well known that zeolite can selective ethylene gas, zeolite content in SEBS of zeolite-SEBS composite/perforated polyolefins (LDPE and BOPP) double-layered films higher than 5% should be investigated.

5.2.2 The adhesion at interphase between SEBS and supporting layer can be improved. Thus, surface of supporting layer should be modified before fabrication.

5.2.3 It is well known that gas permeation can be permeated through the amorphous phase. To improve the ethylene permeation, SEBS/LDPE blend would also be studied.

5.2.4 For future, the zeolite-SEBS composite/perforated polyolefins (LDPE and BOPP) double-layered films should be investigated for packaging of fresh produces.

REFERENCES

[1] Brody A.L. 2001. **Active Packaging for Food Applications.** USA : Technomic.

[2] Saltveit M.E 1999. "Effect of Ethylene on Quality of Fresh Fruits and Vegetables." **Postharvest Biology and Technology.** 15(3) : 279-292.

[3] Zagory D. and Kader A. 1988. "Modified Atmosphere Packaging of Fresh Produce." **Food Technology.** 42(9) : 70-74.

[4] Shah K., Ling MTK., Woo L. and Nebgen, G. 1998. **Gas Permeability and Medical Film Products.** [online]. Available : http://www.devicelink.com/mpb/archive/98/09/005.html.

[5] Monprasit P. 2009. "Study on Ethylene Gas Permeability of SEBS/LDPE double-layered zeolite composite films." M.Sc. Thesis of King Mongkut's Institute of Thechnology Ladkrabang.

[6] Vemeiren L., Devlieghere F. and Beest MV. 1999. "Development in the Packaging of Foods." **Trend in Food Science and Technology.** 10 : 77-86.

[7] Yahia E.M. 2009. **Modified and Controlled Atmosphere for the Storage, Transpiration and Packaging of Horticultural Commodities.** New York : CRC Press.

[8] Irtwange S.V. 2006. "Application of Modified Atmosphere Packaging and Related Technology in Postharvest Handling of Fresh Fruits and Vegetables." **Agricultural Engineering International: the CIGR Ejournal Invited Overview.** 3(4) : 178-187.

[9] Suwandi M.S. and Anhar S. 1987. **Membrane Technology : Proceedings of the Fourth ASEAN (Training) Workshop on Membrane Technology Held at National University of Malaysia in April 15-25.** Bangi : Asean Working Group on Food Waste Materials.

[10] Sci-Tech Encyclopedia. 2008. **Membrane Separations.** [online]. Available : http://www.answers.com/topic/membrane-separation?cat=technology.

[11] Rowan University. 2005. **Membrane Gas Separation.** [online]. Available : http://users. rowan.edu/~savelski/uol/gas.html.

[12] Apisittinet S. 2007. "Study on Ethylene Gas Permeability of Zeolite-LDPE and Zeolite-SEBS composite Film." M.Sc. Thesis of King Mongkut's Institute of Thechnology Ladkrabang.

[13] Comyn J. 1985. **Polymer Permeability.** London : Elsevier Applied Science Publishers.

[14] Young S. 2004. **Gas and Liquid Diffusion in Membranes.** [online]. Available : http:// www.psrc.usm.edu/mauritz/diffuse.html.

[15] Wikipedia. 2008. **Low-Density Polyethylene.** [online]. Available : http://en.wikipedia. org/wiki/LDPE.

[16] The University of Southern Mississippi. 2005. **Polyethylene.** [online]. Available : http://www.pslc.ws/macrog/pe.htm.

[17] Interactive Learning Paradigms Incorporated. 2006. **Polymerization.** [online]. Available : http://www.ilpi.com/msds/ref/polymer.html.

[18] Encyclopedia Britannica Inc. 2007. **Low-Density Polyethylene.** [online]. Available : http://www.britannica.com/EBchecked/topic-art/349692/2948/The-branched-form-of-polyethylene-known-as-low-density-polyethylene#tab=active~checked%2Citems~ checked.

[19] Encyclopedia Britannica Inc. 2007. **Propylene.** [online]. Available : http://www.britannica.com/EBchecked/topic-art/349692/2948/The-branched-form-of-polyethylene-known-as-low-density-polyethylene#tab=active~checked%2Citems~ checked.

[20] Wikipedia. 2008. **Propylene.** [online]. Available : http://en.wikipedia. org/wiki/PP

[21] Application plastic. 2007. **Propylene.** [online]. Available : http://www.rotex.com/04downloads/downloads/English/material_plasticpellets.pdf

[22] Legge N.R., Holden G. and Schroeder HE 1987. **Thermoplastic Elastomers.** New York : Hanser Publishers.

[23] Eastman Chemical Company. 2008. **Block Copolymer.** [online]. Available : http://www. eastman.com/Markets/Tackifier_Center/Block_Copolymer.htm.

[24] Specialchem and Omnexus. 2008. **Block Copolymers Based on Styrene and Butadiene (TPE-S or SBS, SEBS).** [online]. Available : http://www.omnexus.com/plastics-channels/rubber-replacement/performances.aspx?id=tpes.

[25] Kraton Polymer LLC. 2006. **An Introduction to Kraton Polymer.** [online]. Available : http://www.kraton.com/content/includes/An%20Intro%20To%20Kraton.pdf.

[26] Soroka W. 1995. **Fundamentals of Packaging Technology.** Virginia : Institute of Packaging Professionals.

[27] Global Business Hub for the Packaging Industry. 2008. **Plastic Film.** [online]. Available : http://www.packaging-films.com/plastic-films.html.

[28] Rooney M.L. 2005. **Active Packaging Research at the Food Research Laboratory.** [online]. Available : http://www.regional.org.au/au/roc/1991food/p-15.htm.

[29] Food Science Australia. 2008. **Active Packaging.** [online]. Available : http://www.foodscience.csiro.au/actpac.htm.

[30] Dixell. 2008. **Ehtylene Gas - The Silent Killer of Produce and Flowers.** [online]. Available : http://www.dixellasia.com/index.php?tpid=0222&pgid=0223.

[31] Mangaraj S. 2009. "Aplication of Plastic Films for Modified Atmosphere Packaging of Fruits and Vegetables : A Review" **Food engineering.** 1:133-158

[32] Auerbach S.M., Ford M. H. and Monson P.A. 2003. **Handbook of Zeolite Science and Technology.** New York : Basel.

[33] Wikipedia. 2008. **ZSM-5.** [online]. Available : http://en.wikipedia.org/wiki/ZSM-5.

[34] Roy A.H., Broudy R. and Vining J. 2009. Teaching Materials that Matter: An Interactive, Multi- media **Module on Zeolites in General Chemistry.** [online]. Available : http://samson.chem.umass.edu/~auerbach/pub_pdf/pap24.pdf.

[35] University of California San Diego. 2008. **ZSM-5 Catalyst.** [online]. Available : http://chemelab.ucsd.edu/methanol/memos/ZSM-5.html.

[36] Lenntech. 2008. **Zeolite Application.** [online]. Available : http://www.lenntech.com/zeolites-applications.htm.

[37] Wilmot J. 2008. **Zeolite Adsorbents.** [online]. Available : http://www.cefic.be/Templates/shwAssocDetails.asp?NID=473&HID=429&ID=177.

[38] Rooney M.L. 1995. **Active Food Packaging.** London : Blackie Academic and Professional.

[39] Suslow T. 1997. "Performance of Zeolite Based Products in Ethylene Removal." **Perishables Handling Quarterly.** 92 : 32-33.

[40] Hassan F.A.S. 2010. "Effect of 1-methylcyclopropene (1-MCP) treatment on sweet basil leaf senescence and ethylene production during shelf-life" **Postharvest Biology and Technology.** 55 : 61-65

[41] Entrepreneur Inc. 2008. **New Consumer Bags Provide Longer-Life Produce.** [online]. Available : http://www.entrepreneur.com/tradejournals/article/178482503.html.

[42] Mujica P. H., Guillardb V., Reynesa M. and Gontardb N. 2005. "Ethylene Permeability of Wheat Gluten Film as a Function of Temperature and Relative Humidity." **Journal of Membrane Science.** 256 (1-2) : 108-115.

[43] LIU W., Chen W., Chun C. and LI J. 2009. **Effects of perforated polyethylene fresh-keeping bags of different diameters on vegetables**. [online]. Available : http://en.cnki.com.cn/Article_en/CJFDTotal-SPKJ200901088.htm

[44] Kraton Polymer LLC. 2006. **Data Document Kraton ® G1652M Polymer.** [Online]. Available : http://www.kraton.com/content/includes/An%20Intro%20To%20Kraton.pdf.

[45] Zeolyst International. 2006. **Data Sheet of ZSM-5 Type Zeolite Product (MFI).** [Online]. Available : http://www.zeolyst.com/html/zsm5.asp.

[46] **Data Sheet of BOPP**. A.J. Plast Public Co., LTD. 2010.

[47] ASTM D882 Committee on standard. 1998. **Standard Test Method for Tensile Properties of Thin Plastic Sheet.** New York : American Society for Testing Materials.

[48] Wang Y. and Easteal A.J. 1998 "Ethylene and Oxygen Permeability through Polyethylene Packaging Films." **Journal of Packaging Technology and Science.** 11(4) : 169-178.

[49] Freeman B.D. 1999. "Basis of Permeability/Selectivity Trade off Relations in Polymeric Gas Separation Membrane." **Macromolecules.** 32(2) : 375-380.

[50] Metz S.J., Van de ven W.J.C., Potreck J., Mulder M.H.V. and Wessling M. 2005. "Transport of Water Vapor and Inert Gas Mixtures through Highly Selective and Highly Permeable Polymer Membranes." **Journal of Membrane Science.** 251 (1-2) : 29-41.

[51] Kentaro N., Niijima K., Nakata S. and Shiraishi Y. **Breathing film.** U.S. patent no. 6395071. May 2002.

[52] Laidler K.J. and Meiser J.H. 1999. **Physical chemistry.** New York : Houghton Mifflin.

APPENDICES

APPENDIX A

LDPE FILM

Table A.1 LDPE (30) film from blowing process.

Parameter	Data
Film blowing instrument	Single screw extruder connected with film blowing unit
Extruder barrel temperature range	180-210 °C
Die zone temperature	215 °C
Blow up ratio	1.86
Cross head speed	320 rpm
Wide size of film	15.5 cm

APPENDIX B

WEIGHT FRACTION OF SEBS AND SUPPORTING LAYERS (LDPE OR BOPP)

The weight fractions of SEBS and supporting layers (LDPE or BOPP) in the double-layered film were determined for the calculation of the normalized %crystallinity. The double-layered film was cut into a square shape with 3 × 3 cm^2. After that, it was soaking in hot toluene (around 50 °C) for 1 hr in order to dissolve the SEBS. Then, the remained LDPE or BOPP layer was cleaned with fresh toluene and then weighed. The %weight of SEBS and supporting layers in the double-layered films can be calculated by following equation and was shown in Table B.1. Data presented are average of 5 replicated tests.

$$\%\text{Weight of the supporting layer} = \frac{\text{Weight of the remained supporting layer}}{\text{Weight of the double-layered film}} \times 100$$

%Weight of the SEBS layer = 100 - %Weight of the supporting layer (LDPE or BOPP)

Table B.1 %Weight of SEBS, LDPE and BOPP layers in the double-layered films.

Sample	%Weight of LDPE layer	%Weight of SEBS layer
DB_LD	49.46	50.54
5Z_DB_LD	50.03	49.97
Sample	**%Weight of BOPP layer**	**%Weight of SEBS layer**
DB_BOPP	48.91	51.09
5Z_DB_BOPP	48.09	51.91

APPENDIX C

CALCULATION

C1: %Crystallinity.

Sample	DB_LD	DB_BOPP
%Weight of supporting layer	49.46	48.91
ΔH_f(J/g)	39.11	44.51

ΔH_f^0 (J/g) = 293 J/g (100% crystallinity of PE)

ΔH_f^0 (J/g) = 125 J/g (100% crystallinity of PP) **[52]**

$$\textbf{\%Crystallinity} = \frac{\Delta H_f}{\Delta H_f^{\circ}} \times \frac{100}{\textbf{\%W of the supporting layer}} \times 100$$

Example %Crystallinity in LDPE layer

$$= \frac{39.11}{293} \times \frac{100}{49.46} \times 100$$

$$= 23\ \%$$

C2: Ethylene permeability

Peak area of standard ethylene, 589 ppm (A_s) 4024 count

Peak area of the permeated ethylene (A_E) 1100 count

$\therefore$ Concentration of the ethylene in permeated gas $= \frac{589 \times 1100}{4024}$

$= 154$ ppm or μL/L

$= 0.154$ mL/L

Flow rate of the permeated gas (F_x) $= 30.58$ ml/min

$\therefore$ Transmission rate of ethylene (J) $= 0.154 \times 30.58$

$= 4.72$ ml · ml/L · min

$= 0.00472$ ml/min

Surface area of the film (A_F) = 0.000314 m^2

Film Thickness (Δx) = 0.060 mm

Partial pressure difference of ethylene (Δp) = $Pi_{feed} - Pi_{permeate}$

= $Pi_{feed} - 0$

Partial pressure of C_2H_4 in feed (Pi_{feed}) = total absolute pressure × volume fraction of ethylene

Ethylene concentration in feed stream (%v)	20	40	60	80	100
Δp (atm)	0.202	0.404	0.606	0.808	1.01

Flux of ethylene = J / A_F

= 0.00472 / 0.000314

= 15.03 ml / $min.m^2$

= 21643 cm^3 / m^2.day

$\therefore$ Ethylene transmission rate (ETR) = $J / (A_F \cdot \Delta p)$

$$= \frac{0.00472}{0.000314 \times 1.01}$$

= 14.88 ml / $min.m^2$

= 21428 cm^3 / m^2.day.atm

$\therefore$ Ethylene permeation (EP) = $(J \cdot \Delta x) / (A_F \cdot \Delta p)$

or = ETR × Film thickness

= 21428 × 0.060

= 1285 cm^3.mm / m^2.day.atm

APPENDIX D

TGA THERMOGRAM

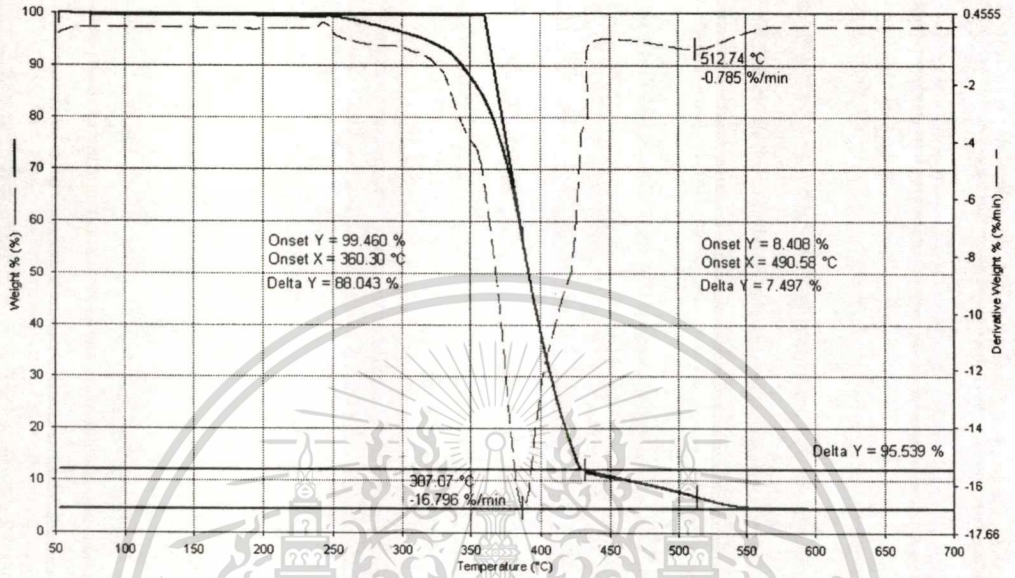

Figure D.1 Thermogram of 5Z_SEBS by spin coating 1st measurement zone.

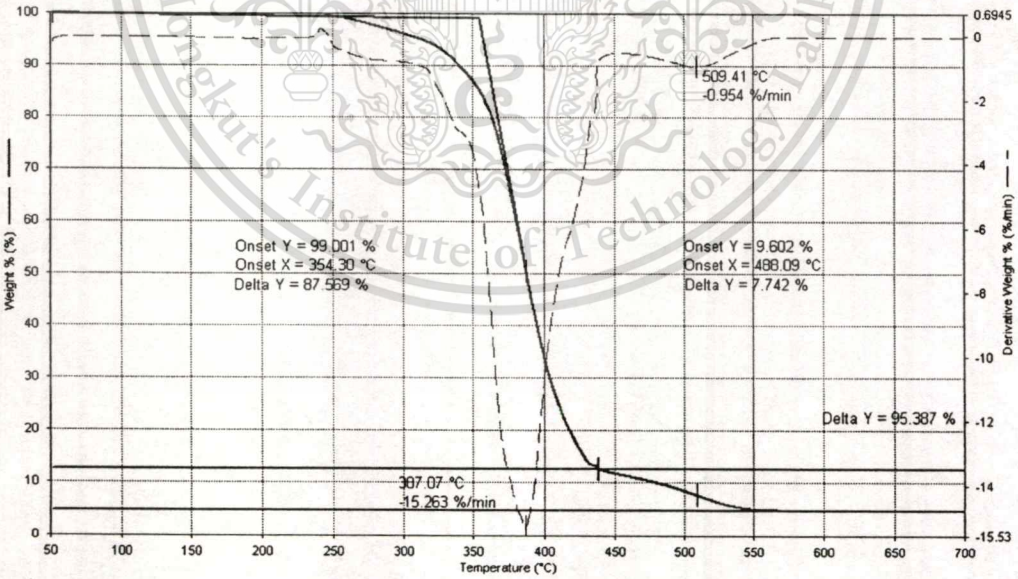

Figure D.2 Thermogram of 5Z_SEBS by spin coating 2nd measurement zone.

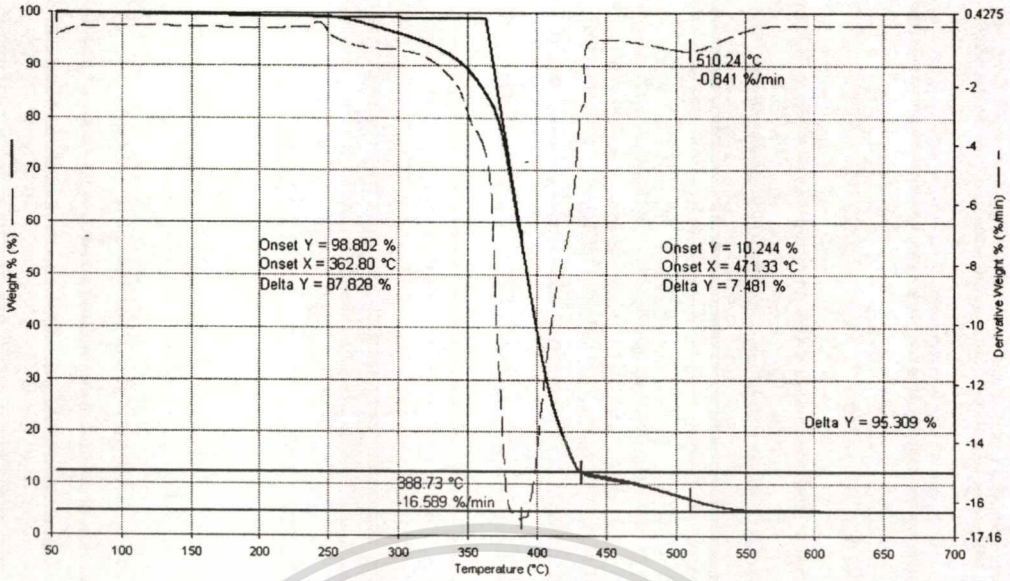

Figure D.3 Thermogram of 5Z_SEBS by spin coating 3rd measurement zone.

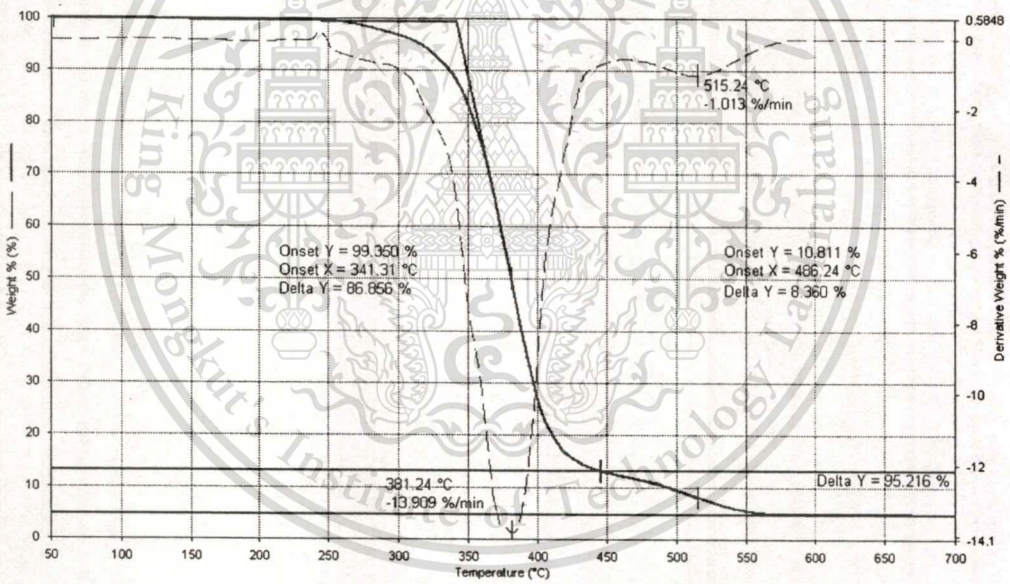

Figure D.4 Thermogram of 5Z_SEBS by solution casting 1st measurement zone.

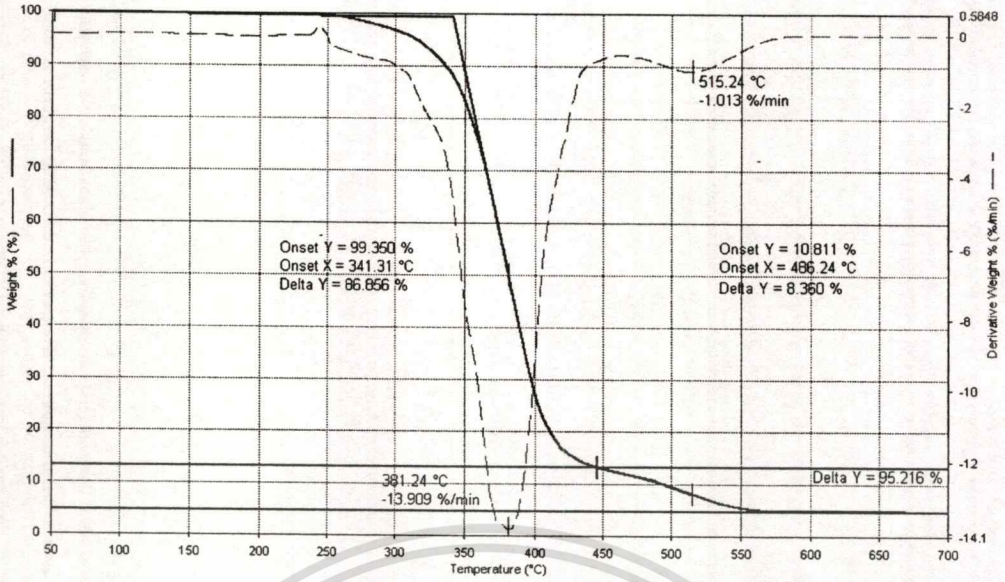

Figure D.5 Thermogram of 5Z_SEBS by solution casting 2nd measurement zone.

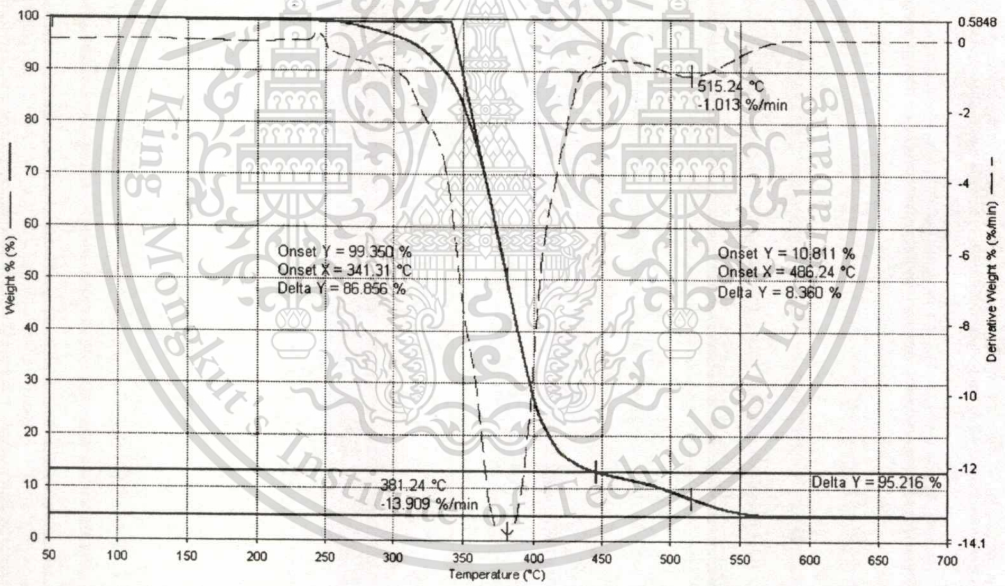

Figure D.6 Thermogram of 5Z_SEBS by solution casting 3rd measurement zone.

APPENDIX E

DSC THERMOGRAM

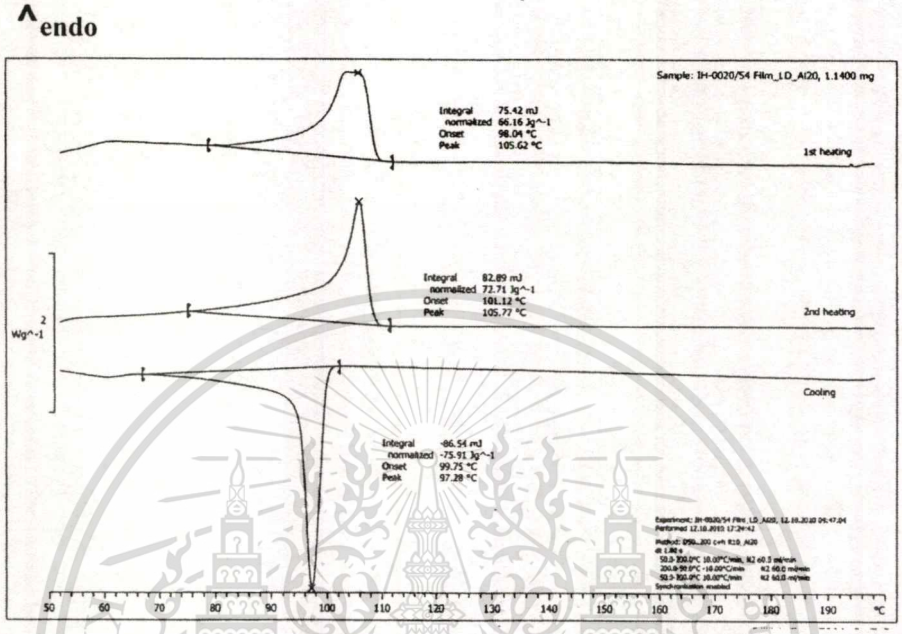

Figure E.1 Thermogram of LDPE film.

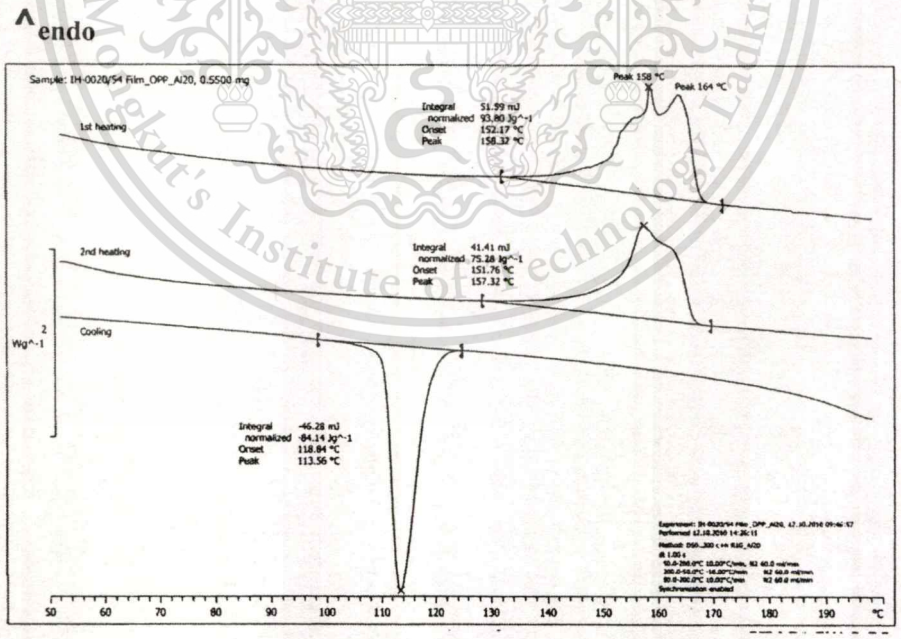

Figure E.2 Thermogram of BOPP film.

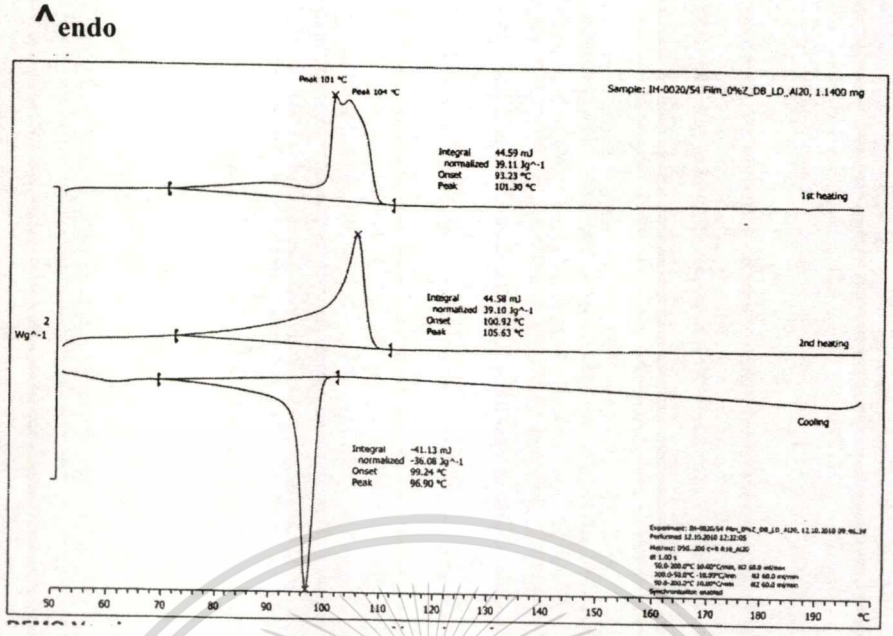

Figure E.3 Thermogram of DB_LD film.

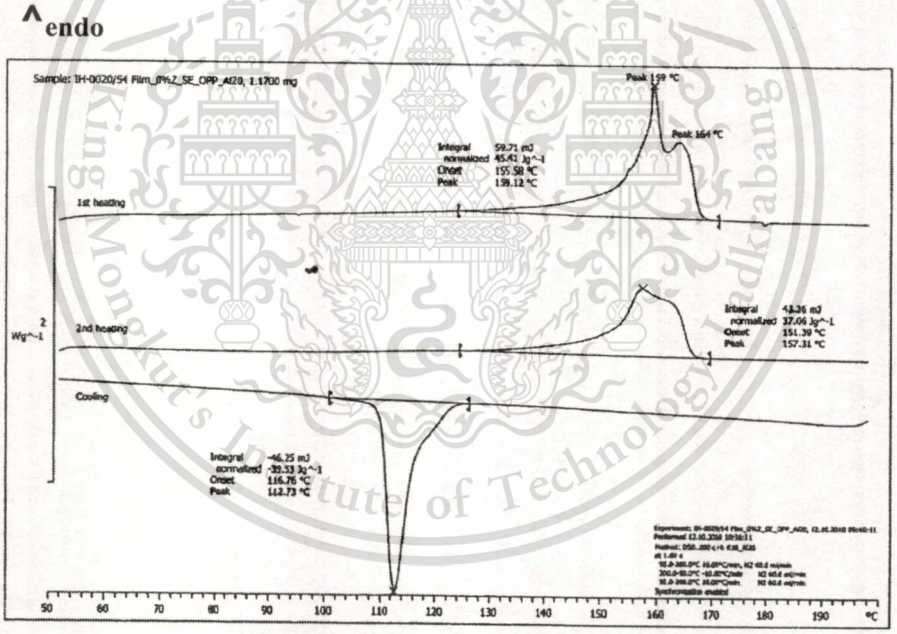

Figure E.4 Thermogram of DB_BOPP film.

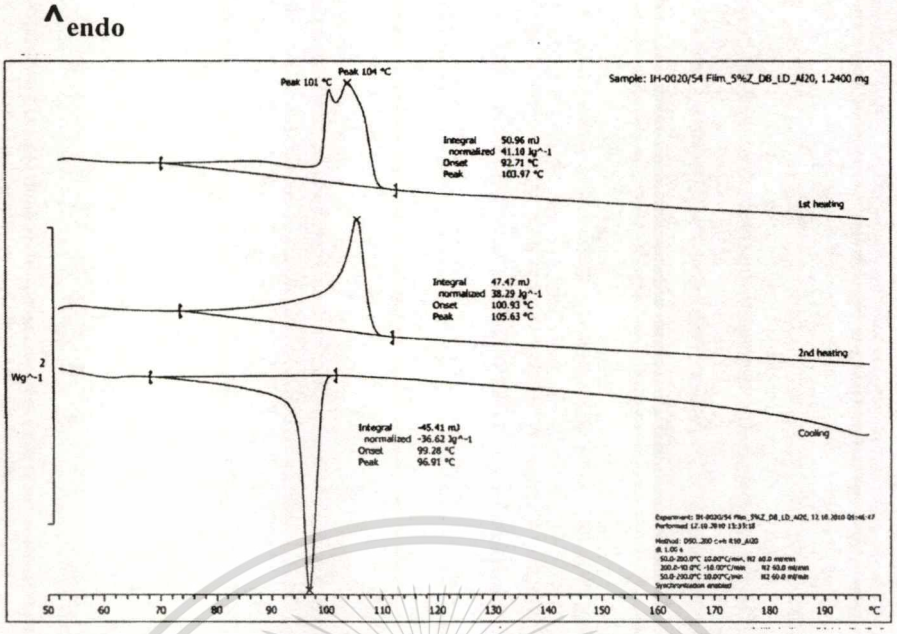

Figure E.5 Thermogram of 5Z_DB_LD film.

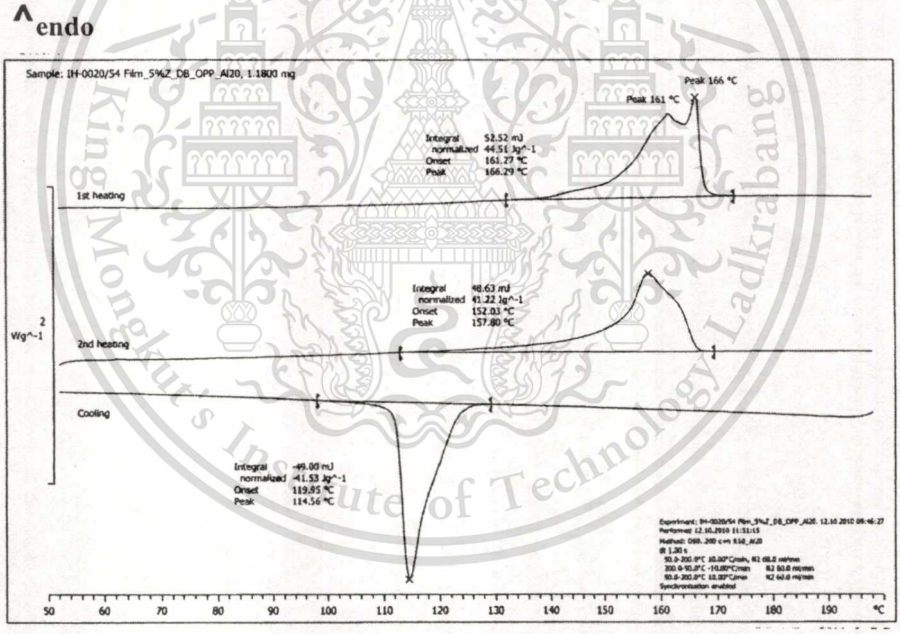

Figure E.6 Thermogram of 5Z_DB_BOPP film.

APPENDIX F

OPTICAL MICROGRAPH

(a)

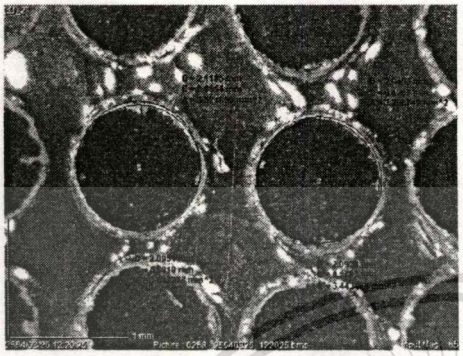

(b)

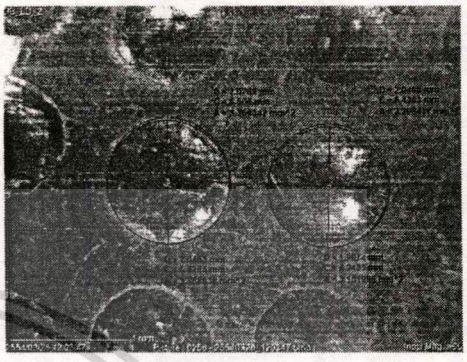

(c)

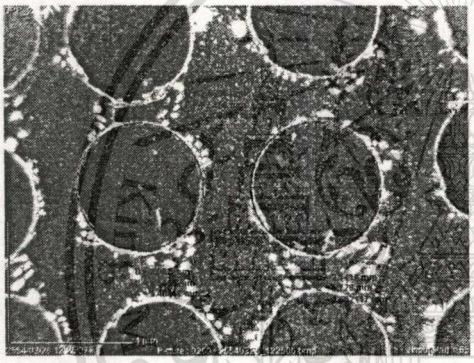

(d)

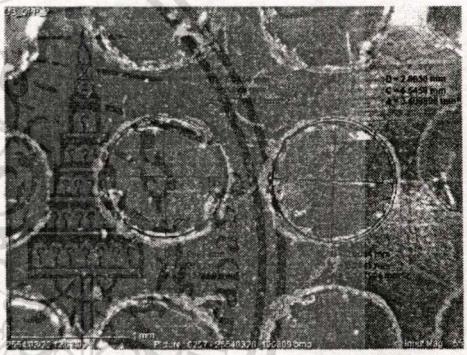

Figure F.1 Optical micrograph at perforated area, perforated size 2 mm:
(a) LDPE, (b) DB_LD, (c) BOPP and (d) DB_BOPP.

APPENDIX G

TENSILE PROPERTIES

Table G.1 Tensile properties of LDPE (30), BOPP (30) and SEBS (50).

Sample	Direction	Stress at yield (MPa)	Young's modulus (MPa)
SEBS (30)	No direction	2.80±0.2	39.3±3.1
LDPE (30)	MD	9.6±0.5	94.1±5.1
	TD	8.6±0.2	93.9±12.4
BOPP (30)	MD	28.9±3.7	264.1±24.7
	TD	68.3±7.8	826.9±72.3

Table G.2 Tensile properties of double-layered films with various perforated areas (0-100%).

Sample	perforated areas (%)	stress at yield (MPa)	Young's modulus (MPa)
DB_LD	0	5.7±0.2	57.1±2.4
	10	4.8±0.5	55.9±2.4
	20	4.3±0.1	53.2±2.6
	30	3.9±0.1	44.3±1.8
	40	3.7±0.3	42.4±5.3
	100	2.8±0.2	39.4±3.1

Table G.3 Tensile properties of double-layered films with various perforated sizes (2, 3 and 5 mm).

Sample	Perforated sizes (mm)	Stress at yield (MPa)	Young's modulus (MPa)
DB_LD	2	3.4±0.3	42.4±5.9
	3	2.8±0.0	35.9±1.4
	5	2.8±0.0	33.1±2.3
DB_BOPP	2	6.6±0.5	106.9±5.8
	3	6.9±0.8	95.6±7.6
	5	9.5±0.9	106.6±16.5

Table G.4 Tensile properties of double-layered films with SEBS thickness (30-50 μm).

Sample	SEBS thickness (um)	Stress at yield (MPa)	Young's modulus (MPa)
DB_LD	30	2.8±0.0	35.6±3.9
	40	2.8±0.0	30.7±4.5
	50	2.8±0.0	37.5±3.4
DB_BOPP	30	13.5±0.2	122.6±8.7
	40	13.0±1.9	119.8±10.9
	50	12.2±1.0	107.1±4.5
5Z _DB_LD	30	2.8±0.0	29.1±6.7
	40	2.8±0.0	31.4±2.3
	50	2.8±0.0	35.3±1.9
5Z _DB_BOPP	30	12.1±1.4	136.8±11.4
	40	10.7±0.8	121.0±10.3
	50	7.5±1.9	85.9±13.9

APPENDIX H

PERMEATION

Table H.1 Ethylene transmission rate (0-100% perforated areas).

Sample	Thickness (μm)	ETR (cm^3/m^2.day.atm)	EP (cm^3.mm/m^2.day.atm)
SEBS (50)	51	67481	3442
	56	61879	3465
	53	69584	3688
Mean	53±3	66315±3982	3532±136
LDPE (30)	33	19167	671
	34	17509	595
	33	18420	589
Mean	33±3	18365±830	606±45
DB_LD	84	19538	1641
	85	19723	1676
	81	18180	1473
Mean	86±3	19147±843	1589±109
DB_LD (2.25 %P)	86	19224	1653
	87	18793	1635
	81	20410	1653
Mean	86±3	19476±838	1636±11
DB_LD (6.25 %P)	85	25265	2148
	86	21803	1875
	83	24368	2023
Mean	85±2	23812±1797	2024±136
DB_LD (12.25 %P)	78	18569	1448
	79	19818	1566
	85	19735	1638
Mean	78±3	19374±698	1511±96

Table H.1 Ethylene transmission rate (0-100% perforated areas) (continued).

Sample	Thickness (μm)	ETR (cm^3/m^2.day.atm)	EP (cm^3.mm/m^2.day.atm)
DB_LD (20.25 %P)	81	25748	2086
	87	24730	2152
	80	24606	1968
Mean	83±3	25028±627	2077±93
DB_LD (30.25 %P)	84	36383	3056
	85	38777	3296
	84	37623	3160
Mean	84±2	37594±1197	3158±120
DB_LD (42.25 %P)	83	35500	2947
	79	36241	2863
	85	36796	3128
Mean	83±4	36179±651	3003±135
DB_LD (64 %P)	90	46265	4164
	85	45936	3905
	80	48071	3846
Mean	85±5	46757±1150	3974±169
DB_LD (90.25 %P)	85	60158	5113
	89	62392	5553
	82	56938	4669
Mean	85±4	59829±2742	5085±442

* (X %P) mean % perforated area.

Table H.2 Ethylene transmission rate as various perforated sizes.

SEBS thickness (μm)	Sample	Thickness (μm)	ETR (cm^3/m^2.day.atm)	EP (cm^3.mm/m^2.day.atm)
2	DB_LD	83	37005	3071
		80	48785	3903
		86	47173	4057
	Mean	83±2	44321±6387	3679±530
3	DB_LD	85	42969	3652
		80	35706	2856
		83	45579	3783
	Mean	82±2	41418±5116	3396±520
5	DB_LD	85	53026	4507
		80	44409	3553
		87	44130	3839
	Mean	85±3	47188±5057	4011±490
2	DB_BOPP	78	41423	3231
		75	42012	3151
		81	47849	3876
	Mean	78±3	43761±3553	3413±397
3	DB_BOPP	79	49844	3938
		80	52422	4194
		79	52708	4164
	Mean	79±2	51658±1577	4081±140
5	DB_BOPP	83	52420	4351
		80	58018	4641
		85	56813	4829
	Mean	83±4	55750±2947	4627±241

Table H.3 Ethylene transmission rate as various SEBS thicknesses.

SEBS thickness (μm)	Sample	Thickness (μm)	ETR (cm^3/m^2.day.atm)	EP (cm^3.mm/m^2.day.atm)
30	SEBS	32	83833	2683
		32	89399	2861
		33	86488	2854
	Mean	32 ± 1	86616±3936	2772±101
40	SEBS	42	78015	3277
		42	68095	2860
		43	66012	2839
	Mean	42 ± 1	73055±7014	3068±247
50	SEBS	52	63374	3295
		52	63535	3304
		53	55695	2952
	Mean	52 ±1	63454±4481	3300±201
30	5Z_SEBS	32	85653	2741
		35	94071	3292
		32	92550	2962
	Mean	32±2	90758±4486	2904±278
40	5Z_SEBS	40	77579	3103
		40	69433	2777
		41	76334	3130
	Mean	40±1	74449±4388	2978±196
50	5Z_SEBS	51	61074	3115
		50	66810	3341
		53	69945	3707
	Mean	53±1	65943±4498	3495±299

Table H.3 Ethylene transmission rate as various SEBS thicknesses. (continued).

SEBS thickness (μm)	Sample	Thickness (μm)	ETR (cm^3/m^2.day.atm)	EP (cm^3.mm/m^2.day.atm)
30	DB_LD	65	54342	3532
		65	50990	3314
		66	61090	4032
	Mean	66±1	55474±5144	3661±368
40	DB_LD	74	48650	3600
		74	44677	3306
		73	51230	3740
	Mean	75±1	48186	3614±211
50	DB_LD	86	46818	4026
		80	42281	3382
		83	35741	2967
	Mean	83±3	41613±5569	3454±534
30	5Z _DB_LD	61	62466	3810
		60	57325	3440
		63	64743	4079
	Mean	61±2	61511±3800	3752±321
40	5Z _DB_LD	72	50078	3606
		72	56288	4053
		73	58152	4245
	Mean	72±1	54840±4227	3948±328
50	5Z _DB_LD	87	48609	4229
		85	48895	4156
		88	38177	3360
	Mean	86±2	45227±6107	3890±482

Table H.3 Ethylene transmission rate as various SEBS thicknesses. (continued).

SEBS thickness (μm)	Sample	Thickness (μm)	ETR (cm^3/m^2.day.atm)	EP (cm^3.mm/m^2.day.atm)
30	5Z _DB_BOPP	63	37502	2363
		64	48802	3123
		62	46484	2882
	Mean	63±1	44263±5969	2789±389
40	5Z _DB_BOPP	72	33189	2390
		69	41852	2888
		66	41996	2772
	Mean	69±3	39012±5044	2692±261
50	5Z _DB_BOPP	82	29627	2429
		83	33515	2782
		81	42180	3417
	Mean	82±1	35107±6427	2879±500

Table H.4 Ethylene transmission rate as various ethylene concentrations in the presence of other gases.

Sample	Ethylene concentration (%v)	Ethylene transmission rate ($cm^3/m^2.day.atm$)		
		Under N_2	Under air zero	Under CO_2
DB_LD	20	10950	55249	7308
	40	21098	12821	15023
	60	36993	24584	33004
	80	48160	38530	48490
	100	55249	48923	55249
5Z_DB_LD	20	11467	11678	7310
	40	22052	27267	15856
	60	38395	40861	35051
	80	51151	56408	53623
	100	61255	61255	61255
5Z_DB_BOPP	20	7245	8426	5088
	40	13556	19716	10586
	60	28589	26549	24812
	80	33592	44320	32170
	100	45083	45083	45083

Table H.5 Oxygen permeation.

Sample	Oxygen flux ($cm^3/m^2.day$)	Thickness (μm)	OP ($cm^3.mm/m^2.day.atm$)
SEBS (30)	50142	32	1605
	52934	33	1694
Mean	51538	32	1649
LDPE (30)	5875	33	194
	7630	34	252
Mean	6753	33	223
BOPP (30)	2420	32	77
	2200	33	70
Mean	2310	32	74
DB_LD	31452	67	2076
	36224	65	2391
Mean	33838	66	2233
5Z_DB_LD	32752	62	1998
	25666	61	1566
Mean	29209	61	1782
5Z_DB_BOPP	18756	63	1144
	23606	64	1440
Mean	21181	63	1292

Table H.6 Carbon dioxide permeation.

Sample	Carbon dioxide flux ($cm^3/m^2.day$)	Thickness (μm)	CO_2P ($cm^3.mm/m^2.day.atm$)
SEBS (30)	82299	33	2633
	77542	33	2481
Mean	79920	32	2557
LDPE (30)	17496	33	577
	17820	34	588
Mean	17658	33	583
BOPP (30)	4437	32	141
	3785	33	121
Mean	4111	32	132
DB_LD	50202	67	3263
	56400	65	3778
Mean	53301	66	3517
5Z_DB_LD	52215	62	3246
	55013	61	3355
Mean	54114	61	3300
5Z_DB_BOPP	42521	63	2678
	44857	64	2825
Mean	43689	63±1	2752

Table H.7 Water vapor permeation.

Sample	WVTR ($g/m^2.day$)	Thickness (μm)	WVP ($g.mm/m^2.day$)
SEBS (30)	43.4	53	2.30
	43.3	52	2.29
Mean	43.10	52	2.26
5Z_SEBS (30)	71.1	29	2.06
	59.0	38	2.24
Mean	65.60	33	2.17
LDPE (30)	13.0	33	0.43
	12.9	32	0.42
Mean	13.2	32	0.43
BOPP (30)	5.13	30	0.16
	5.29	31	0.16
Mean	5.10	30	0.16
DB_LD	33.4	69	2.32
	33.1	71	2.35
Mean	33.28	70	2.34
5Z_DB_LD	26.7	72	1.92
	28.9	70	2.02
Mean	27.93	71	1.98
5Z_DB_BOPP	26.8	67	1.80
	21.4	70	1.50
Mean	24.60	68	1.68

AUTHOR BIOGRAPHY

Mr. Sarawut Laowakul was born on December 21, 1985 in Phichit. He received him B.Sc. in Chemistry from Naresuan University, Phitsanulok, Thailand, in 2007. He has been studied in Master programe in Polymer Technology, Faculty of science, King Mongkut's Institute of Technology Ladkrabang, since 2008.

This thesis had two publications in i) Study on tensile properties of SEBS/LDPE and SEBS/BOPP double-layered films for packaging application, Poster presentation in The 6th International Symposium on Advanced Materials in Asia – Pacific Rim (ISAMAP), Chulalongkorn University, Bangkok, Thailand, 21-23 November 2009 and ii) Ethylene transmission rate through zeolite modified double-layered films for packaging of fresh produces, Oral presentation in The 7th International Symposium on Advanced Materials in Asia – Pacific Rim (ISAMAP), Ishikawa High-Tech Exchange Center, Ishikawa, Japan, 30 September-1 October 2010

SCHOLARSHIP:

2009 National Science and Technology Development Agency (NSTDA), Pathumtani, Thailand